Design and Analysis of Chassis Frame for Four Wheel Rotary Potato and Maize Cultivator Machine

By

Moges Zewdu

A thesis submitted to partial fulfilment of the requirements for the award of the degree of Master of Science in Automotive Engineering

Department of Mechanical Systems and Vehicle Engineering

School of Mechanical, Chemical and Materials Engineering

Office of Graduate Studies

Adama Science and Technology University

Adama, Ethiopia

October, 2019

Design and Analysis of Chassis Frame for Four Wheel Rotary Potato and Maize Cultivator Machine

By

Moges Zewdu

Advisor: Mr. Mekonnen Liben (Asst. professor)

A thesis submitted to partial fulfilment of the requirements for the award of the degree of Master of Science in Automotive Engineering

Department of Mechanical Systems and Vehicle Engineering

School of Mechanical, Chemical and Materials Engineering

Office of Graduate Studies

Adama Science and Technology University

Adama, Ethiopia

October, 2019

Approval of Board of Examiners

We, the undersigned, members of the Board of Examiners of the final open defense by Moges Zewdu have read and evaluated his thesis entitled **“Design and Analysis of Chassis Frame for Four Wheel Rotary Tiller Machine Used for Potato and Maize”** and examined the candidate. This is, therefore, to certify that the thesis has been accepted in partial fulfillment of the requirement of the Degree of Master of Science in Automotive Engineering.

______________________	______________________	______________________
Supervisor/Advisor	Signature	Date
______________________	______________________	______________________
Chairperson	Signature	Date
______________________	______________________	______________________
Internal Examiner	Signature	Date
______________________	______________________	______________________
External Examiner	Signature	Date

DECLARATION

I hereby declare that this MSc Thesis is my original work and has not been presented for a degree in any other university, and all sources of material used for this thesis have been duly acknowledged.

Moges Zewdu	________________	________________
Student	Signature	Date

This MSc Thesis has been submitted for examination with my approval as thesis advisor

Mekonnen Liben	________________	________________
Advisor	Signature	Date

ACKNOWLEDGMENT

First of all I would like to thank the almighty God for his blessings.

My deepest gratitude also goes to my advisor, Mr. Mekonnen Liben (Asst. Professor) for their Sound advice and encouragement throughout this thesis. Their maximum effort and motivational speaking helps me to be strong and makes me to go forward.

My classmate, Mulugeta Denanto helped me a lot during prototype construction. I got a lot of constructive ideas from him. I wish God blessings for him and his family throughout his life.

Lastly, but not the least, I would like to forward my thanks to all my friends and my family members who gave me special advice and support.

TABLE OF CONTENTS

CONTENT PAGE

LIST OF TABLES

LIST OF FIGURES

LIST OF ACRONYMS

FEA	Finite Element Analysis
SCDM	Space Claim Design Modeler
FOS	Factor of Safety
MoA	Ministry of Agriculture
GDP	Gross Domestic Product
GR	Green Revolution

LIST OF NOMENCLATURES

K_{eq}	Equivalent Stiffness
ω_n	Natural Frequency
R_{total}	Total Resistance Force
R_{rl}	Rolling Resistance Force
Ra	Air Resistance Force
V	Speed
W	Weight
C_d	Coefficient of Drag Resistance
A_{PF}	Projected Frontal Area
P_r	Power Required for Rotary Mechanism
P_b	Maximum Brake Power
R_{RR}	Reaction Force at Right Rear Wheel
R_{RL}	Reaction Force at Left Rear Wheel
N	Newton
S_{UT}	Ultimate Tensile Strength
S_Y	Yield Strength
P_{axle}	Axle Load
w	Width
b	Breadth
t	Thickness
I_{XX}	Areal Moment of Inertia about X-X Axis

ABSTRACT

Agriculture has been the backbone of the Ethiopian economy and it will continue to remain so for a long time. Over the years, agricultural practices have been carried out by small scale farmers cultivating using human labor and traditional tools such as wooden plough, yoke, leveler, harrow, spade etc. The objective of this thesis work is to design a chassis frame of four wheel rotary tiller machine. The machine is used during the growth of crops such as potato and maize cultivated linearly for small land holder farmers. Our country is still using traditional farming system which is very tedious and time consuming. Therefore agricultural vehicle able to do such operations is needed to minimize the farmers' fatigue and to get the required product. In this thesis work, a chassis frame used to mount rotary tiller tools was designed. The ladder chassis frame have been modeled by considering channel cross-section longitudinal members and five cross members with three different cross-sections. I.e. C, I and cylindrical. The modeling was done using ANSYS fluent SCDM 18.1 and the analysis was done with the same software workbench. Reaction forces were determined using static equations by considering fixed supports at the four wheels and the gross weight of the vehicle was taken to be applied at the center of gravity of the vehicle. Both static (bending, torsion and combined bending and torsion) analysis and dynamic (impact and modal) analysis were done by taking four different materials such as ASTM A710 steel, ASTM A302 steel, AISI 4140 tempered and quenched at 205^{o}C and aluminum 6063 T-6 alloys to evaluate total stress and maximum deflections (deformations) and a factor of safety was calculated for each case. Based on the result of the analysis, AISI 4140 tempered and quenched at 205 ^{o}C was found to be fit for both the longitudinal and cross members due to its good strength and stiffness. It had a factor of safety of 1.47 and 1.59 for compressive and tensile strengths respectively in dynamic analysis approximately equal to the recommended factor of safety (1.5) which made the design safe.

Keywords: modeling, static analysis, dynamic analysis, rotary tiller.

CHAPTER ONE

INTRODUCTION

1. Background

Agriculture has been the backbone of the Ethiopian economy and it will continue to remain so for a long time. Over the years, agricultural practices have been carried out by small land holders cultivating using human labor and traditional tools such as wooden plough, yoke, leveler, harrow, spade etc. These tools are used in land preparation, for sowing of seeds, weeding and harvesting.

By adopting scientific farming methods we can get maximum yield and good quality crops which can save a farmer from going bankrupt but majority of farmers still use primitive method of farming techniques due to lack of knowledge or lack of investment for utilizing modern equipment. Modern agricultural techniques and equipment's are not used by small land holders because these equipment's are too expensive and difficult to acquire.

The use of hand tools for land cultivation is still predominant in Ethiopia because modern agricultural machineries require resources that many Ethiopian farmers do not have accessed easily. The need for agricultural mechanization in Ethiopia must therefore be assessed with a deeper understanding of the small land holder farmer‘s activities. There is huge gap in technology adoption and implement used with small and marginal farmers. Sustainable improvement in the livelihoods of poor farmers in developing countries depends largely on the adoption of improved resource conserving cropping systems. While most of the necessary components already exist, information on the availability and performance of equipment is lacking and effective communication between farmers and agricultural research and development department is unsuccessful.

Crops requirements for soil conditions are expressed in terms of looseness of soil, the depth of loosened layer, crumbly soil structure and moisture content that are necessary for emergence, root growth and plant development. From germination to seedlings' initial development the state of the top 10 centimeter layer (seed bed and seed bed base),while during the growing season the state of the soil from the surface to the depth of root growing but at least the state of top 0-45 cm layer is particularly important (Marta Birkas, 2014).

Tillage machines are fundamental for crop establishment, growth and amount of yield. For these reasons manufacturers have designed numerous types of tillage, sometimes especially designed according to farmers' requirements for a particular crop or a particular cultivated land. Tillage machines are classified according to their use for primary or secondary tillage operations and possible hitching configuration.

When designing a self-propelling machine, three main things should be considered. i.e. Power train system, body and chassis frame of the propelling body (vehicle). Chassis is a French term used to denote the frame parts of the vehicle and is called as carrying unit of a vehicle. The components of the vehicle like power plant, transmission system, axles, wheels and tires, Suspension, Controlling Systems like braking, steering etc., and also electrical system parts are mounted on the chassis frame. It is the main mounting for all the components including the body. Being the main load bearing structure of the vehicle, well-conditioned design of the chassis frame is paramount to the success of the vehicle as a whole.

Design of the vehicle chassis has to be started from identification of load types and there are five basic load cases to be considered during the design of chassis of any vehicle (Ashutosh and Vivek, 2009). These loads are bending caused by loading in vertical plane, torsion case, combined of bending and torsion loads and lateral loading generated at the tire to ground contact patch and fore and aft loading generated when vehicle accelerates and decelerates inertia forces should also be considered.

The mechanization of farming in developing countries has been very uneven. In certain parts of Africa, in Java, and in many hilly regions, farmers still till their fields with hand tools even though animal tillage has been common in other parts of the world for thousands of years. While draft animals have completely disappeared in North America, Europe, and Japan, they have been widely accepted in Senegal only in the past few decades. Even in countries where farming is beginning to be mechanized, power tillers and tractors are still restricted to tillage and a few other operations. The pattern and speed of mechanization is heavily influenced by relative scarcities of capital and labor, and other macroeconomic variables. The responsiveness of invention and innovation to economy wide factors has become known as the process of induced innovation (Hans, 2014).

The early history of the tractor owes a lot to the development of the steam engine. As far as we could trace back, the first ever steam engine mounted on a vehicle, dates to 1769, when Joseph Cugnot, a French military engineer, presented his “fardier a vapeur”. Cugnot was the first inventor to convert the alternate motion of a steam piston into rotary motion. He built a second wagon, dating from 1771, which was able to transport 5 tons at a speed of 3.5 km/h. This was a very heavy vehicle, hard to maneuver with two rear wheels and one in the front, supporting the steam boiler. The steam engines were adapted and evolved for agricultural use. Many of the first steam traction engines of the 1800’s were mounted on wheels, transported to the field by horses and standing still would haul ploughs and other implements by cable. British soil scientists welcomed these innovations for they prevented soil compression associated with horse cultivation. The aim of farmers though was to create a machine capable of pulling implements or cultivating the soil directly, turning the soil more efficiently than a traditional plough. To encourage such a development, in 1854 the Royal Agricultural Society of England offered a 500 pound prize for the most efficient and economic steam cultivator and John Fowler was the winner, presenting a machine that could draw an agricultural implement, like a plough, back and forth across the field using a windlass (figure1.1). The Fowler Company kept improving their machines through the 19th century, expanding their market to Eastern Europe). Another inventor, Thomas Rickett, developed a rotary steam cultivator, which was an enormous 10 ton machine designed to break and aerate the soil, that became popular at the time (Vanessa et al., 2016).

Figure 1. 1. Fowler´s traction engine pulling a plough (Source: Steam Plough Club, www.steamploughclub.org.uk/pictures.htm)

The introduction of the farm tractor in United Sates farms was responsible for the reduction of the farm work force, the reduction of draft animals and accounted for an increase of 8.4% of the US GNP in 1954. From 1910 to 1955, the fraction of total workforce applied in agriculture was reduced from 30% to 10% and the number of horses and mules decreased from 24 million to 4.3 million in the same period (Vanessa et al., 2016).

Agricultural Engineering profession and practice in China is greatly supported by the central government policies and support. The support is in the area of adequate funding for research and development, training and extension. In the last twenty years, the central government at the beginning of every year issues policies documents and working plan related to agriculture, rural areas and farmers issue. The attendant results is the contribution of agricultural engineering to ensuring adequate food supply and enhancing the income of the farmers (Kehinde, 2014). Agricultural engineering development in China has promoted mechanization and industrialization of agricultural production, development of cooperative organizations of farmers, advanced research in new techniques, competitiveness of agricultural products and environmental protection and ecological development. Many Africa countries are still faced with the inadequate supply of food to feed their population. The attendant results are hunger, malnutrition, and sometimes political instability. The model of China experience can be adapted to revolutionize the Africa agriculture. Government heavy investment in all aspects of agriculture is highly needed, researches into new and improved mechanization agricultural system is urgently needed. Farmers need incentives and increased income to avoid urban migration thereby depleting rural labor. Rural transportation needs to be overhauled and post-harvest technology needs great improvement. Appropriate government deliberate supportive policies are required. A lot of Africa countries have the required resources and experts to develop agriculture and make Africa self-sufficient in food production. However, government efforts, investment and favorable policies are still inadequate in most Africa countries. Huge food importation being employed by Nigeria and some governments to supplement local production will not augur well for sustainable efforts to be self- dependent in food production. Instead local investment should be made to encourage local investors in agricultural sector (Kehinde et al., 2014).

Given the relatively high land-to-labor ratio on agricultural endowments in many African countries, mechanization may play a greater role in African agricultural intensification than it did in the intensification processes observed in the Asian Green Revolution (GR). In most Asian countries during the GR, land-to-labor ratio was low and rural non-farm employment opportunities were few. In general, demand for mechanization emerges at the point when it becomes cost effective for farmers to use it over other available options. Thus, policy interventions aimed at promoting mechanization must first confirm whether sufficient demand is indeed present (Xinshen et al., 2016).

1.1. The rotary tiller

The rotary tiller is used to tillage operation for potato and maize cultivated land. The whole assembly of the rotary tiller will be mounted between the third and fourth cross members of the chassis frame. The tilling attachments rotate about the vertical axis on the horizontal plane and used to tilt the cultivated land around each crop which helps to aerate the soil and remove weeds.

1.1.1. Power transmission to the rotary tiller and its working principle

For operation of power tiller, the power is obtained from the Engine, fitted on the power tiller. The engine power goes to the main clutch. From main clutch, the power is divided in two routes, one goes to transmission gears and then to the wheel. The other component goes to the tilling attachment by belt drives. The power from the engine is made to rotate the rotary tiller tools about the vertical axis by using bevel gear assembly as shown in the Figure 1.2 below.

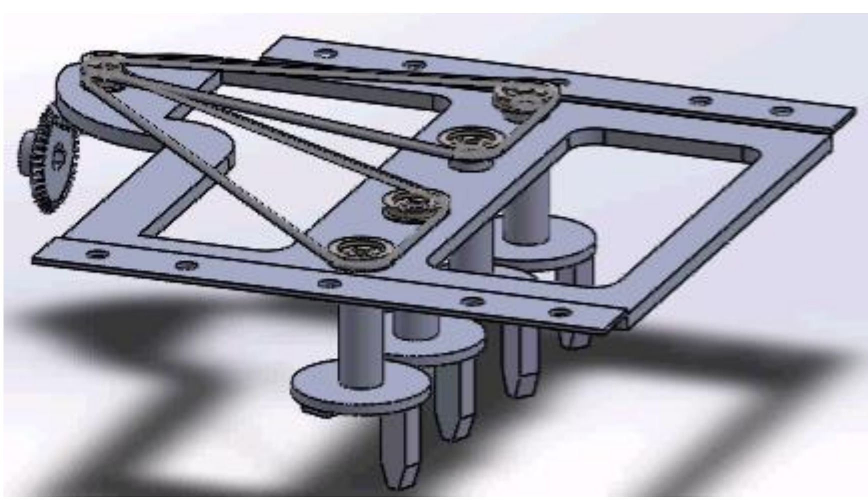

Figure 1. 2. Rotary tiller tool

1.2. Chassis types, layouts and its main components

There are three types of chassis frames.

- Conventional frame
- Integral frame
- Semi-integral frame

Conventional Frame: The Conventional type of chassis frame has two long side members and 5 to 6 cross members joined together with the help of rivets and bolts. The frame sections used are generally classified as Channel Section, Tabular Section and Box Section. It is non load carrying frame. The loads of the vehicle are transferred to the suspensions by the frame. This suspension in the main skeleton of the vehicle which is supported on the axles through springs. The body is made of flexible material like wood and isolated frame by inserting rubber mountings in between. The frame is made of channel section or tubular section of box section. Such chassis frame is used for trucks. It has the advantage when the vehicle is met with accident the front frame can be taken easily to replace the damaged chassis frame (Prashanth, 2017).

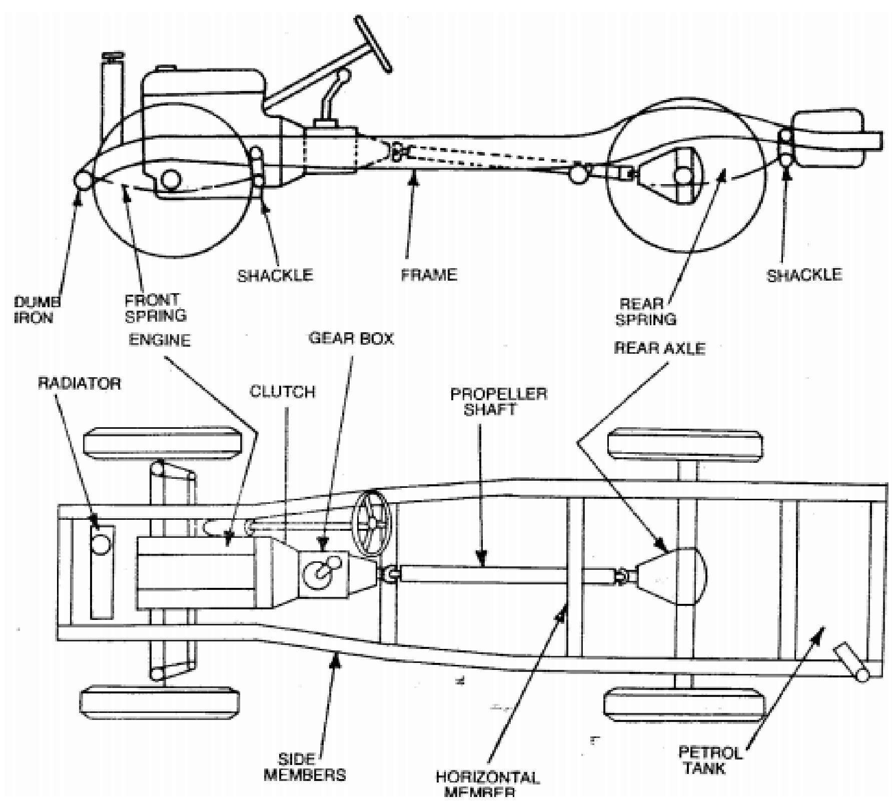

Figure 1. 3. Layout of conventional chassis and its main components (source: https://perticos. wordpress.com/2016/02/09/automobile-chassis-and-body-engineering/)

Semi-integral Frame: In this case the rubber mountings used in conventional frame between frame and suspension are replaced by more stiff mountings. Because of this some of the vehicle load is shared by the frame also. This type of frame is heavier in construction (Prashanth, 2017). In some vehicles half frame is fixed in the front end on which engine gear box and front suspension is mounted which is called Semi-Integral chassis Frame This type of frame is used in FIAT cars and some of the European and American cars (Julian, 2002).

Integral Frame: In this type of construction, there is no frame. It is also called unitized frame body construction. In this case, the body shell and underbody are welded into single unit. The underbody is made of floor plates and channel and box sections welded into single unit. This assembly replaces the frame which decreases the overall weight compared to conventional separate frame and body construction (Prashanth, 2017). On the Integral chassis Frame, there is no frame and all the assembly units are attached to the body. All the functions of the frame carried out by the body itself. Due to elimination of long frame it is cheaper and due to less weight most economical also. Only disadvantage is repairing is difficult (Julian, 2002).

1.3. Statement of the problem

Our country is still using traditional way of agricultural mechanisms. This traditional way of farming is very tedious and time consuming. Due to this reason, farmers are not able to fulfill crops requirements for soil conditions, expressed in terms of looseness of soil, the depth of loosened layer, crumbly soil structure and moisture content that are necessary for root growth and plant development. In addition to this crops are damaged by weed due to absence of modern way of farming and farmers are not able to get high crop product. So secondary tiller machines used to break and aerate the soil during the growing period of crops are important.

1.4. Objectives

1.4.1. General objective

The general objective of this thesis work is to design a chassis frame of four wheel rotary tiller machine used during the growing period of potato and maize crops cultivated linearly for small land holder farmers. The chassis frame is used to mount the rotary tiller on it.

1.4.2. Specific objectives

The specific objectives are:

- To design the longitudinal and cross members of the chassis frame
- To model chassis frame and related components using ANSYS SCDM 18.1 software.
- To do the strength analysis by ANSYS software and select appropriate materials
- To do the prototype of the chassis frame.

1.5. Significance of the thesis

The significance of this thesis work are the following:

- It helps in reducing farmers' fatigue.
- Since it can cover large areas with in minimum time, the required farming activity will be done with in the recommended period of time and so crop growth could not affected by weeds.
- It plays a great role for the productivity of crops.

1.6. Delimitation (Scope)

The scope of this project is to design a chassis frame for four wheel agricultural rotary dibber machine for some selected cpops such as maize and potato which grow in linear pattern. Prototype construction of the chassis frame will be done based on the design results.

1.7. Limitations

Different challenges were faced during the execution of this thesis work. The first challenge is non availability of the required material types with appropriate dimensions and lack of modern workshops which enable to manufacture the designed project with appropriate dimensions. The second limitation is that the time of budget allowance was very late which is directly related with the university management problems which makes us to start our project late.

CHAPTER TWO

LITERATURE REVIEW

There has been a large amount of research into designing vehicles appropriate for agricultural purposes. Among these designed and used vehicles soil tillage vehicles are largely used in different parts of the world.

2.1. Purpose of tillage

Tillage, the mechanical manipulation of soil to provide suitable conditions for crop growth and development, may be required for a number of reasons such as creating seedbed, loosen compacted soil layers, for aeration, to incorporate crop and weed residues in to the soil and to facilitate irrigation, water infiltration and soil moisture (Mitchel, 2004).Broadly defined, tillage is mechanical manipulation of soil and plant residues to prepare seedbed, for crop planting. Even if tillage plays vital role for the development of crops, however intensive tillage can also have negative impact on environmental quality by accelerating soil loose (Shrestha, 2006).

(Marta, 2014) Stated about crop requirements for soil conditions and the purpose of tillage was well explained. It also explained the international trend of soil tillage and relevant points of good agricultural practice.

Harsha (2017) aimed on the design, development and the fabrication of the vehicle which can dig the soil, sow the seeds, leveler to close the soil and pump to spray water, these whole systems of the vehicle works with the battery and solar power, the vehicle is controlled by toggle switch.

Kataoka (2009) explained about the beginning of mechanization in agriculture in Hokkaido and the evolution of agricultural machineries. Different tractor types such as McCormic Deering Tractor, wheat reaper and the structure of a steam engine tractor and benz tractor are clearly shown. In addition to this it is also explained that rotary tillers or the power harrows are used for making seedbed of fine soil in spring.

2.3. Chassis types and their cross-sections

Kumar and Deepanjali (2016) entitled as design and analysis of automobile chassis focused on finding out best material and most suitable cross-section for an Eicher E2 TATA truck ladder chassis with the constraints of maximum shear stress, equivalent stress and deflection of the chassis under maximum load condition with materials namely ASTM A710 Steel, ASTM A302 alloy Steel and Aluminum Alloy 6063-T6 subjected to the same load. The different vehicle chassis have been modeled by considering three different cross-sections namely C, I and rectangular box (hollow) type cross sections. The result of the analysis shows that the shear stresses were found minimum in Aluminum alloy 6063-T6 and maximum in ASTM A710 steel under given boundary conditions, Von Mises stresses were found minimum in Aluminum alloy 6063-T6 and maximum in ASTM A710 steel under given boundary conditions and the rectangular box cross-section type of ladder chassis was having least deflection, Von Mises stress and maximum shear stress for aluminum alloy 6063-T6 in all the three types of materials of three different cross section type of ladder chassis.

2.4. Load types and boundary conditions

Normally the main function of the chassis is to safely carry the maximum load holding all components together while driving, accommodate twisting on uneven road surface enduring shock loading and it must absorb engine & driveline torque. Various loads acting on the chassis frame are (Wankhade, 2014).

1. Short duration load - while crossing a broken patch.
2. Momentary duration load - while taking a curve.
3. Impact loads - due to the collision of the vehicle.
4. Inertia load - while applying brakes.
5. Static loads - loads due to chassis parts and weight of vehicle.

When the vehicle is at rest and moving at a constant velocity on an even road, the loads are treated as static loading type and can be solved using static equilibrium balance, resulting in set of algebraic equations. On the other hand dynamic loads include the load types during vehicle moving on a bumpy road even at constant velocity. Such problems can be solved using dynamic equilibrium balance resulting in differential equations. Due to the above conditions five basic load cases may exist on the chassis frame. These loading cases are bending case, torsion case, combined bending and torsion, lateral loading and fore and aft loading. The bending case happens due to loading on the vertical plane and due to weight of components along the vehicle frame (Paulina, 2014).

The punishing treatment received by the vehicle bodies in service, together with the great variety of use and abuse, means the combinations of many load cases have to be considered in finding the worst one, for the realistic use in the analysis. Before moving directly to these conditions, it will be a fair practice to visit the simplified representation of the structure, and the actual representation of the load over it. The structure can be simply assumed as beam, with uniformly distributed load due to cabin & body over its length, and the point loads at the engine, transmission and various heavily loaded accessories. It is fixed at its four wheels or suspensions.

Whilst adequate durability under dynamic conditions is a design requirement for the vehicle structures, the static load cases cannot be disregarded. The values for the individual load cases are taken from the expected service conditions of the particular vehicle. The worst-case loading conditions (distribution of the load) as well as overloading must be considered for the static load case. The factors usually applied to the static load case, especially for those vehicles with a long overhang containing concentrated loads (e.g., rear engine buses). Such loads result in high bending moments over the rear axle (Ashutosh and Vivek, 2009).

Adequate durability under dynamic conditions is a design requirement for the vehicle structures, the static load cases cannot be disregarded. The values for the individual load cases are taken from the expected service conditions of the particular vehicle. The punishing treatment received by the vehicle bodies in service, together with the great variety of use and abuse, means the combinations of many load cases have to be considered in finding the worst one for the realistic use in the analysis. Before moving directly to these conditions, it will be a fair practice to visit the simplified representation of the structure, and the actual representation of the load over it.

Grzegorz et al. (2014) listed the process that a chassis design consists such as load case, chassis type and structural analysis. Here it was clear that Design of the vehicle chassis had been started from analysis of load cases which are five basic types.

Bending case: This is loading in a vertical plane, the x–z plane due to the weight of components distributed along the vehicle frame which cause bending about the y-axis.

Torsion case: The vehicle body is subjected to a moment applied at the axle center lines by applying upward and downward loads at each axle in this case. These loads result in a twisting action or torsion moment about the longitudinal x-axis of the vehicle

Combined bending and torsion: In practice, the torsion case cannot exist without bending as gravitational forces are always present. Therefore, the two cases must be considered together when representing a real situation (Julian, 2002).

Lateral loading: This condition occurs when the vehicle is driven around a corner or when it slides against a kerb.

Fore and aft loading: During acceleration and braking longitudinal forces are generated (along the x-axis). Traction and braking forces at the tire to ground contact points are reacted by mass times acceleration (deceleration) inertia forces.

The most important cases are those of 1 (bending), 2 (torsion) and 3 (bending and torsion) as these are paramount in determining a satisfactory structure. The lateral loading and fore-aft loading cases require attention when designing the suspension mounting points to the structure but are less significant on the structure as a whole. Other localized loading conditions such as loads caused by door slamming, seat belt loads, etc., are not considered in this work (Julian, 2002).

Olofsson (2015) concerned on rationalizing Chassis calculations for use in truck Frame design. The subject for analysis was a six-wheeled articulated truck, and the load cases under study was Lateral Loading, Frame Torsion and Vertical Load on Kingpin. Making robust deformation and stress models with a calculation time succinctly short and accuracy consistently high for efficient design work is an arduous task.

Whilst adequate durability under dynamic conditions was a design requirement for the vehicle structures, the static load cases cannot be disregarded. The values for the individual load cases were taken from the expected service conditions of the particular vehicle. The worst-case loading conditions (distribution of the load) as well as overloading were considered for the static load case. The factors usually applied to the static load case, especially for those vehicles with a long overhang containing concentrated loads (e.g., rear engine buses). Such loads result in high bending moments over the rear axle. Lateral forces act on the Roll Center of vehicle during cornering. A line joining the roll centers of the suspensions is roll axis. The lateral separation between the suspensions causes them to develop roll resisting moment proportional to the difference in the roll angle between the body and the axle (Ashutosh and Vivek, 2009).

According to Ashutosh and Vivek (2009), the cross members & side members are severely stressed when the diagonally opposite wheels of the vehicle are on the bump. Here, the suspensions whose wheels are on bumps are given the maximum displacement (permissible for the suspension) in the vertical direction. The non-bump wheels spring mounting locations are made constrained in the vertical direction. Heights of the bumps are taken such that the diagonally opposite suspensions undergo the maximum deflection. The maximum stress is coming near the fuel tank mountings, as the fuel tank will add to the rigidity due to its own section modulus. The diagonally opposite bumps will twist the chassis, due to which the rear most cross member will undergo the high torsional stresses.

The modal analysis is the field of measuring and analyzing the dynamic response of structure when excited by an input disturbance. Modal analysis of the system is closely associated with the natural frequency of the system. Stiffness (k) and mass (M) of the system are the deciding factors for the natural frequency (Kallappa, 2015).

Cavazzuti (2010) presented computer aided rear-central engine high performance car chassis design. The method was potentially extended to chassis design in general once the performance targets and the suspensions scheme are given. The methodology presented makes use of collaborative design techniques and aims at finding more efficient layout solutions for the chassis framework.

The effects of different twisting angles generated by an electrohydraulic vibration simulator on a farm trailer's chassis were determined and it is explained that the twisting moment of the trailer's chassis is important for stability and lifetime (Bahattin, 2008).

Erwin (2004) gave the compulsory specification for agricultural tractors and agricultural tractor was defined as power-driven vehicle, either wheeled or track laying, which had at least two axles, and whose function depends essentially on its tractive power, and that is specially designed to pull, push, carry or actuate certain implements, machines or trailers intended for use in agriculture.

Atsbaha and Tessema (2010) listed the major crops and vegetables of Ethiopian farmers and the farming methods used. It was stated that the effort is focused on making the country self-sufficient through increased food production and higher farm productivity, with the final goal being ending the country's dependence on external food aid.

Kiran et al. (2014) used numerical analysis using finite element technique to find the critical stress. The monologue and ladder frame for static load condition with the stress, deflection bending moment are analyzed and the analysis of two different chassis with same as above frame were analyzed. i.e. the kit car chassis and the other one is Chevy truck chassis. The drawback of this work was that the analysis is done by considering only static loading type and the load applied was taken as loads applied on cantilever beam.

Jatin (2014) focused on Automobile Chassis for Prevention of Rolling Over of a Vehicle. The first part of this paper dealt with the structural analysis of automobile frame and design modification to reduce weight of the chassis and the second part was the study of rolling over effect and the multiple axle drives with active bogies for chassis levelling and the final part was the implementation of the active bogies and multiple axle drives for the prevention of rolling over. Using Active weights are suggested in order to prevent the rolling over of a vehicle.

Srinivasa et al. (2017) reviewed typical natural frequency values, excitation sources and mode shape of parallel ladder type frame with box section chassis of a Suzuki jeep truck model chassis of mass approximately 75kg and the dimension of an existing truck chassis was measured. For the analysis case, the numerical method of analysis is adopted, in which ‘finite element technique' is used. The analysis of this paper shows that duralumin is better than structural steel of the same weight for the case of static analysis.

Gaurav (2016) aimed on the design and analysis of a go kart chassis. The main intention of the project focused to do design and static analysis of go-kart chassis and the maximum deflection was obtained by analysis. The paper highlights the material used and structural formation of chassis, the strength of material, and rigidity of structure and energy absorption characteristics of chassis is discussed. Boundary value analysis testing technique is used to identify errors at boundaries rather than finding those exist in center of input domain. Here the main short coming of the project is dynamic loading conditions are not considered. i.e. only static analysis is done.

Madhu (2014) studied about Static Analysis, Design Modification and Modal Analysis of Structural chassis Frame. In this paper static analysis, modification of chassis frame based on results and modal analysis of structure was achieved. Results indicated Von Mises stress below yield strength of the material, which satisfies the design and deflection is about 5.648mm. Modification of design was carried out to reduce deflection of structure. Deflection of the modified structure is 3.706mm.

Kallappa et al.(2015) gave the emphasis on dynamic analysis of chassis and the modal analysis is carried out using both analytical and FEA techniques. According to the analysis of this journal the results were found to be in good agreement with each other and the chassis structure is optimized by varying the design parameters with the help of acceleration response of the system.

2.5. Chassis materials

The amount of carbon in steel is important to determine the strength, hardness, and machining characteristics. Material selection of the frame plays an important role in providing desired strength, endurance, safety and reliability of the vehicle. The material used for chassis are various grades of steel or aluminum alloys. The main component of steel is carbon which increases the hardness of material of chassis. Aluminum alloy is expensive than steel so mainly steel is used to constructs the chassis (Gaurav et al., 2016)

An important design consideration in chassis design is the natural frequencies and mode shapes for dynamic loading conditions along with strength. With high strength to weight ratio carbon nanotubes (CNT) reinforced polymer composite material are used in automobile industry. CNT are used as a reinforced materials because of higher strength, toughness specific tensile strength and ability to resist vibrations (Vinodbabu et al, 2015).

Kumar and Deepanjali (2016) entitled as design and analysis of automobile chassis focused on finding out best material and most suitable cross-section for an Eicher E2 TATA Truck ladder chassis with the constraints of maximum shear stress, equivalent stress and deflection of the chassis under maximum load condition with materials namely ASTM A710 Steel, ASTM A302 Alloy Steel and Aluminum Alloy 6063-T6 subjected to the same load. The different vehicle chassis have been modeled by considering three different cross-sections namely C, I and Rectangular Box (hollow) type cross sections. The result of the analysis shows that the Shear stresses were found minimum in Aluminum alloy 6063-T6 and maximum in ASTM A710 steel under given boundary conditions, Von Mises stresses were found minimum in Aluminum alloy 6063-T6 and maximum in ASTM A710 Steel under given boundary conditions and the Rectangular Box Cross-section Type of Ladder Chassis is having least deflection, Von Mises stress and Maximum Shear stress for Aluminum Alloy 6063-T6 in all the three types of materials of three different cross section type of Ladder Chassis.

Vijayan et al. (2015) described design and analysis of heavy vehicle chassis as prime objective of any automotive industries. The pertinent information of an existing heavy vehicle chassis of EICHER was taken for modeling and analysis by considering polymer composite materials such as s-glass, Epoxy, and cross-sections such as C, I and Box section subjected to identical load as that of steel chassis. The numerical results are validated with analytical calculation considering the stress distribution. The result of this paper shows that it is inferred that by employing a S-Glass Epoxy composites heavy vehicle chassis for same load carrying capacity, there is a reduction in weight when compared to steel but main downside is S-Glass Epoxy induces high deformation and stress distribution when compared to steel except in 'I' section. Based on the results it was inferred that steel with 'I' section has superior strength to withstand high load and induced low deformation and stress distribution when compared to S-Glass Epoxy composites material.

2.6. Finite element method

The finite element method (FEM), sometimes referred to as finite element analysis (FEA), is a computational technique used to obtain approximate solutions of boundary value problems in engineering. Simply stated, a boundary value problem is a mathematical problem in which one or more dependent variables must satisfy a differential equation everywhere within a known domain of independent variables and satisfy specific conditions on the boundary of the domain. Boundary value problems are also sometimes called field problems. The field is the domain of interest and most often represents a physical structure. The field variables are the dependent variables of interest governed by the differential equation. (DAVID, 2004)

2.6.1. Finite element analysis steps

There are certain steps in formulating a finite element analysis of physical problems. There are three main steps, namely: preprocessing, solution and post processing steps.in the preprocessing (model definition) includes :define the geometric domain of the problem, the element types to be used, the material properties of the elements, the geometric properties of the elements (length, area…),the element connectivity(mesh the model),the physical constraints(boundary conditions) and the loadings. A perfectly FE solution is of absolutely no value if it corresponds to the wrong problem. The next step is the solution. In this step the governing equation in matrix form and computes the unknown values of primary field variables are assembled. Actually the features in this step such as matrix manipulation, numerical integration and equation solving are carried out automatically through commercial software. The last step is post processing during which the analysis and evaluation of result is done which includes sorting element stresses in order of magnitude, check equilibrium, calculate factors of safety, plot deformed structural shape and animate dynamic model behavior (Madenci, 2007).

2.6.2. Modal analysis

The modal analysis is the most basic and important part of analysis of dynamic character. This modern method used find the natural frequency and mode shapes of the structures. The rigidity could be analyzed and the resonance vibration could be avoided. The main characteristics of each mode of the structure can be figured out through the modal analysis, and the actual vibration response under this frequency range can be predicted. The results from modal analysis can be used as reference value for other dynamic analysis like random analysis, harmonic analysis (Madhu, 2014).

The modal analysis is the field of measuring and analyzing the dynamic response of structure when excited by an input disturbance (Kallappa, 2015). The modal analysis of the chassis frame should be carried out to determine the natural frequency and mode shapes of the system. The rigidity of the system should be analyzed and their resonance could be avoided (Madhu, 2014).

$$\omega_n = \frac{1}{2\pi}\sqrt{K/m} \tag{2.1}$$

Where: ω_n = natural frequency

K = Stiffness of the chassis frame

M = mass of the model

2.6.3. Static analysis

The FEM is a common tool for stress analysis. FEM with required boundary conditions was used to determine critical regions in the chassis frame. Static structural analysis is performed to identify critical regions and based on the results obtained design modification has been done (Madhu, 2014).

2.6.4. Comparison of finite element and exact solutions

The process of representing a physical domain with finite elements is referred to as meshing, and the resulting set of elements is known as the finite element mesh. As most of the commonly used element geometries have straight sides, it is generally impossible to include the entire physical domain in the element mesh if the domain includes curved boundaries (David, 2004). Such a situation is shown in Figure 2.6 a, where a curved-boundary domain is meshed (quite coarsely) using square elements. A refined mesh for the same domain is shown in Figure 2.6.b, using smaller, more numerous elements of the same type. Note that the refined mesh includes significantly more of the physical domain in the finite element representation and the curved boundaries are more closely approximated. (Triangular elements could approximate the boundaries even better.)

If the interpolation functions satisfy certain mathematical requirements a finite element solution for a particular problem converges to the exact solution of the problem. That is, as the number of elements is increased and the physical dimensions of the elements are decreased, the finite element solution changes incrementally. The incremental changes decrease with the mesh refinement process and approach the exact solution asymptotically.

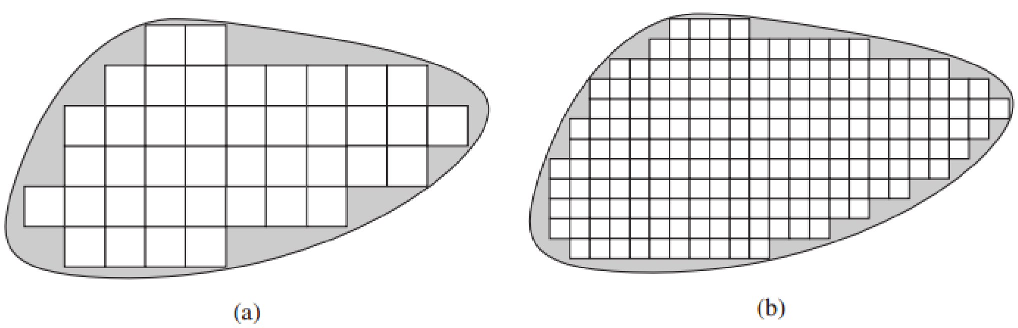

Figure 2. 1. (a) Arbitrary curved-boundary domain modeled using square elements. (b) Refined finite element mesh.

From the above literatures, it is clear that the boundary conditions of the chassis frame analysis depends on the load case applied to the chassis frame. The natural frequency of the chassis frame should be higher than the excitation frequency of the all vibrating bodies in order to avoid resonant frequency.

CHAPTER THREE

MATERIALS AND METHODS

3.1. Materials

The modelling of the chassis frame was done using ANSYS space claim and the static and the dynamic analysis had been done by using the same software work bench. The specification and some important data are taken from Mahindra tractor company manuals.

The ladder type chassis having 5 cross members is used for the analysis. From those cross members, the front is channel section and the cross-members next to front cross member and the rear cross member are tubular cross-section whereas the middle 2 cross members are selected to be double channel section to have good resistance for combined loading

Materials selection depends very much on the skills and experience of the design team although materials databases are now available to help in this process. A successful choice of materials requires knowledge, understanding and experience of working with a wide range of materials. Performance of the material must meet specific requirements. It is necessary to match the task, which the component or device may have to perform, with the material resources. It is important to consider the whole range of service requirements that are likely to arise, such as the mechanical loads and loading regimes, hardness, rigidity, flexibility and particularly weight, in vehicle design, as well as a range of physical properties. These can then be surveyed and matched with the properties and characteristics of suitable materials. The requirements of both properties and processing are often needed in various combinations for particular applications (Julian, 2002).

These and other requirements can now be explored and tested with computer software packages, particularly with plastics and polymers, so that comparisons can be made. In this way, the materials choice can be narrowed and a suitable selection becomes possible

For this project, the materials used for comparison are ASTM A710, ASTM A302 steel alloys and aluminum alloy 6063-T6.The material properties are given on the table 3.1 below

Table 3. 1. Material Properties

Property	ASTM A710 steel alloy	ASTM A302 steel alloy	aluminum alloy 6063-T6	AISI 4140 Q&T at 205^{0}C
Density(kg/m^3)	7850	7790	2800	7835
Yield Strength(MPa)	450	340	220	1640
Ultimate tensile strength (MPa)	515	590	250	1770
Young's modulus (GPa)	205	210	69	200
Poisons Ratio	0.29	0.33	0.32	0.3
Shear Modulus (GPa)	80	78	26	80
Max. Elongation (%)	20	22	8	21.5

Source: Kumar and Deepanjali (2016) and Shigley's (2015) mechanical engineering design,tenth edition.

3.2. Method

3.2.1. Literature review

Literature review was used as a main tool to see the previously done projects and to identify the existing problem. Totally, more than thirty journals, books, proceedings of conference and other publications are reviewed. The load types applied on the chassis frame, the boundary conditions used and requirements including the speed limit for agricultural vehicle are generally viewed from previous works. In addition to these points the general procedures followed and the main types of analysis important for chassis design are well explained in some works.

3.2.2. Vehicle specification

To do the design of the chassis, specifications of the vehicle components and the overall dimensions and weight of the vehicle including the location of axles with respect to the center of gravity is known.

The chassis frame is done by taking Specification of Mahindra E-Max S-22 Gear Tractor as to have equivalent overall dimension given in the table 3.2 below (Mahindra, 2017).

Table 3. 2. Specification of Mahindra E-Max S-22 Gear Tractor

Tractor model		e-max s-22 gear
Engine rated power hp (kw)		22(16.4) @2800 rpm
Weight (Kg)		968
Over all dimensions (mm)	Length	2553
	Width	1290
	Height	1778
Engine dimensions	Length (mm)	925
	Width (mm)	694
	Height (mm)	432
	Weight (kg)	381

The chassis of this machinery has five cross-members on which the first cross-member starts at the front. The first cross member is C-channel cross-section, the second and the fifth cross members are tubular cross-sections and the third and fourth cross members are double C cross-section forming an I-section as shown in Figure 3.1 below. The reason why these three types of combination used is to resist all loading types. i.e. bending loads, torsion loads and combination of these load types.

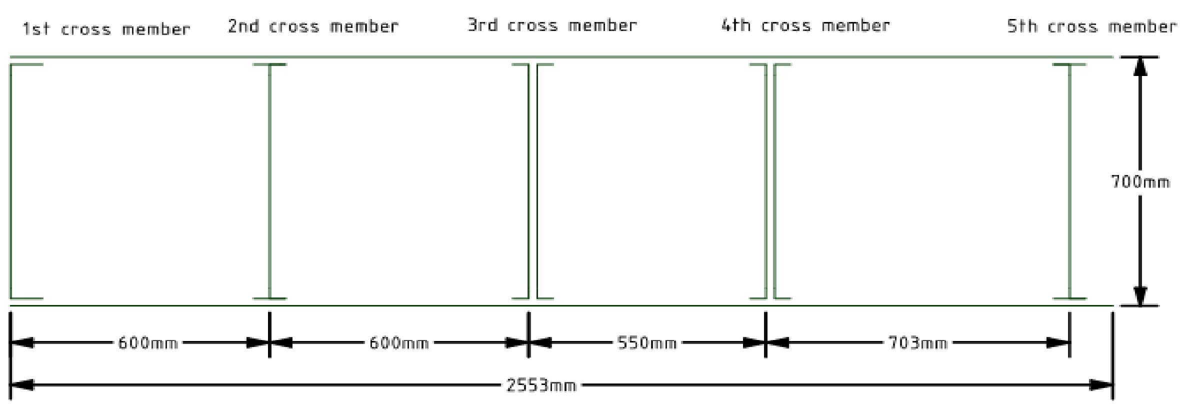

Figure 3. 1. Chassis frame specification and location of chassis cross-members

3.2.2. Location of loading components on the chassis frame

The different components of the vehicle that are engaged to the chassis frame are located as shown on the Figure 3.2 below.

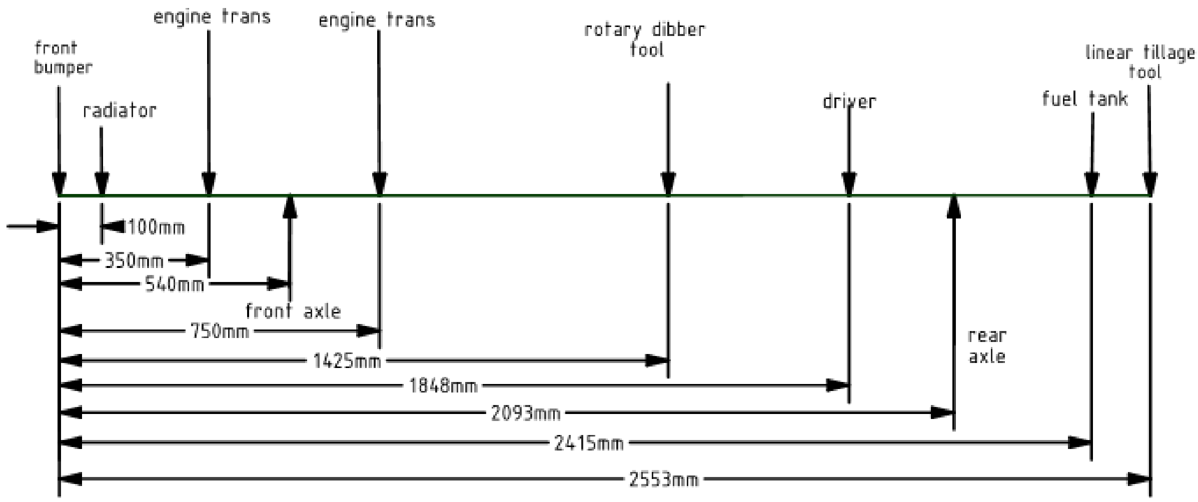

Figure 3. 1. Typical loading locations on chassis frame

3.3. Solid modeling

A solid model of an object is a clear and complete representation which provides more about the geometrical information of an object which enables to read unambiguously. The solid mode of both parts and assembly were done by ANSYS fluent 18.1 software.

3.3.1. Solid modeling of parts

The software used for solid modeling of this project is SCDM 18.1, a version of ANSYS fluent 18.1 which is simple to use and allows access to modify the dimensions and shapes of the object easily whenever required. All the parts required for frame construction are modeled by this software as shown on Figures 3.3 to 3.7 and the dimensions were modified according to the result of the analysis.

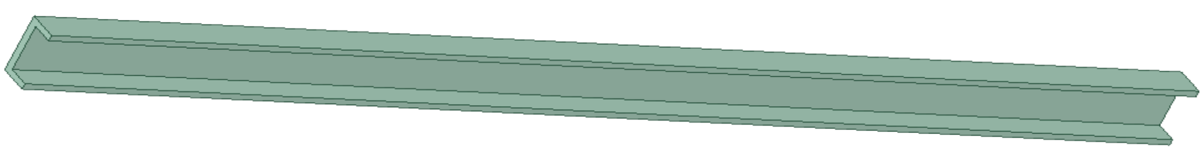

Figure 3. 2. Channel section main side member of the chassis frame

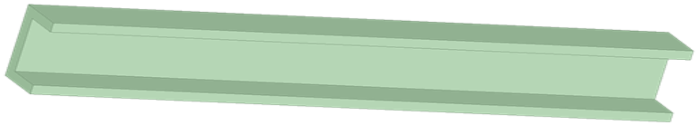

Figure 3. 3. First cross member

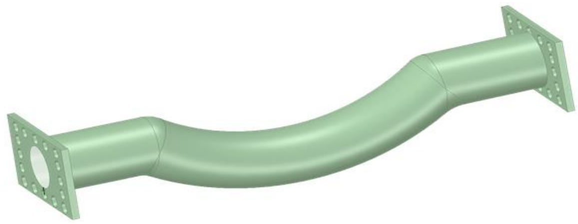

Figure 3. 4. Second crossmember

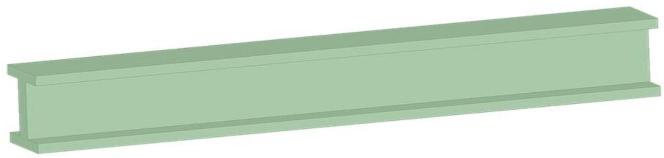

Figure 3. 5. Third and fourth cross member

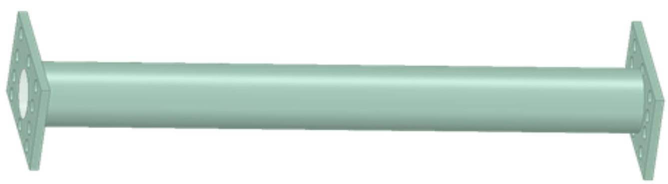

Figure 3. 6. Fifth cross-member

In addition to the above components gussets and connection plates show on Figures 3.8 and 3.9 are used for withstanding the stress induced at the connection between the main side member and each cross-members and to strengthen the joints.

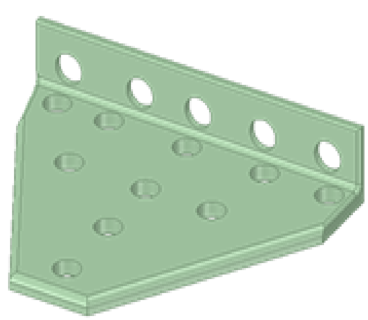

Figure 3. 7. I & C cross-section connection plate

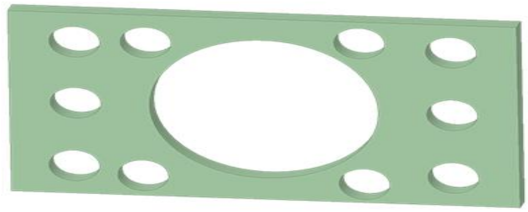

Figure 3. 8. 2nd & fifth connection plate

3.3.2. Assembly drawing

The components that are generated in the part are assembled with the same software. All components are assembled to give meaning full model shown on Figure 3.10 below for analysis.

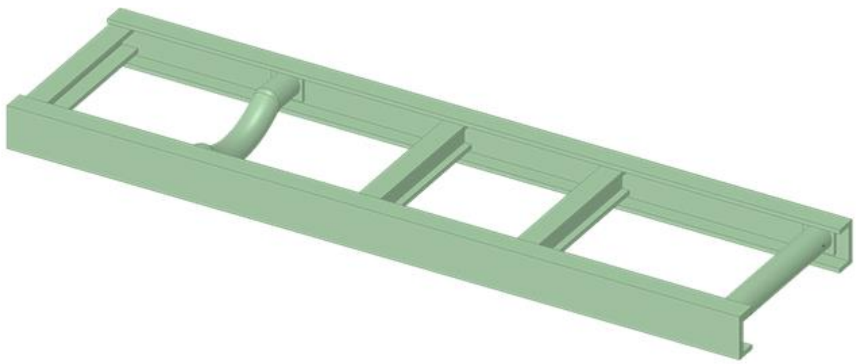

Figure 3. 9. Chassis frame assembly

3.4. Importing the solid model to ANSYS work bench

After assembling the parts on SCDM18.1, the model had been imported directly to ANSYS fluent 18.1 work bench for analysis. On this workbench, both static analysis such as bending analysis, torsional analysis and combined loading (bending and torsion) analysis and dynamic analysis such as impact and Modal analysis had been done.

Generally the methodology followed is concluded by a flow chart shown on Fig.3.11 bellow.

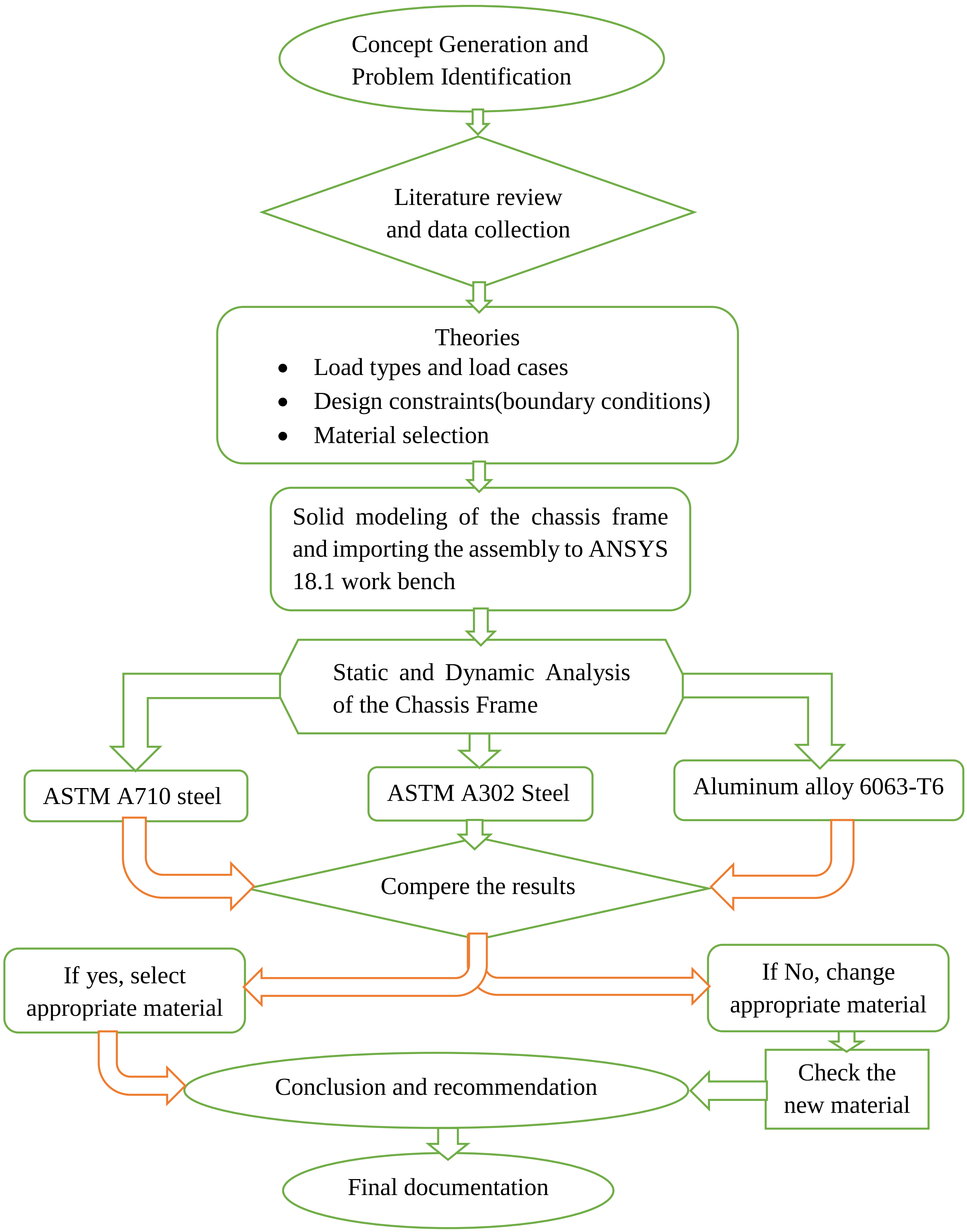

Figure 3. 10. Flow chart showing over all work flow of the thesis

3.5. Design and analysis

As per the objective of the project, static analysis and dynamic analysis are performed. Static analysis is done by assuming the vehicle as it is at rest. As stated on chapter two of this document, the vehicle is subjected to different load case such as bending loads, torsion loads and combination of these two load cases and other dynamic loadings caused as the vehicle traverses uneven ground and as the driver performs various maneuvers. The following five basic load cases are considered. So using finite element analysis commercial software (ANSYS), the response of the different loads on the chassis is analyzed for both static and dynamic load cases including the modal analysis.

3.5.1. Bending case

The bending conditions depend upon the weights of the major components of the vehicle. The first consideration is the static condition by determining the load distribution along the vehicle. The axle reaction loads are obtained by resolving forces and taking moments from the weights and positions of the components (i.e. the equations of statics). The structure can be treated as a two-dimensional beam as the vehicle is approximately symmetric about the longitudinal x-axis. Here the engine weight and corresponding power train components are taken from manuals.

The engine with its specification is taken from (Mahindra, 2017) tractor manuals. The loads taken for calculating axle reactions are in simplified form as follows

Engine = 9.53 N/mm

Bumper = 130 N

Radiator = 400 N

Rotary system = 550 N

Driver = 800 N

Fuel tank & exhaust system = 600 N and

Body weight = 339 kg/2253 mm = 1.5 N/mm

Having the above values, the front and rear axle loads R_A and R_B are 3986N and 5802N respectively and the location of center of gravity is 942 mm from the front axle.

Figure 3.12 below shows a typical list and types of the major components of the vehicle that are considered. The distributed loads are estimates of the weight per unit length for the engine and body of the vehicle. Other loads are approximated as point loads. The unsprang masses consisting of wheels, brake discs/ drums and suspension links are of course not included as they do not impose loads on the structure.

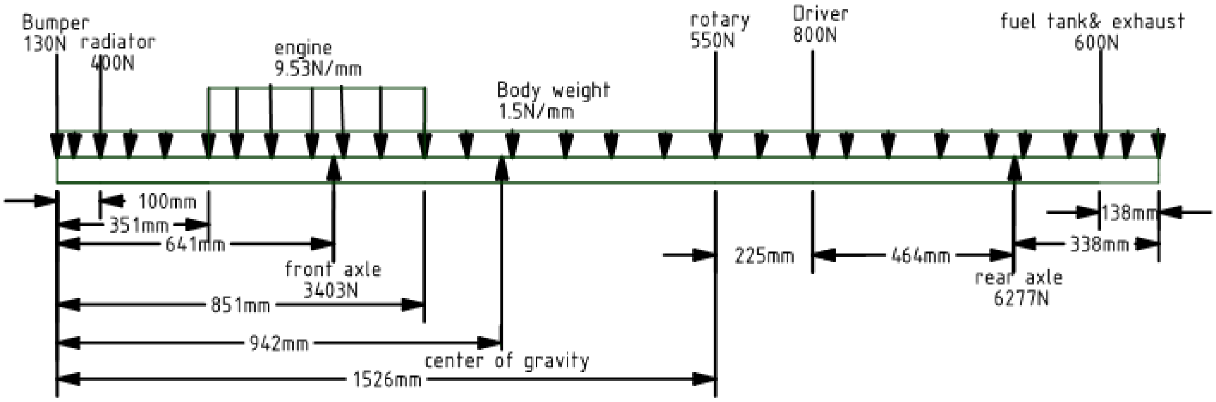

Figure 3. 11. Loads of the chassis frame

From the above Figure, the shear force diagram and bending moment diagram can be constructed in the normal way (using static analysis) as in Figure 3.13 and Figure 3.14 below. The Values taken from these diagrams can be used to determine stress conditions on a chassis frame.

Figure 3. 12. Shear force diagram of the chassis frame

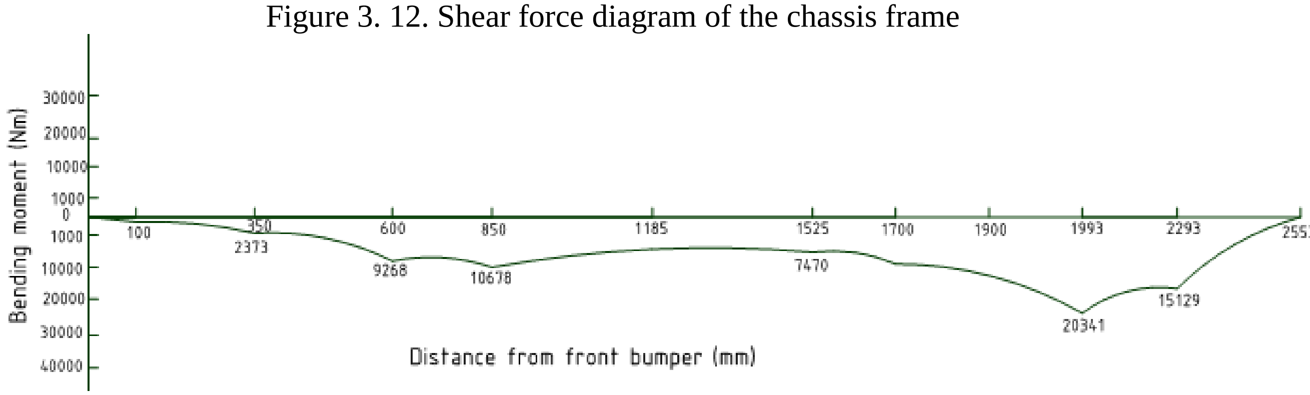

Figure 3. 13. Bending moment diagram of chassis frame

As shown on the Figures 3.13 and 3.14 above, both the shear force and bending moment, 4844N and 20341 Nm are found at rear axle. So this point is used to determine the thickness of the chassis frame. Since these loads are applied on both chassis frames, the shear force and bending moment applied for each chassis frame at the same point are 2422N and 10170.1Nm respectively.

3.5.2. Torsion case

The case of pure torsion can be considered simply as being applied at one axle line and reacted at the other axle. The condition of pure torsion cannot exist on its own because vertical loads always exist due to gravity, as mentioned in chapter two. However, for ease of calculation the pure torsion case is assumed. The vehicle body is subjected to a moment applied at the axle center lines by applying upward and downward loads at each axle in this case. These loads result in a twisting action or torsion moment about the longitudinal axis of the vehicle

The maximum torsion moment is based on the loads at the lighter loaded axle, and its value is the wheel load on that lighter loaded axle multiplied by the wheel track.

Torsion moment on the chassis frame due to reaction at front axle is given by:

$$T_F = \frac{R_F}{2} x \; t_f \qquad (3.6)$$

Where: t_f = front track

T_F =torsional moment of the chassis due to front axle reaction

R_F = front axle reaction

Substituting the values for equation 3.6, the value of torque is;

$$T_F = \frac{3986N}{2} \times 0.7m = 1395.1Nm$$

Once again this load is based on static reaction loads but dynamic factors in this case are typically 1.3 for road vehicles. For trucks and off road vehicles which often go off road 1.5 and for cross-country vehicles a factor of 1.8 may be used (Julian, 2002).

3.5.3. Combined bending and torsion

This represents the situation arising if one wheel of the lighter loaded axle is raised on a bump of sufficient height to cause the other wheel on that axle to leave the ground. (Julian, 2002) recommended that a maximum bump height of 200 mm should be considered as most cars have a suspension bump to rebound travel of 200 mm or less. The present writer considers the 200 mm bump height will lift the other wheel of the same axle off the ground. In this condition all the load of the lighter axle is applied to one wheel. If this principle is applied to the vehicle assuming the front track t_f = rear track t_r = 700 mm, the load on one wheel of the front axle will be the total axle load R_e=3986N, the torque on the body, T=2790.2Nm and R'_R is equal to R_e which is 3986N. This is because rear track is equal to the front track.

Resultant wheel loads at the rear axle are:

$$\text{Right wheel: } R_{RR} = \frac{R_R}{2} - \frac{R'_R}{2} \tag{3.7}$$

$$R_{RR} = 2901N - 1993N = 908N$$

$$\text{Left wheel: } R_{RL} = \frac{R_R}{2} + \frac{R'_R}{2} \tag{3.8}$$

$$R_{RL} = 2901N + 1993N = 4894\text{N}$$

If the left rear wheel had been lifted instead of the right front wheel, the same situation would have occurred, i.e. the left front wheel load will reduce to zero before the right rear wheel. Any further lifting of the left rear wheel (or right rear wheel) will not increase the torque applied to the vehicle structure.

3.5.4. Lateral loading

When cornering, lateral loads are generated at the tire to ground contact patches which are balanced by the centrifugal force $\frac{MV^2}{R}$where M is the vehicle mass, v is the vehicle forward speed and R is the radius of the corner. The worst possible condition occurs when the wheel reactions on the inside of the turn drop to zero, that is when the vehicle is about to roll over. In this condition the structure is subject to bending in the x–y plane. The condition approaching the roll-over depends upon the height of the vehicle center of gravity and the track. At this condition the resultant of the centrifugal force and the weight passes through the outside wheels contact patch.

3.5.5. Longitudinal loading

When the vehicle accelerates or decelerates, the mass times acceleration or inertia force is generated. As the center of gravity of the vehicle is above the road surface the inertia force provides a load transfer from one axle to another. While accelerating, the weight is transferred from the front axle to the rear axle and vice versa for the braking or decelerating condition. To obtain a complete view of all the forces acting on the body the heights of the centers of gravity of all components will be required. These are often not known, therefore a plot of bending moments along the vehicle is not obtainable. A simplified model considering one inertia force generated at the vehicle center of gravity can provide useful information about the local loading at the axle positions due to traction and braking forces.

3.6. Mass of the chassis and second moment of inertia

3.6.1. Mass of the chassis frame

The mass of an object is the fundamental physical quantity which is the measure of inertia of that object. Materials having good strength with lower mass are preferable for vehicle design which is directly related to the fuel consumption and hydrocarbon emission. Here the mass of the chassis frame is given for the three materials. The volumes of the chassis frame used for all the three materials are the same which are 2.1488×10^7 mm^3.

$$\text{Mass} = \text{volume} \times \text{density} \qquad (3.9)$$

By substituting the values for each material in equation 3.9 above;

A. Mass of ASTM A710 steel alloy

   Given the density of ASTM A710 = 7850kg/m^3

   M = 7850 kg/m^3 × 0.021488 m^3 = 168.7 kg

B. Mass of ASTM A302 steel alloy

   Given the density of ASTM A302=7790 kg/m^3

   M = 7790 kg/m^3 × 0.021488 m^3 = 167.4 kg

C. Mass of Aluminum 6063 T-6 Alloy

   Given the density of Aluminum 6063 T-6 Alloy =2800 kg/m^3

   M = 2800 kg/m^3 × 0.021488 m^3 = 60.17 kg

D. Mass of AISI 4140 steel alloy

   Given the density of ASTM A710 = 7850 kg/m^3

   M = 7835 kg/m^3 × 0.021488 m^3 = 168.4 kg

3.6.2. Area moment of inertia

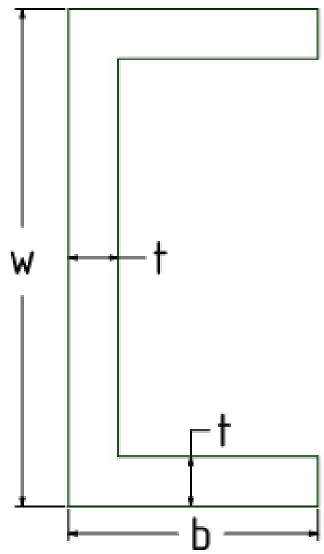

Figure 3. 14. Cross-sectional view of chassis frame

The second areal moment of inertia about the symmetrical (neutral axis), (I_{XX}) is given as follows:

$$I_{XX} = \frac{1}{12}(bw^3 - (b-t)(w-2t)^3) \tag{3.10}$$

Substituting 150 mm and 75 mm for w and b respectively in equation 3.10 above, we will get the second moment of inertia in terms of thickness, t as follows.

$$I_{XX} = \frac{1}{12}(-8t^4 - 270000t^2 + 10147500t)$$

$$(I_{XX})_{\text{channel section}} = \frac{1}{12}(-16t^4 + 4200t^3 + 9720000t^2 + 10125000t)$$

3.7. Allowable stress and bending stiffness

3.7.1. Allowable stress

The load conditions discussed in sections 3.5.1 to 3.5.5 results in stresses occurring throughout the vehicle structure. It is important that under the worst load conditions that the stresses induced into the structure are kept to acceptable limits.

Consideration of the static loads factored by an appropriate amount should give a stress level certainly below the yield stress. If the bending case for a vehicle is considered the maximum allowable stress should be limited as follows (Julian, 2002) and (Rutheravan, 2016) :

Stress due to static load × Dynamic Factor ≤ 2/3 ×Yield stress (3.11)

This means that under the worst dynamic load condition the stress should not exceed 67% of the yield stress. Alternatively, the safety factor against yield is 1.5 for the worst possible load condition. A similar criterion is applied to other load conditions.

3.7.2. Bending stiffness

The previous sections have considered loads and stresses and now there is a need to determine whether the structure is sufficiently strong. An equally important design requirement is to assess the structural stiffness; in fact, many designers consider stiffness is more important than strength. It is possible to design a structure which is sufficiently strong but yet unsatisfactory because it has insufficient stiffness. Designing for acceptable stiffness is therefore often more critical than designing for sufficient strength. The bending stiffness is determined by the acceptable limits of deflection.

3.8. Finite element analysis of the chassis frame

Structural analysis uses combination of the fields of applied mechanics, applied mathematics and material sciences to find the structure's physical phenomena such as internal forces, stresses and deformation of the structure which enables us to verify the structures fitness for specific use usually without physical tests.

3.8.1. Static Structural analysis of chassis for bending case

Static analysis calculates the effects of steady load conditions on a structure while ignoring inertia and damping effects, such as those caused by time varying loads (Rajappan and Vivekanandhan, 2013). is based on the condition that the vehicle is being stationary. The ladder chassis frame is treated as a simply supported beam and loads were due to weight of components applied to the beam. For practical calculations, it is recommended that the loads on the chassis frame including its own weight is concentrated at some points. These loads are equivalent to the actual distributed load carried by the vehicle. The stress distribution on the chassis for bending, torsion and combined bending and torsion load have been determined and the magnitude and direction of reaction loads are determined according to the equilibrium conditions for each case.

A linear finite element structural analysis of the ladder chassis finite element models under the vertical directional load was conducted with channel (C) cross-section chassis type. Four different types of materials, AISI 4140 steel, ASTM A710 Steel, ASTM A302 steel Alloy Steel and Aluminum Alloy 6063-T6 were used for analysis. The contour plots of Von Mises stress distribution, Maximum Stress and Deformation contours are shown on each static and dynamic analysis.

There are various steps that should be followed to do the analysis of the structure. The main steps that follows for static structural analysis are importing the model to ANSYS work bench, mesh generation, fixing supports and application of loads and solution evaluation. The thickness of the model imported to the ANSYS work bench was determined by using stress equation as follows:

The stress equation is given by: $\sigma = \frac{My}{I}$ (3.12)

Where: M = the bending moment,

y = the distance from the centroid axis and

I = the second areal moment of inertia.

Correspondingly the maximum stress is:

$$\sigma_{max} = \frac{M_{max} y_{max}}{I}.$$

Substituting $M_{max} = \frac{2341 \text{ Nm}}{2}$ from the bending moment diagram given on Figure, y_{max} = 75 mm and $I_{xx} = \frac{1}{12}(-8t^4 - 270000t^2 + 10147500t)$ for channel section, we can find the following formulas for σ_{max} .

$$\sigma_{max} = \frac{0.5 \times 2.341 \times 10^6\ Nmm \times 75\ mm}{\frac{1}{12}(-8t^4 - 270000t^2 + 10147500t)} = \frac{1.053 \times 10^9 N\ mm^2}{-8t^4 - 270000t^2 + 10147500t}$$

Having the above formulas for maximum stress, we can get the minimum thickness t of the chassis frame from the formula given below.

$$\frac{\sigma_{allow}}{\sigma_{max}} = F.S \qquad (3.13)$$

Where σ_{allow} *is awllowable stress for the material and* $F.S$ *is the factor of safety*

The Dynamic Loading must be considered as the vehicle traverses uneven road surfaces. The resulting impact of the vehicle returning to earth is cushioned by the suspension system but inevitably causes a considerable increase in loading over the static condition. Experience gained by vehicle manufacturers indicates that the static loads should be increased by factors of 2.5 to

3.0 for road going vehicles but off-road or cross-country vehicles may be designed with factors of 4 (Julian, 2002).

Since agricultural vehicles are off-road vehicles, a dynamic factor of 4 is used for pure bending and the above equation will be:

$$\frac{\sigma_{allow}}{4\times\sigma_{max}} = F.S \tag{3.14}$$

For all of the three materials the compressive allowable stresses are lower than the tensile allowable stresses. So finding the thickness of the chassis by using the compressive allowable stresses is better.

Substituting the values on the above formula gives the following values.

a. ASTM A710 steel alloy

$$\frac{450Mpa\times(-8t^4-270000t^2+10147500t)}{4\times1.053\times10^9 N/mm^2} = 1.5$$

$$-8t^4 - 270000t^2 + 10147500t = 4.804 \times 10^7$$

$t =$ (-33788, 6, 32)

b. ASTM A302 steel alloy

$$\frac{340\ MPa\times(-8t^4-270000t^2+10147500t)}{4\times1.053\times10^9\ N/mm^2} = 1.5$$

$$-8t^4 - 270000t^2 + 10147500t = 6.258 \times 10^7$$

$t =$ (-33788, 8.0, 30) mm

c. Aluminum alloy T6063

$$\frac{250MPa\times(-8t^4-270000t^2+10147500t)}{4\times1.053\times10^9\ N/mm^2} = 1.5$$

$$-8t^4 - 270000t^2 + 10147500t = 6.878 \times 10^7$$

t = (-33788, 8.5, 29) mm

From the solution of the above equations, the lowest positive rational number of each equation in each of all the cases will be the probable thickness of the chassis used for further analysis i.e. for both static and dynamic analysis. Here the values are nearly equal for all the three materials and aluminum alloy is the lowest strength material and its minimum thickness value is 8.5 mm.

3.8.2. Importing the model to ANSYS workbench

The model of chassis is done with ANSYS SCDM18.1 which can be directly imported into ANSYS workbench. The model imported to ANSYS workbench is shown in Figure 3.16 below.

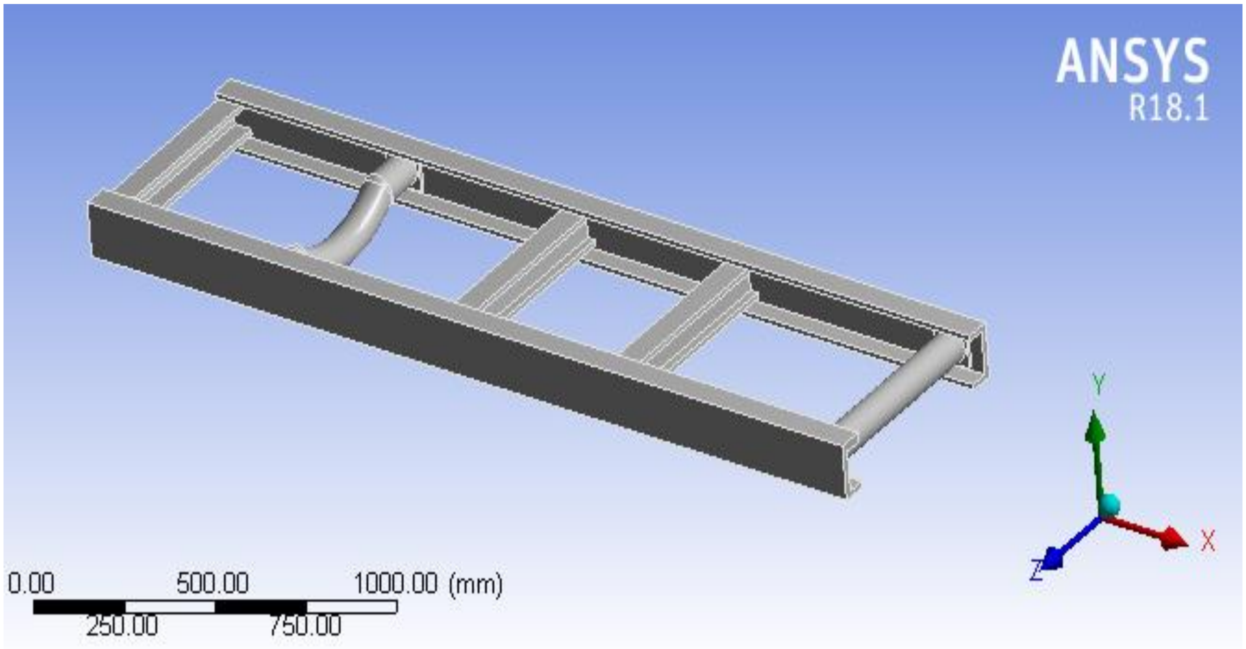

Figure 3. 15. The imported model of the chassis frame

3.8.3. Meshing and boundary conditions

The meshing is done on the model with 25613 number of nodes and 12857 numbers of elements. The chassis model is loaded by static forces from the vehicle body and load. For this model, the maximum loaded weight of vehicle is 9788 N. The load is assumed as a concentrated load at the center of gravity of chassis frame and the reaction forces are taken at the two axels. The finite element model of the chassis with generated mesh and boundary conditions is shown in Figure 3.17 and 3.18 below.

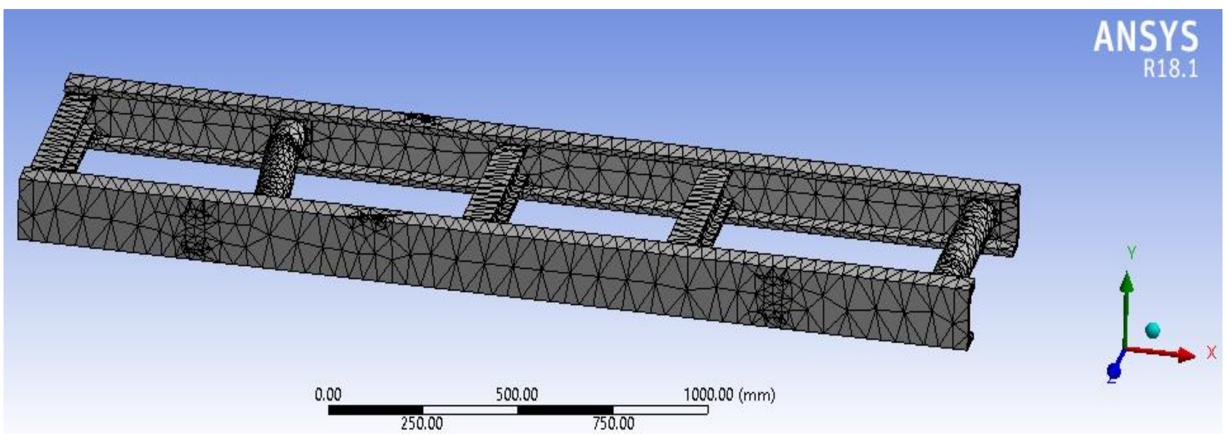

Figure 3. 16. Meshing of the model

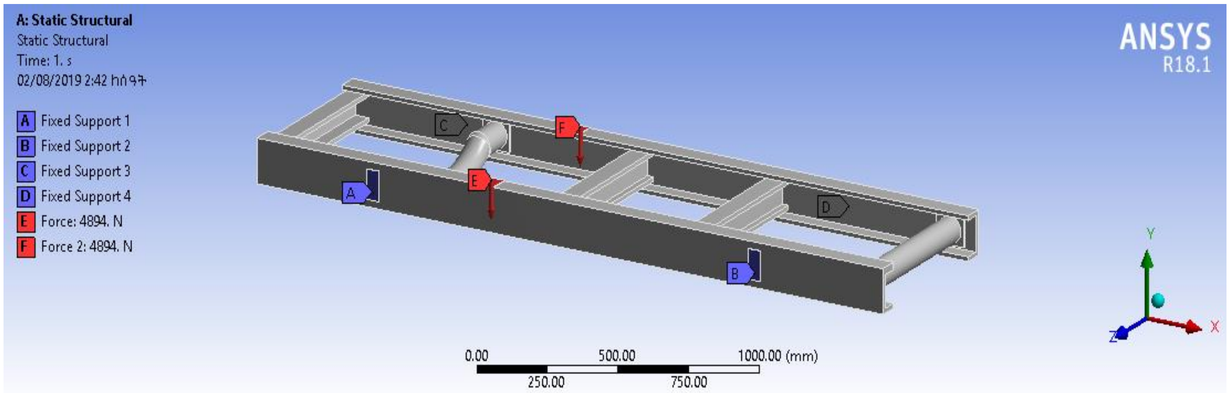

Figure 3. 17. Boundary condition of the chassis frame

3.8.4. Equivalent (Von-Mises) stress distribution and deformation for bending case

A. Von misses stress distribution for ASTM A710 steel alloy

As shown on the Figure 3.19 below, the maximum equivalent (Von Mises) stress is 78.466 MPa and its minimum value is 0.002667 MPa.

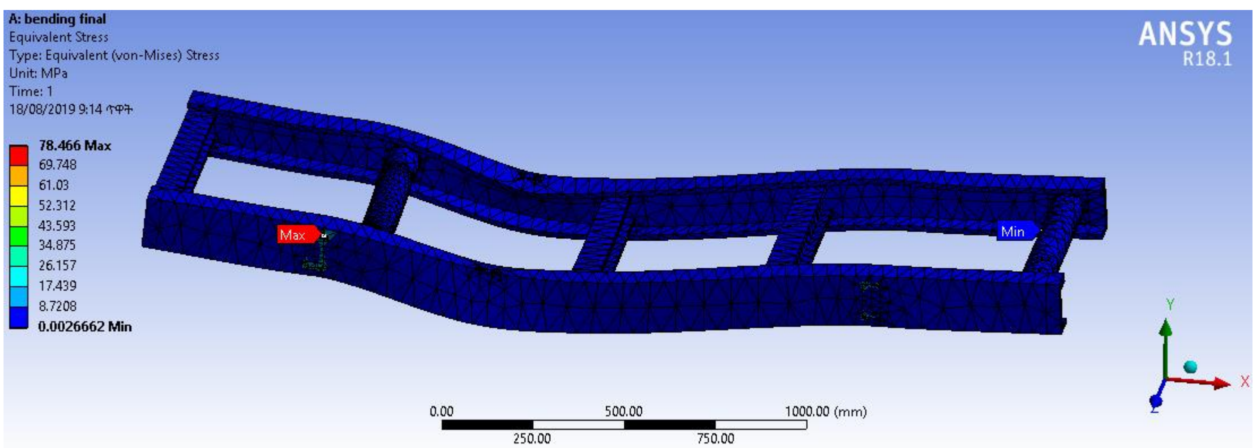

Figure 3. 18. Von misses stress distribution for AISI A710 steel alloy

B. Total Deformation contour of ASTM 710 steel alloy

When an object is subjected to different types of loads, its shape may be changed either temporarily or permanently due to the applied load. This change in shape is called deformation and if the object deforms permanently, it is called plastic deformation and failure happens. On the other side if the structure deforms temporarily, the structure will regain its original shape when load is released which is called elastic deformation. The maximum total deformations of ASTM 710 steel alloy is 0.0467mm as shown on Figure 3.20.

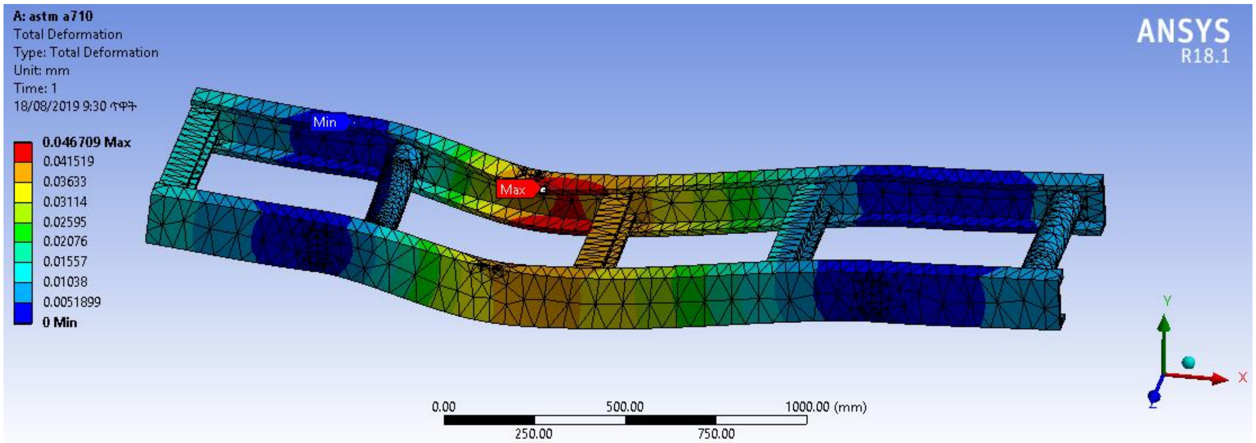

Figure 3. 19. Deformation contour of ASTM A710 steel alloy

C. Von misses stress distribution for ASTM A302 steel alloy

The FEA of the bending analysis showed that maximum equivalent (Von Mises) stress is 78.353 MPa located between the second and third cross member and its minimum value is 0.002355 MPa as shown on the Figure 3.21 below.

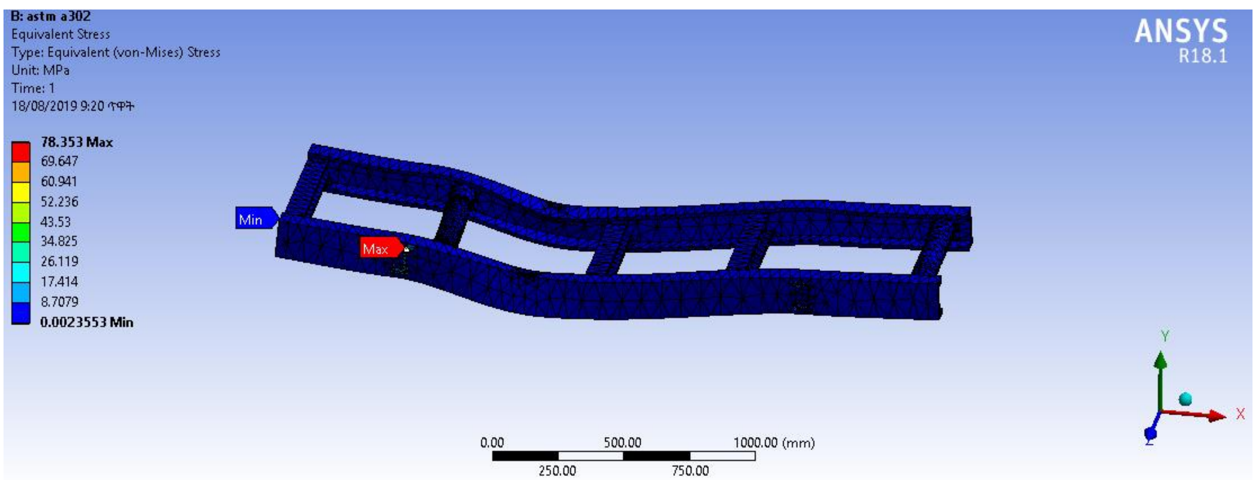

Figure 3. 20. Von misses stress distribution for ASTM 302 steel alloy

D. Total Deformation contour of ASTM A302 steel alloy

The FEA result for bending showed the following result which has almost negligible deformation value.

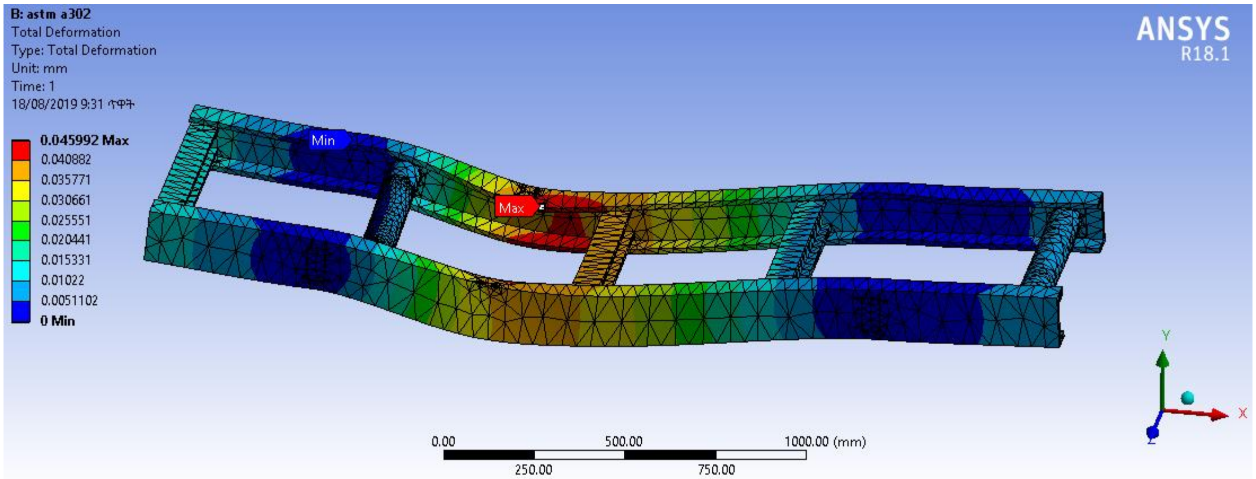

Figure 3. 21. Deformation contour of ASTM 302 steel alloy

E. Von misses stress distribution for aluminum 6063 T-6 alloy

The maximum equivalent (Von Mises) stress and its minimum value for 6063 T-6 aluminum alloy are78.36Mpa and 0.00266 Mpa respectively as shown on the Figure 3.23 below.

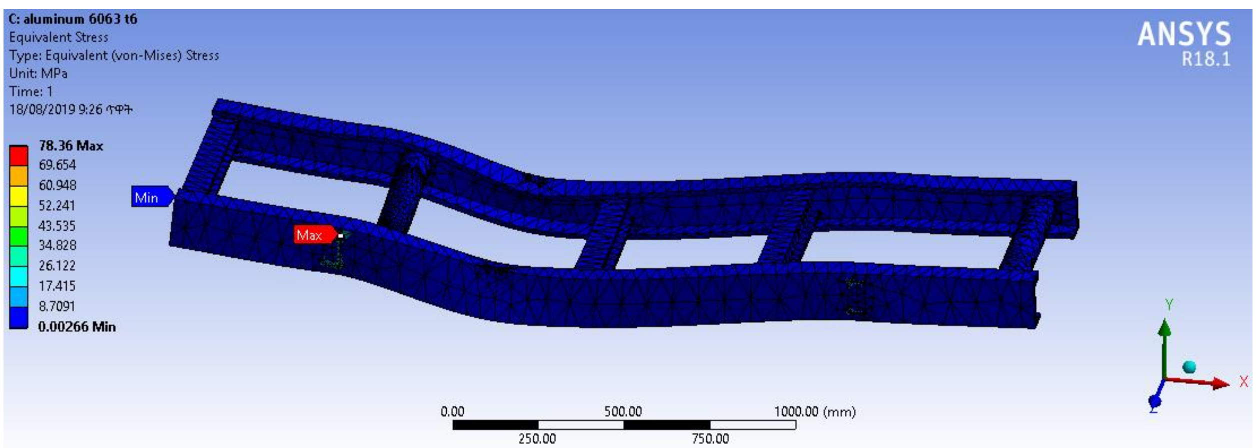

Figure 3. 22. Von misses stress distribution for aluminum 6063 T-6 alloy

F. Deformation contour of aluminum 6063 T-6 alloy

The deformation contour of aluminum alloy showed that its maximum value is greater than both of the steel alloys and located at the point where maximum equivalent stress exists on as shown on Figure 3.24 below.

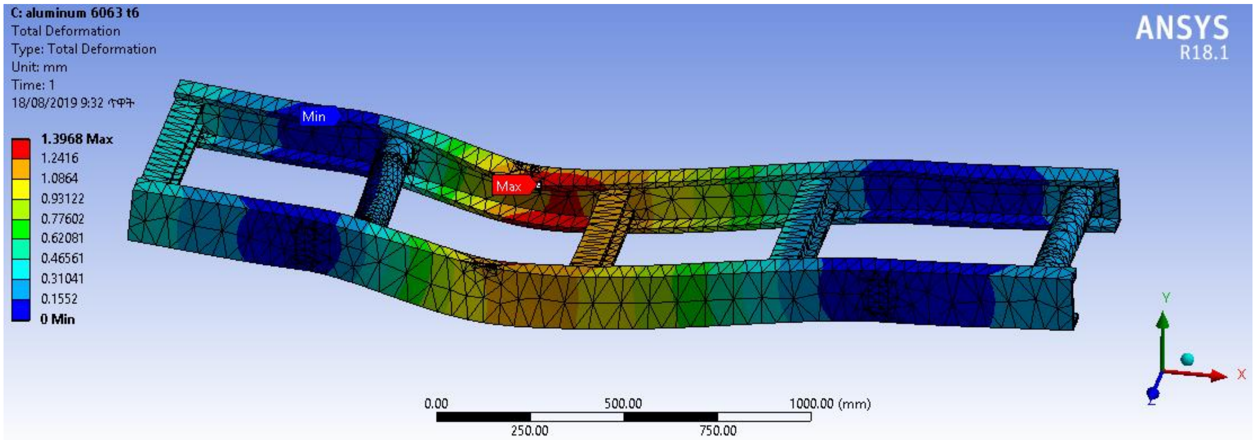

Figure 3. 23. Deformation contour of aluminum 6063 T-6 alloy

4.8.5. Torsional load case

This simulation is based on the condition where by one of the vehicle's wheel rests on a bump where as other three wheels are on the level road causing torsional moment on the chassis about the longitudinal axis. Even if pure torsion does not exist without bending it is important to show its effect on the structure separately. Assume that the front right wheel is at the bump, the torque T reaches maximum when this right wheel lifts off, i.e., when P_R=0.the front axle is the lightest axel having a load of 3986 N. The torque T is given by:

$$T = P_{axle} \times \frac{b}{2} = 3986\ N \times 0.35\ m = 1395.1\ Nm$$

A. Application of load and boundary condition for torsion case

As described above the front right wheel of the vehicles rests on a bump whereas, other three wheels are on the level road causing torsional moment on the chassis about the longitudinal axis. The three wheels are considered not to have both translation and rotational motion at the moment.

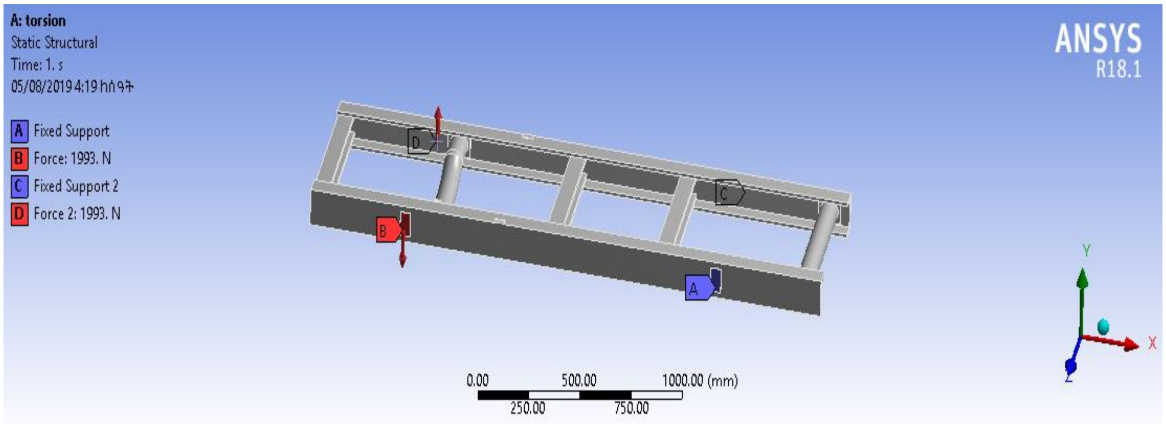

Figure 3. 24. Meshing and boundary condition

B. Von misses stress distribution and deformation contour for ASTM A710 steel alloy

The maximum equivalent (Von Mises) stress is and its deformation value for ASTM A710 steel alloy for torsional loads are 161.76 MPa and 0.8156 mm respectively as shown on the Figures 3.26 and 3.27 below.

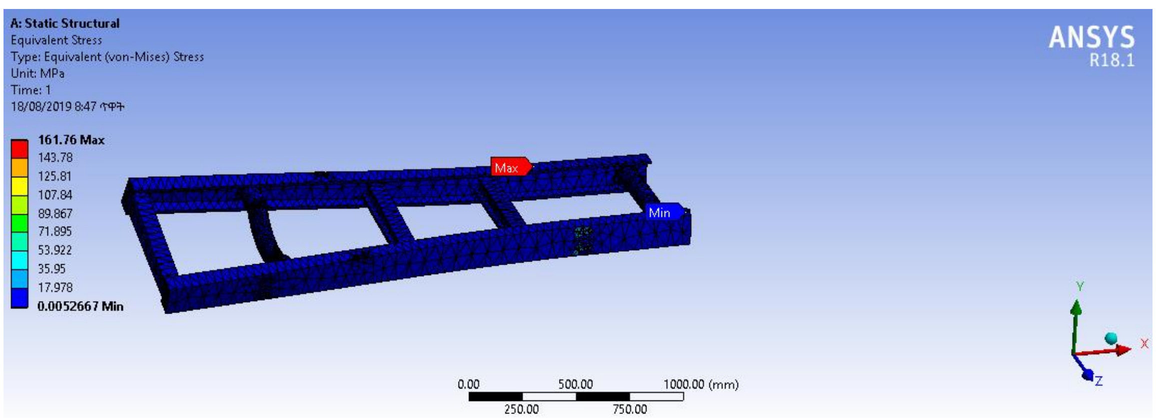

Figure 3. 25. Von misses stress distribution for ASTM A710 steel alloy

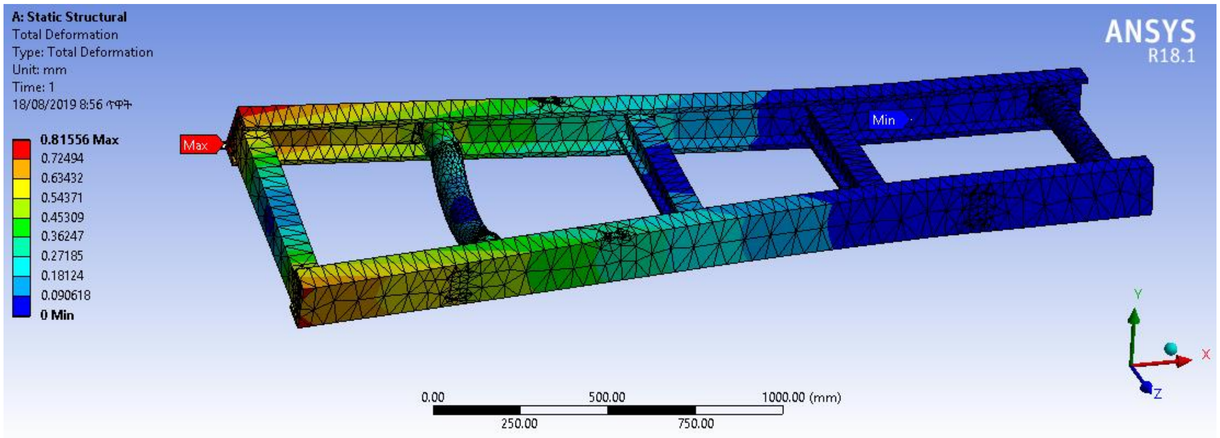

Figure 3. 26. Deformation contour of ASTM 710 steel alloy

C. Von misses stress distribution and deformation contour for ASTM A302 steel alloy

The maximum equivalent (Von Mises) stress and its maximum deformation value are 163.64 MPa and 0.807 mm respectively as shown on Figures 3.28 and 3.29.

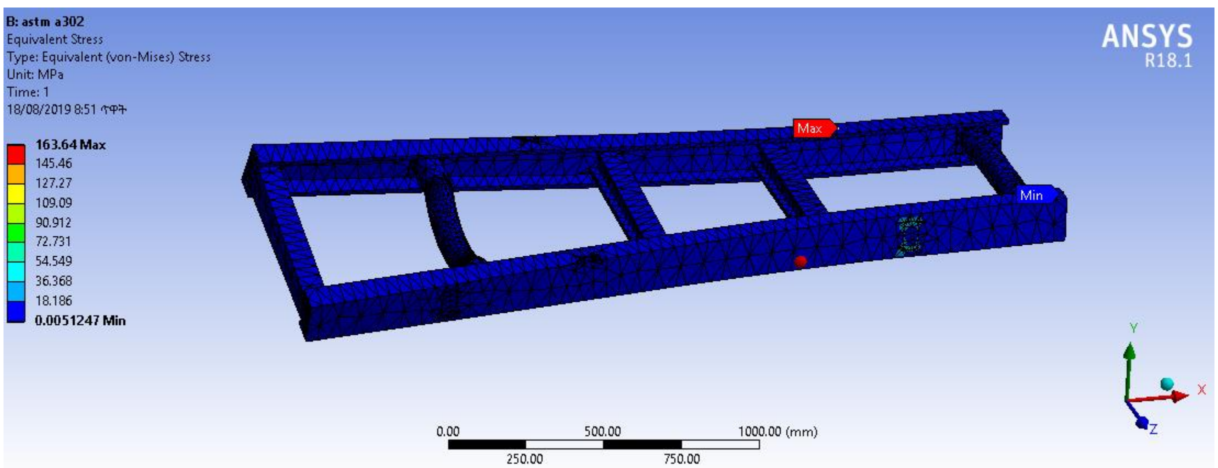

Figure 3. 27. Von misses stress distribution for ASTM A302 steel alloy

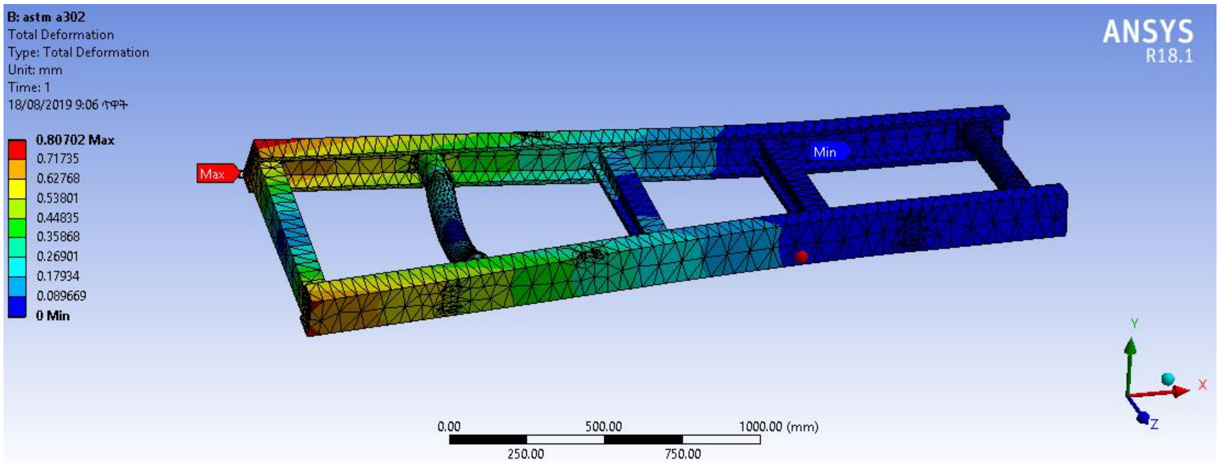

Figure 3. 28. Deformation contour of ASTM 302 steel alloy

D. Von misses stress distribution and deformation contour for aluminum 6063 T-6 alloy

The maximum equivalent (Von Mises) stress is 163.1 MPa and its minimum value is 0.005155 MPa as shown on Figure 3.30. The maximum deformation is 24.48 mm and found at the front right corner of the chassis frame as shown on figure 3.31.

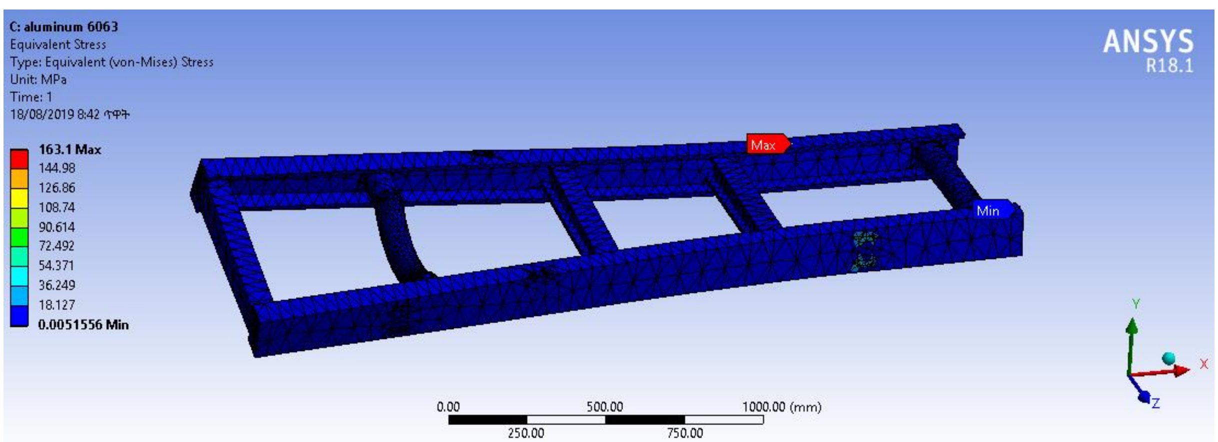

Figure 3. 29. Von misses stress distribution for aluminum 6063 T-6 alloy

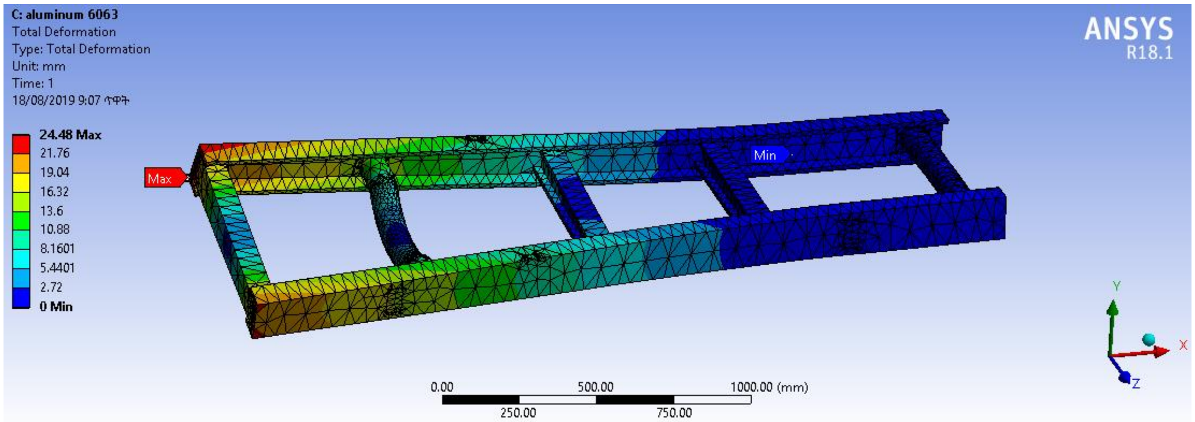

Figure 3. 30. Deformation contour of aluminum 6063 T-6 alloy

3.8.6. Combined bending and torsion case

This represents the situation arising if one wheel of the lighter loaded axle is raised on a bump of sufficient height to cause the other wheel on that axle to leave the ground without ignoring the effect of vehicle weight. If the left wheel of the front axle is on the bump, the load on the right wheel of the front axle will be the total axle load R_e=3986 N, the torque on the body 2790.2 Nm and R'_R is equal to R_e which is 3986 N. This is because rear track is equal to the front track. Resultant wheel loads at the rear axle are:

Right wheel: $R_{RR} = \frac{R_R}{2} - \frac{R'_R}{2} = 2901\ N - 1993\ N = 908\ N$

Left wheel: $R_{RL} = \frac{R_R}{2} + \frac{R'_R}{2} = 2901\ N + 1993\ N = 4894\ \text{N}$

If the left front wheel had been lifted instead of the right rear wheel, the same situation would have occurred, i.e. the left rear wheel load will reduce to zero before the right front wheel as shown on Figure 3.32. Any further lifting of the left front wheel (or right rear wheel) will not increase the torque applied to the vehicle structure.

A. Application of load and boundary condition for combined bending and torsion case

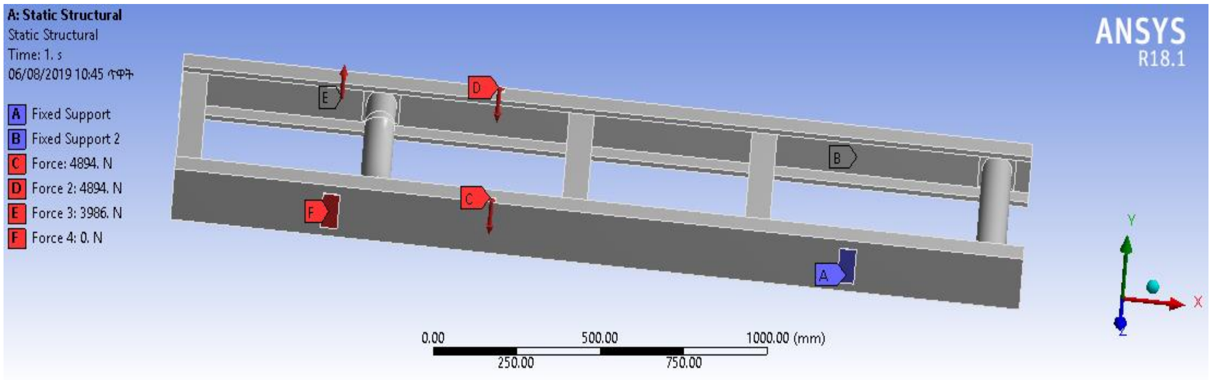

Figure 3. 31. Boundary condition of combined loading

B. Von misses stress distribution for ASTM A710 steel alloy

The maximum equivalent (Von Mises) stress is 325.38 MPa and its minimum value is 0.002764 MPa as shown on Figures 3.33 and 3.34 respectively.

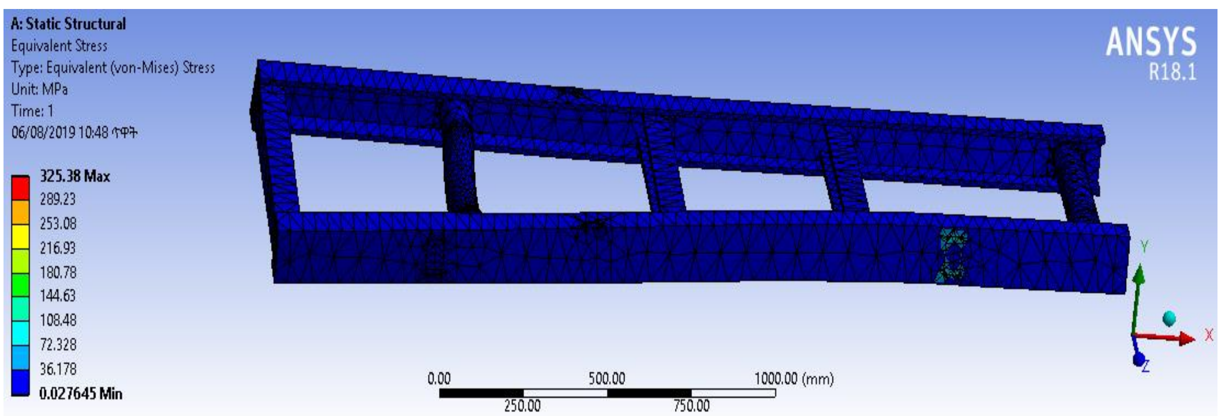

Figure 3. 32. Von misses stress distribution for ASTM 710 steel alloy

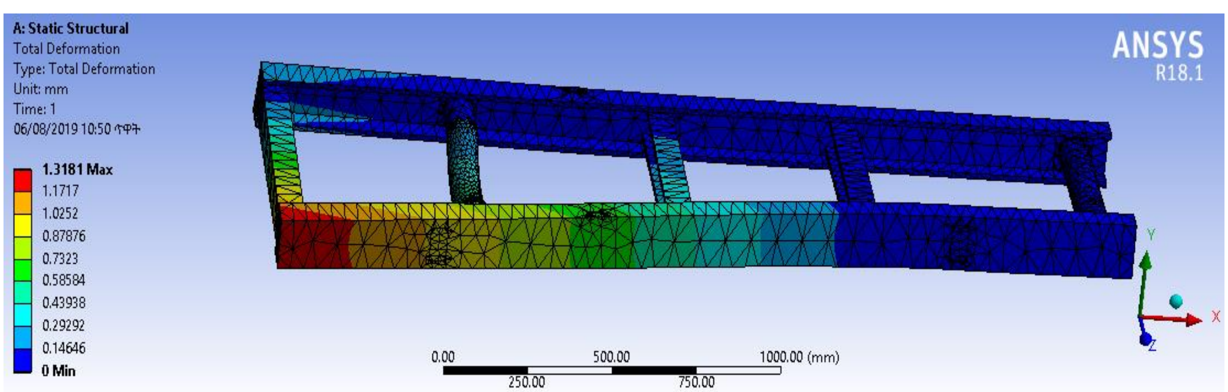

Figure 3. 33. Deformation contour of ASTM A710 steel alloy

C. Von misses stress distribution and deformation for ASTM A302 steel alloy

The maximum equivalent (Von Mises) stress is 327.14 MPa and its maximum deformation value is 1.3007mm as shown on Figures 3.35 and 3.36 below.

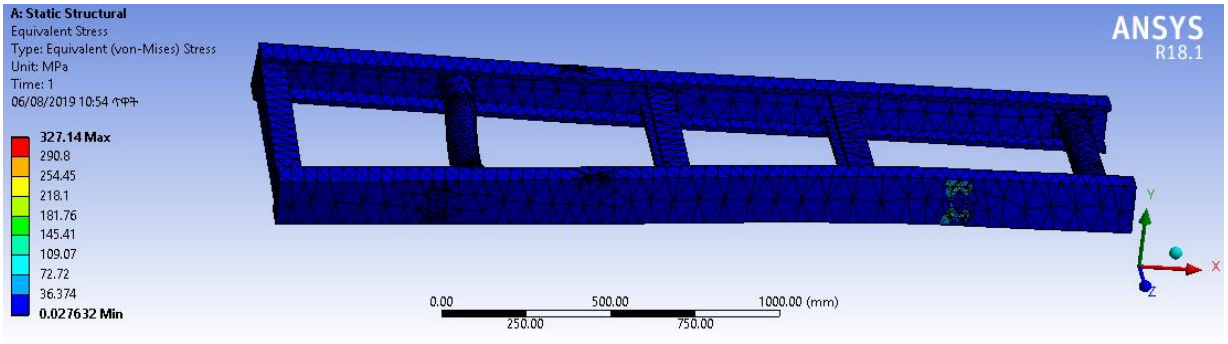

Figure 3. 34. Von misses stress distribution for ASTM 302 steel alloy

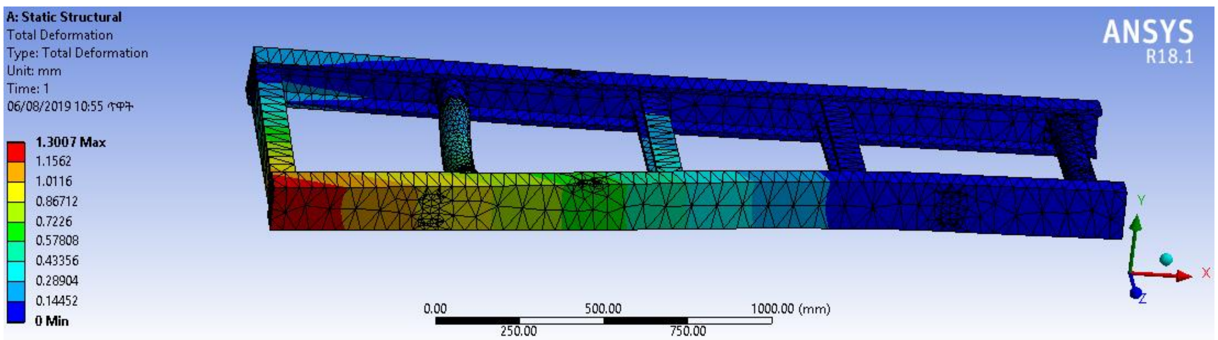

Figure 3. 35. Deformation contour of ASTM A302 steel alloy

D. Von misses stress distribution and deformation contour for aluminum 6063 T-6 alloy

The maximum equivalent (Von Mises) stress is 326.65 MPa and its maximum deformation value is 39.582 mm as shown on Figures 3.37 and 3.38 below.

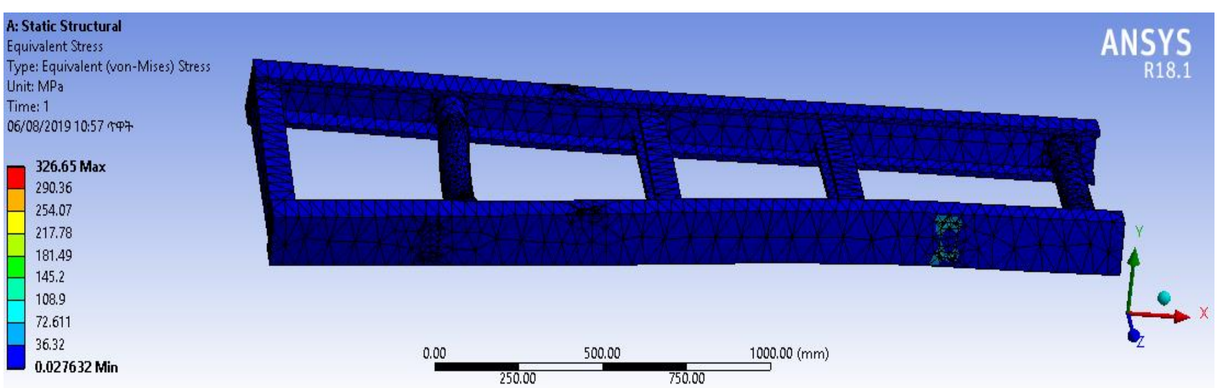

Figure 3. 36. Von misses stress distribution for aluminum 6063 T-6 alloy

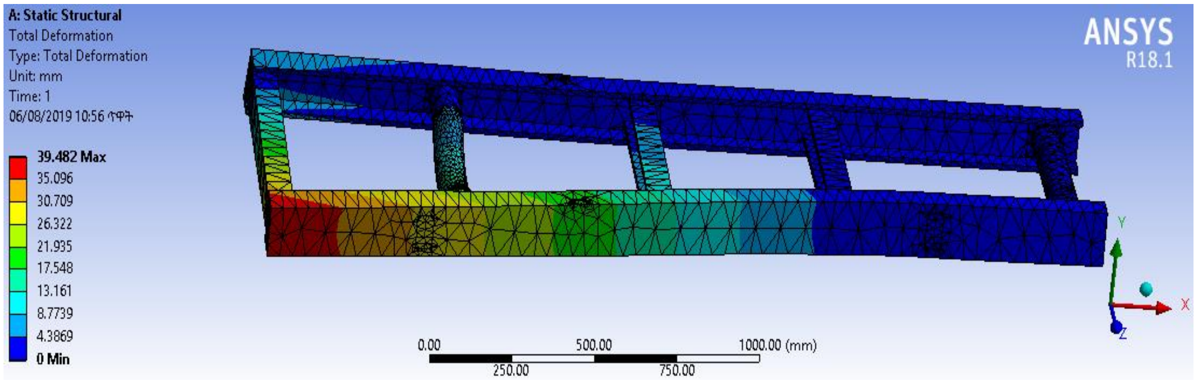

Figure 3. 37. Deformation contour of aluminum 6063 T-6 alloy

3.9. Dynamic analysis of the chassis frame

Today's automobile manufacturers are increasingly using lightweight materials to reduce weight. These include composites, aluminum, magnesium and new types of high strength steels. Many of these materials have limited strength or ductility, in each case rupture is a serious possibility during the crash event. Furthermore, the joining of these materials presents another source of potential failure. Both material and joining failure will have serious consequences on vehicle crashworthiness and must be predicted (Rajappan and Vivekanandhan, 2013).

As the dynamic behavior of structural members is different from the static one, the crashworthiness of the vehicle structures has to be assessed by impact analysis. Hence it becomes necessary to check the car structure for its crash ability so that safety is achieved together with the fuel economy. There are two ways by which this safety feature can be assessed.

a. Performing an actual crash test.
b. Simulating the crash in some FE code

Though the first option is more accurate and reliable, it demands time and high cost. A more practical solution which results in a compromise between the factors of accuracy, cost and time is simulation. With appropriate initial conditions, loads and element formulations, engineers can develop a precise enough FE model to judge the crash response in an actual accident. This technique has superseded the testing using an actual model. Thus computer simulations are used to find the automobile model's crash ability.

ANSYS explicit dynamics engineering simulation solutions are ideal for simulating physical events that occur in a short period of time and may result in material damage or failure. These types of events are often difficult or expensive to study experimentally. Simulation provides insight and a detailed understanding of the fundamental physics taking place and gives engineers a chance to make necessary changes before their products are put into service, when mistakes in design can be costly. Explicit dynamics analysis is used to determine the dynamic response of a structure due to stress wave propagation, impact or rapidly changing time-dependent loads. Momentum exchange between moving bodies and inertial effects are usually important aspects of the type of analysis being conducted. This type of analysis can also be used to model mechanical phenomena that are highly nonlinear.

3.9.1. Impact analysis

In an Explicit Dynamics solution the model preparation steps are: a discretized domain (mesh), assigned material properties, loads, constraints and initial conditions. This initial state, when integrated in time, will produce motion at the node points in the mesh.

- The motion of the node points produces deformation in the elements of the mesh
- The deformation results in a change in volume (hence density) of the material in each element
- The rate of deformation is used to derive material strain rates using various element formulations
- Constitutive laws take the material strain rates and derive resultant material stresses
- The material stresses are transformed back into nodal forces using various element formulations
- External nodal forces are computed from boundary conditions, loads and contact (body interaction)
- The nodal forces are divided by nodal mass to produce nodal accelerations and accelerations are integrated explicitly in time to produce new nodal velocities.
- The nodal velocities are integrated Explicitly in time to produce new nodal positions
- The solution process (Cycle) is repeated until a user defined time is reached

A. ***Meshing and boundary conditions***

The meshing is done on the model with 20077 number of nodes and 10813 numbers of elements. The chassis model is loaded by static forces from the vehicle body and load. For this model, the maximum loaded weight of vehicle is 9788N. The load is assumed as a concentrated load at the center of gravity of chassis frame and the reaction forces are taken at the two axels. The finite element model of the chassis with generated mesh and boundary conditions is shown in Figure 3.39 and 3.40 below.

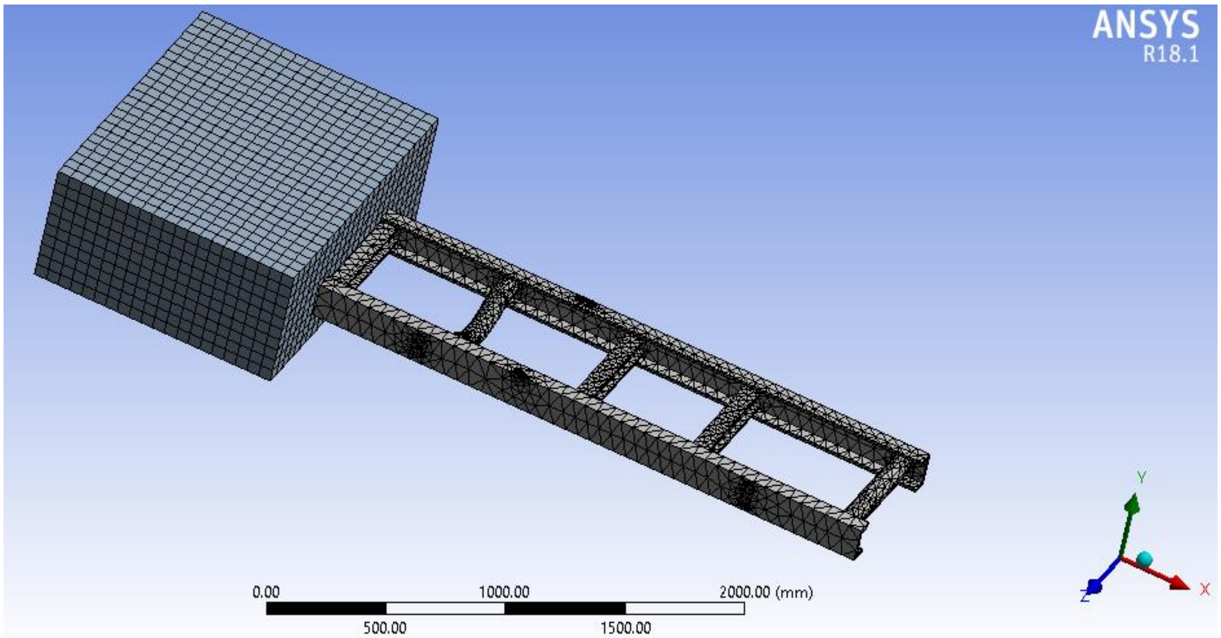

Figure 3. 38. Mesh generation for impact analysis

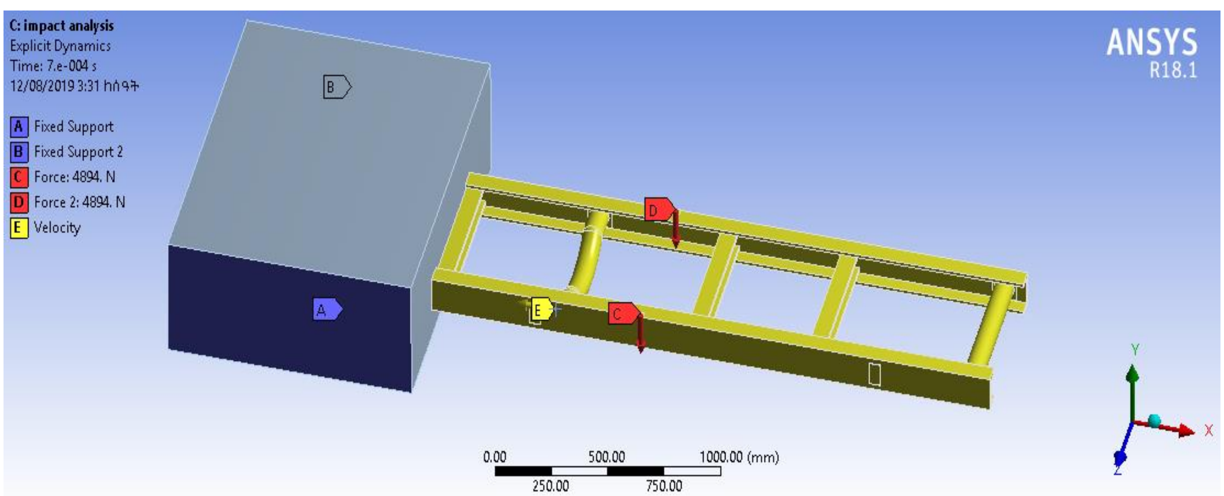

Figure 3. 39. Boundary condition for impact analysis

B. Von misses stress distribution for ASTM A710 steel alloy

The maximum equivalent (Von Mises) stress is 724.53MPa and its maximum deformation value 1.777 mm as shown on Figures 3.41 and 3.42 below.

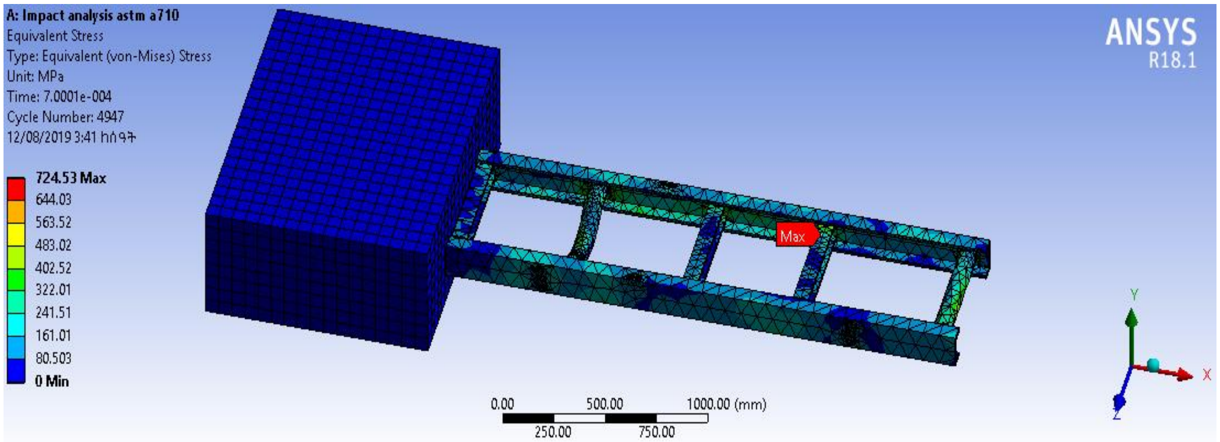

Figure 3. 40. Von misses stress distribution of ASTM A710 steel alloy

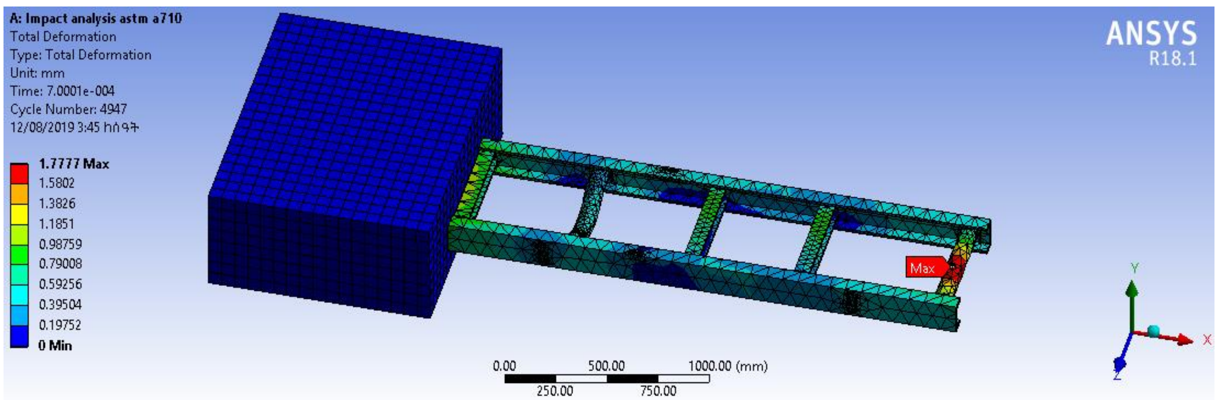

Figure 3. 41. Deformation contour of ASTM A710 steel alloy

C. Von misses stress distribution and deformation for ASTM A302 steel alloy

The maximum equivalent (Von Mises) stress is 712.18 MPa and its maximum deformation value 1.7504 mm as shown on Figures 3.43 and 3.44 below.

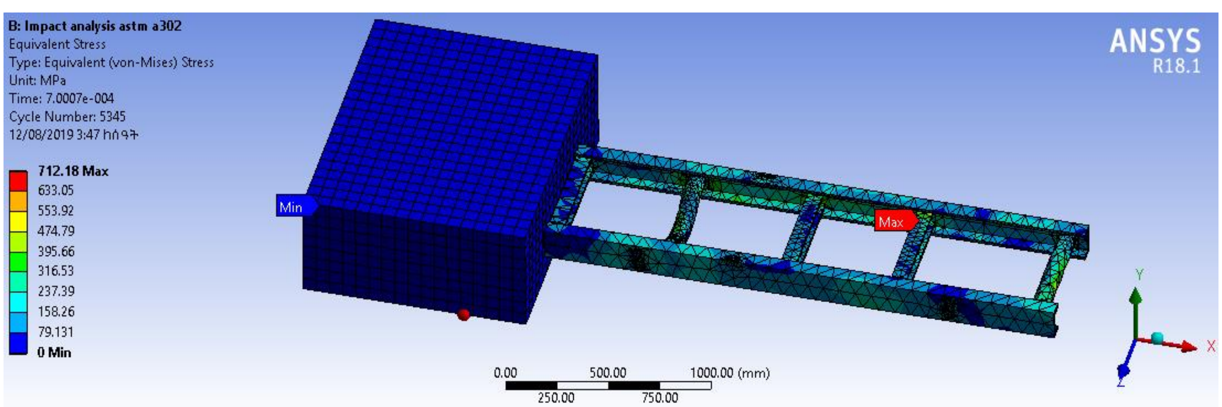

Figure 3. 42. Von misses stress distribution for ASTM A302 steel alloy

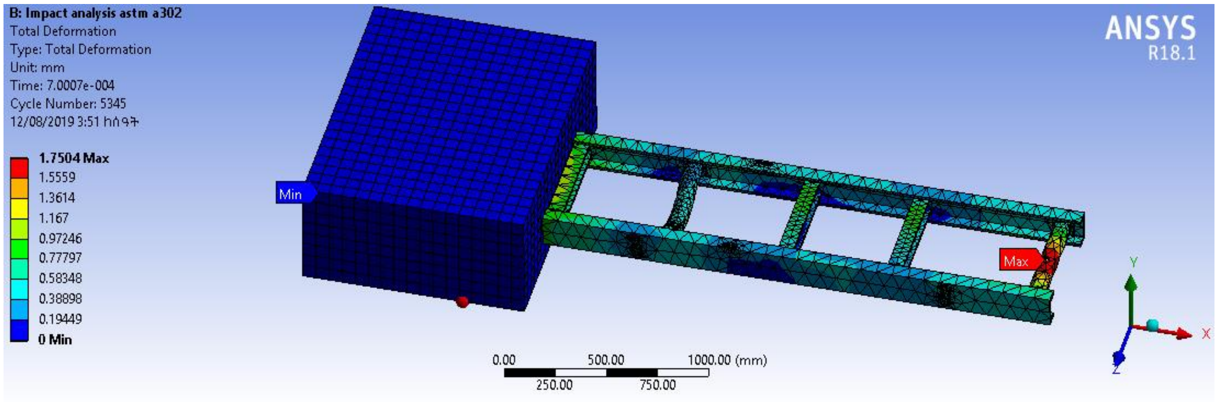

Figure 3. 43. Deformation contour of ASTM A302 steel alloy

D. Von misses stress distribution for AISI 4140 steel alloy

The maximum equivalent (Von Mises) stress is 626.5 Mpa and its maximum deformation value 1.7956 mm as shown on Figures 3.45 and 3.46 below.

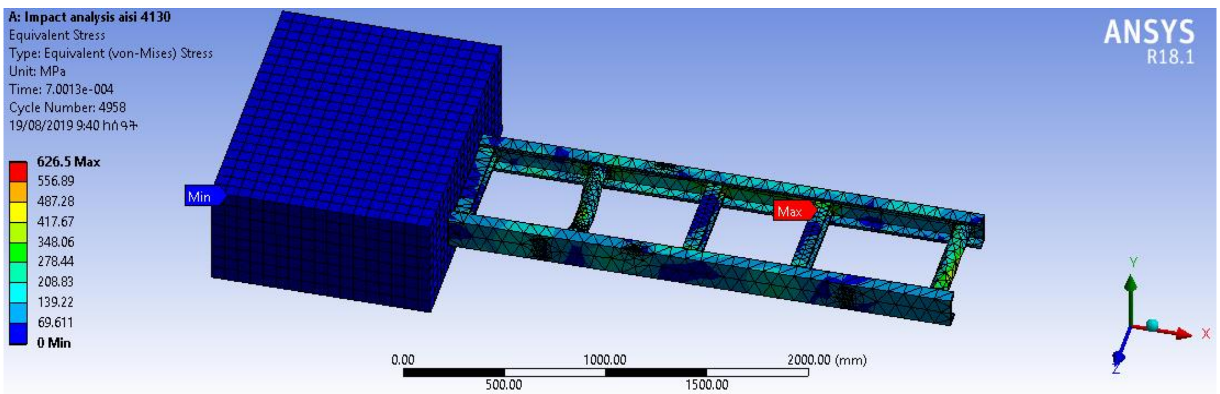

Figure 3. 44. Von misses stress distribution for AISI 4140 steel alloy

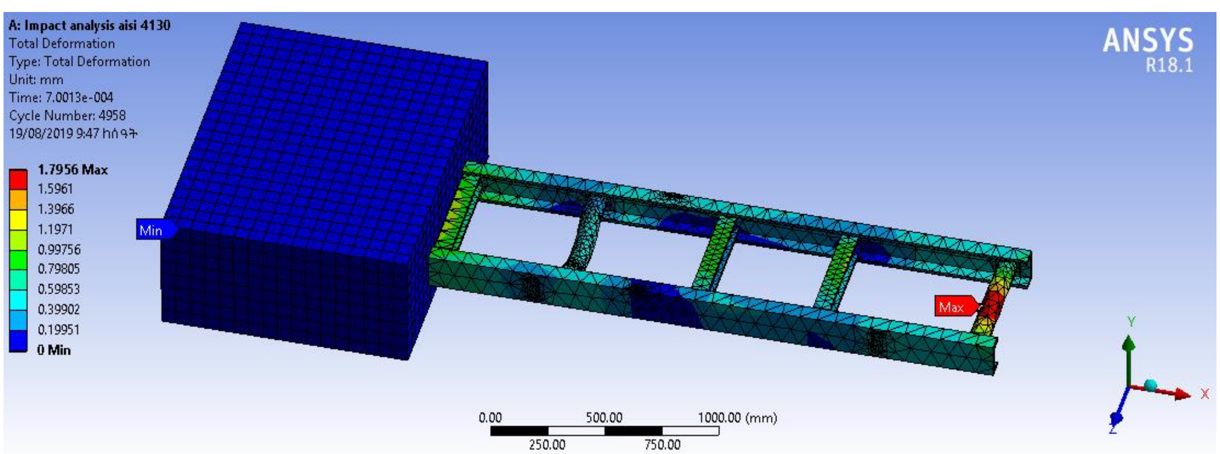

Figure 3. 45. Deformation contour of AISI 4130 steel alloy

3.9.2. Modal analysis

The chassis frame provides necessary support to the vehicle components placed on it. Also the frame should be strong enough to withstand shock, twist, vibrations and other stresses. The chassis frame consists of side members attached with a series of cross members. Stress analysis using Finite Element Method (FEM) can be used to locate the critical point which has the highest stress. This critical point is one of the factors that may cause the fatigue failure. The magnitude of the stress can be used to predict the life span of the chassis. The accuracy of prediction of life of the chassis is depending on the result of its stress analysis (Patel et al., 2012).

Modal analysis is a powerful tool to identify the dynamic characteristics of structures. Every structure vibrates with high amplitude of vibration at its resonant frequency. If any of the excitation frequencies coincides with the natural frequencies of the chassis, then resonance phenomenon occurs and the chassis will undergo dangerously large oscillations, which may lead to excessive deflection and failure. The vibration of the chassis will also cause high stress concentrations at certain locations, fatigue of the structure, loosening of mechanical joints, creation of noise and vehicle discomfort (Rajappan and Vivekanandhan, 2013).It is imperative to know the modal parameters- resonant frequency, mode shape and damping characteristics of the structure at its varying operating conditions for improving its strength and reliability at the design stage (Mukhopadhyay, 2013).

Modal analysis using Finite Element Method (FEM) can be used to determine natural frequencies and mode shapes. In this study, the modal analysis has been accomplished by the commercial finite element software, ANSYS. After constructing finite element model of chassis and appropriate meshing with shell elements, model has been analyzed and first 10 frequencies that play important role in dynamic behavior of chassis, have been expanded. In addition, the relationship between natural frequencies and engine operating speed has been explained. In addition to road excitation, the engine vibration is also the main disturbance source for the chassis as the chassis natural frequencies lie within the road and the engine excitation frequency range. Therefore it is important to include the dynamic effect in designing the chassis.

The engine works in the range 0f 0 to 3000 rpm engine speed which is equivalent to an excitation frequency of 0-50 Hz.

At low speed, there is no risk of vibration effect due to engine excitation but excitation of road disturbance is more risky and which ranges from 0- 100Hz (Rajappan and Vivekanandhan, 2013).

3.9.3. Deformation and mode shape of AISI 4140 steel alloy

A. First mode shape of AISI 4140 steel alloy

In the first mode, only bending exists. The maximum displacement of the chassis is 3.75mm which exists around the center of its longitudinal axis as shown on the Figure 4.47 below.

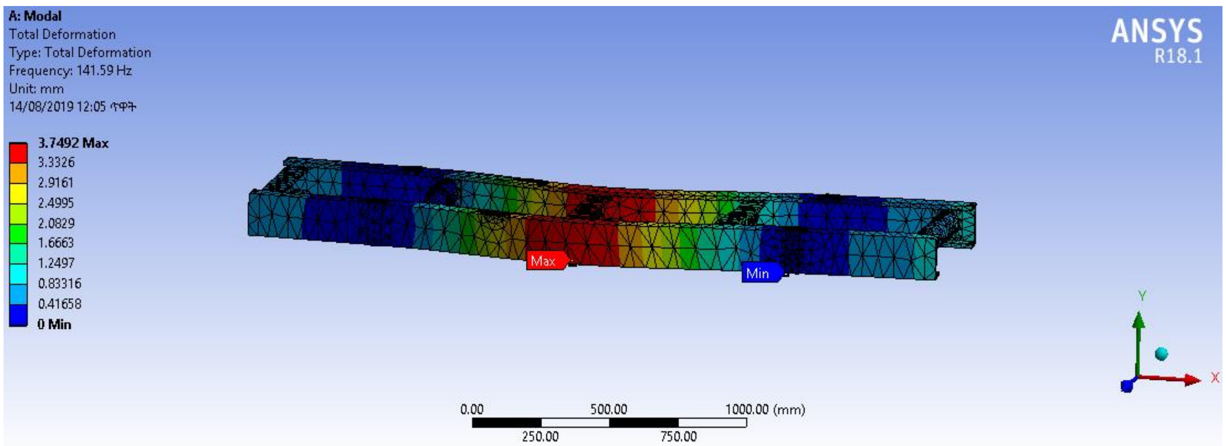

Figure 3. 46. Deformation of first mode shape of AISI 4140 steel alloy

B. Second mode shape of AISI 4140 steel alloy

The second mode showed that bending exists in front of the front axle and at the rear of rear axle and also small twisting is show at the front cross member about the vertical axis. Here the maximum displacement of the chassis is 5.106 mm which exists at the front end as shown on the Figure 4.48 below.

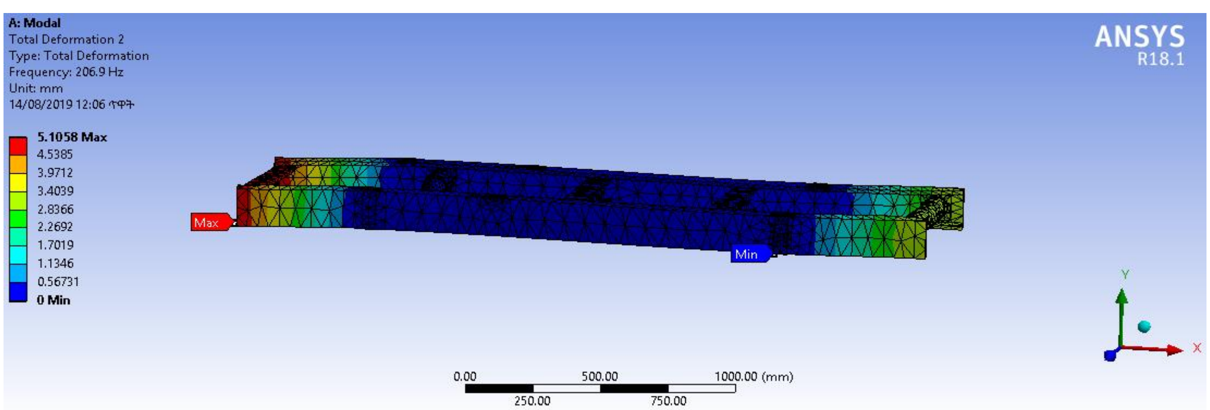

Figure 3. 47. Second mode shape of AISI 4130 steel alloy

C. Third mode shape of AISI 4140 steel alloy

The third mode showed that bending about the 'Z' axis exists and twisting about the x-axis is shown at the front and rear ends. Here the maximum displacement of the chassis is 5.499 mm which exists at the rear end as shown on the Figure 4.49 below.

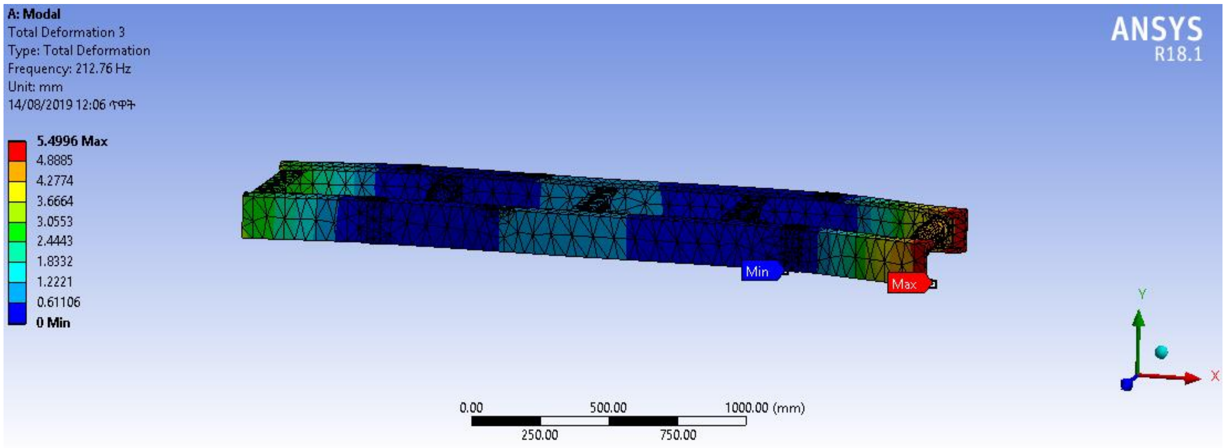

Figure 3. 48. Third mode shape of AISI 4130 steel alloy

D. Fourth mode shape of AISI 4140 steel alloy

In the fourth mode, only simple bending exists and the maximum deflection of the chassis is 4.42mm which exists around the center of its longitudinal axis as shown on the Figure 4.50 below.

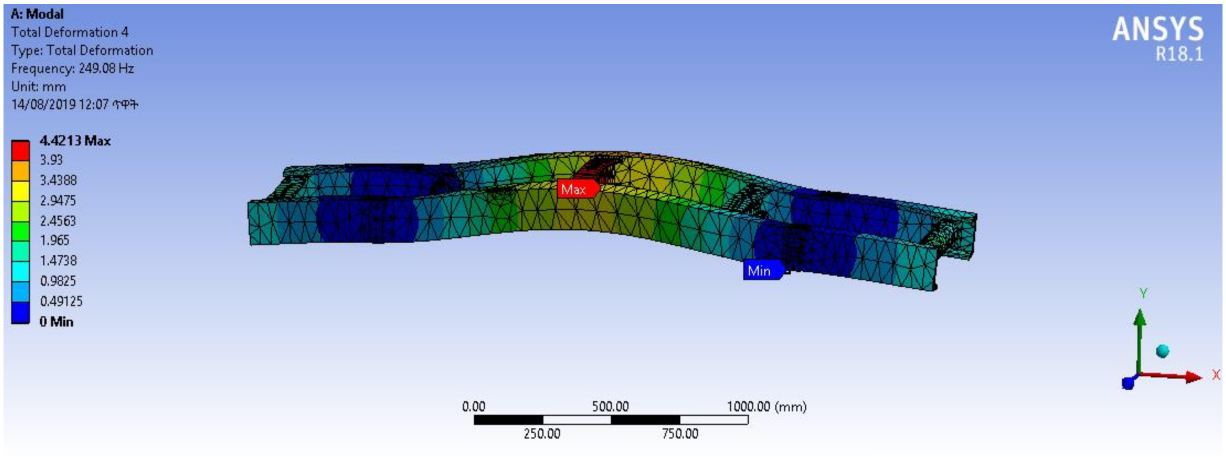

Figure 3. 49. Fourth mode shape of AISI 4130 steel alloy

E. Fifth mode shape of AISI 4140 steel alloy

The fifth mode showed that the bending of the longitudinal members about the 'Z' axis exists and bending of the front and rear ends about x-axis. Here the maximum displacement of the chassis is 6.715 mm which exists at the front end as shown on the Figure 4.51 below.

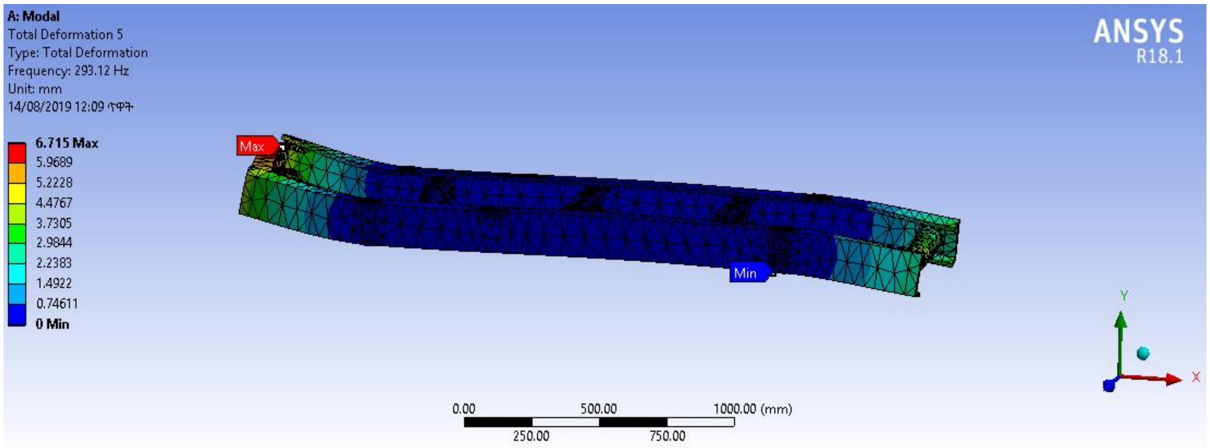

Figure 3. 50. Fifth mode shape of AISI 4130 steel alloy

F. Six mode shape of AISI 4140 steel alloy

The Sixth mode showed that the bending of the longitudinal members about the 'Z' axis exists and bending of the front and rear ends about x-axis. Here the maximum displacement of the chassis is 7.15 mm which exists at the center of the rear cross member as shown on the Figure 4.52 below.

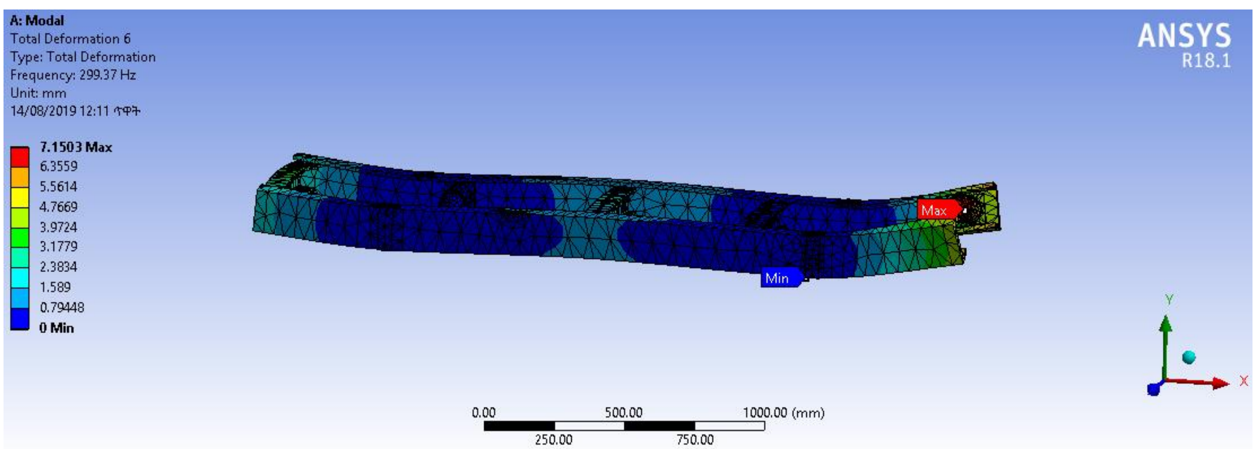

Figure 3. 51. Six mode shape of AISI 4130 steel alloy

G. Seventh mode shape of AISI 4140 steel alloy

The seventh mode showed that the bending of the longitudinal members about the 'Z' axis exists and twisting of the whole system about x-axis is shown. Here the maximum displacement is 6.715 mm which exists at the longitudinal member near to the third cross member as shown on the Figure 4.53 below.

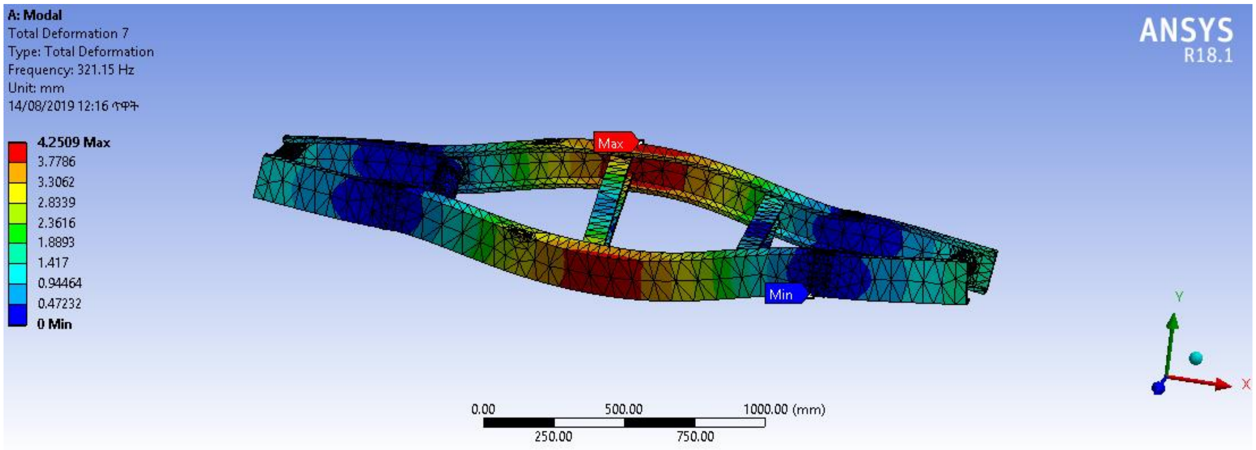

Figure 3. 52. Seventh mode shape of AISI 4130 steel alloy

H. Eighth mode shape of AISI 4140 steel alloy

Here the maximum displacement is 4.1819 mm which exists at the longitudinal member between the third and fourth cross member as shown on figure 3.54 below.

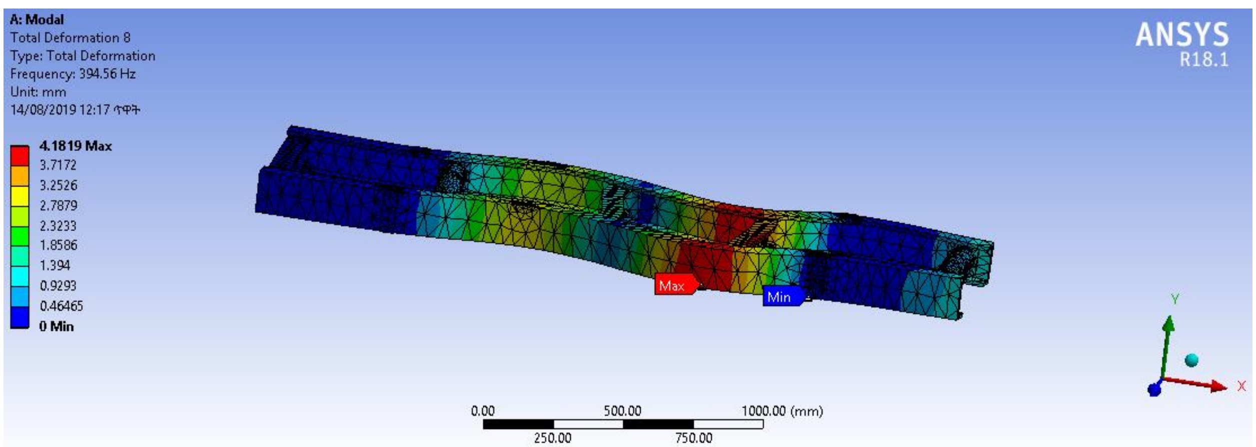

Figure 3. 53. Eighth mode shape of AISI 4130 steel alloy

I. Ninth mode shape of AISI 4130 steel alloy

The maximum displacement for the ninth mode shape is 8.3166 mm which exists at the rear end of the chassis frame as shown on figure 3.55 below.

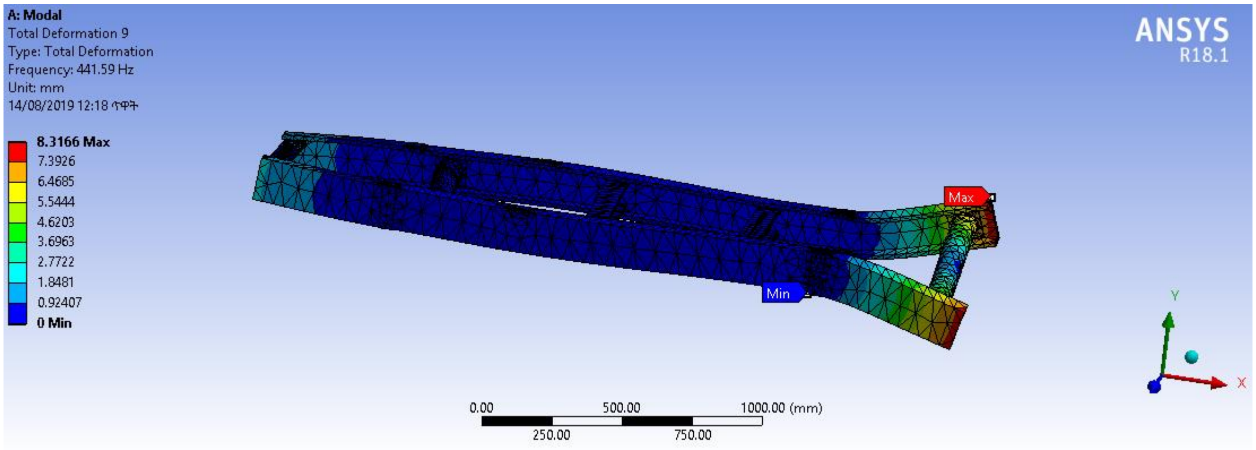

Figure 3. 54. Ninth mode shape of AISI 4130 steel alloy

J. Tenth mode shape of AISI 4140 steel alloy

The maximum displacement for the tenth mode shape is 4.8438 mm which exists at the front end of the chassis frame as shown on figure 3.55 below.

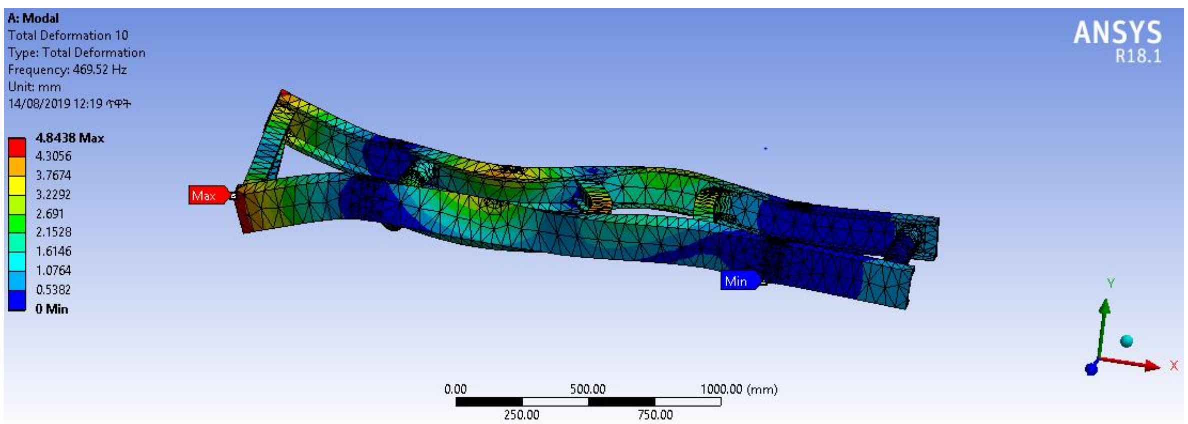

Figure 3. 55. Tenth mode shape of AISI 4130 steel alloy

CHAPTER FOUR

RESULTS AND DISCUSSION

In this section, the results of design and analysis made by Finite Element Methods are presented in tabulated form and the results are interpreted for both static and dynamic analysis such as bending analysis, torsional analysis, combined bending and torsional analysis, impact and modal analysis.

4.1. Results of pure bending load analysis

The results of bending analysis for the three materials are given in Tables 4.1, 4.2 and 4.3 below.

Table 4. 1. Bending Analysis Results for ASTM A710 Steel Alloy

Object Name	*Equivalent Stress*	*Maximum Principal Stress*	*Maximum Shear Stress*	*Total Deformation*
Minimum	2.6662e-003 MPa	-1.54 MPa	1.5317e-003 MPa	0. mm
Maximum	78.466 MPa	55.813 MPa	44.799 MPa	4.6709e-002 mm

Table 4. 2. Bending Analysis Results for ASTM A302 Steel Alloy

Object Name	*Equivalent Stress*	*Maximum Principal Stress*	*Maximum Shear Stress*	*Total Deformation*
Minimum	2.3553e-003 MPa	-1.9427 MPa	1.2931e-003 MPa	0. mm
Maximum	78.353 MPa	57.005 MPa	44.847 MPa	4.5992e-002 mm

Table 4. 3. Bending Analysis Results for Aluminum 6063 T-6 Alloy

Object Name	*Equivalent Stress*	*Maximum Principal Stress*	*Maximum Shear Stress*	*Total Deformation*
Minimum	2.66e-003 MPa	-1.6981 MPa	1.4633e-003 MPa	0. mm
Maximum	78.36 MPa	56.676 MPa	44.823 MPa	1.3968 mm

As shown on the Table 4.1 above, the maximum equivalent (Von Mises) stress for ASTM A710 steel alloy is 78.466Mpa and its maximum deformation value is 0.0467mm. The ultimate tensile strength and the compressive yield strengths of ASTM A710 steel alloy are 515Mpa and 450Mpa respectively as given on the material property table 3.1.

The factor of safety (FOS) of the chassis frame for ASTM A710 steel alloy is given by:

Factor of safety $=\frac{\text{ultimate stress}}{4\times\text{developed stress}}$ (equ.3.14)

FOS $=\frac{S_{UT}}{4\times developed\ stress}$

FOS $= \frac{515Mpa}{4\times78.466} = 1.64$ (Tensile strength)

Factor of safety $=\frac{yield\ stress}{F_{dy}\times developed\ stress}$

FOS $=\frac{S_Y}{4\times developed\ stress}$

$FOS = \frac{450Mpa}{4\times78.466} = 1.43$ (compressive strength)

The maximum equivalent (Von Mises) stress for ASTM A302 steel alloy is 78.353Mpa and its maximum deformation value is 0.04599mm as shown in the Table 4.2 above. The ultimate tensile strength and the compressive yield strengths of ASTM A302 steel alloy are 590Mpa and 340 Mpa respectively as given in the material property table 3.1.

The factor of safety (FOS) of the chassis frame for ASTM A302 steel alloy is given by:

Factor of safety $=\frac{yield\ stress}{4\times developed\ stress}$

FOS $=\frac{S_Y}{4\times developed\ stress}$

FOS $= \frac{340Mpa}{4\times78.353} = 1.09$ (compressive strength)

Factor of safety $=\frac{ultimate\ \ stress}{4\times developed\ stress}$

FOS $=\frac{S_{UT}}{4\times developed\ stress}$

FOS$= \frac{590\ Mpa}{4\times78.353\ MPa} = 1.88$ (Tensile strength)

The maximum equivalent (Von Mises) stress for Aluminum 6063 T-6 alloy is 78.36 MPa and its maximum deformation value is 1.3967 mm as shown in the Table 4.3 above. The ultimate tensile strength and the compressive yield strengths of Aluminum 6063 T6 alloy are 250 MPa and 220MPa respectively as given on the material property table 3.1.

The factor of safety (FOS) of the chassis frame for aluminum 6063 T-6 alloy is given by:

Factor of safety $=\frac{yield\ stress}{4\times developed\ stress}$

FOS $=\frac{S_Y}{4\times developed\ stress} = \frac{220\ MPa}{4\times78.36\ MPa} = 0.7$ (compressive strength)

Factor of safety $=\frac{ultimate\ \ stress}{4\times developed\ stress}$

$$\text{FOS} = \frac{S_{UT}}{4 \times developed\ stress} = \frac{250\ MPa}{4 \times 78.36 MPa} = 0.8 \qquad \text{(Tensile strength)}$$

Table 4. 4. Summary of Finite Element Analysis Results for Bending Case

Material	Von Misses Stress (MPa)	Max.deformation (mm)	Factor of safety		Remark
			Tensile	Compressive	
ASTM 710 Steel Alloy	78.466	0.0467	1.64	1.43	Pass
ASTM 310 Steel Alloy	78.353	0.04	1.88	1.09	Risk for compressive
Aluminum 6063 T-6 Alloy	78.38	1.397	0.8	0.7	Fail

The factor of safety for bending analysis result showed that only ASTM A710 steel alloy is safe for all tensile and compressive strengths. Whereas ASTM A302 steel alloy had good factor of safety for its tensile strength even if its compressive factor of safety is not enough. This can be improved by increasing the thickness of the chassis around the point where maximum stress is located. But the result of Aluminum 6063 T-6 alloy is not in good condition for this case.

4.2. Results of torsional load analysis

This simulation is based on the condition where by one of the vehicles wheel rests on a bump where as other three wheels are on the level road causing torsional moment on the chassis about the longitudinal axis. Even if pure torsion does not exist without bending it is important to show its effect on the structure separately. Assume that the front right wheel is at the bump, the torque T reaches maximum when this right wheel lifts off, i.e., when P_R=0.the front axle is the lightest axel having a load of 3986 N. The torque T is given by:

$$T = P_{axle} \times \frac{b}{2} = 3986\ N \times 0.35\ m = 1395.1\ Nm$$

The results of torsional analysis are given in Tables 4.5, 4.6 and 4.7 below.

Table 4. 5. Torsion Analysis Results for ASTM A710 Steel Alloy

Type of analysis	Equivalent (von-Mises) Stress	Total Deformation	Maximum Principal Stress	Directional Deformation	Minimum Principal Stress	Maximum Shear Stress
Minimum	5.2667e-003 MPa	0. mm	-2.766 MPa	-3.9891e-002 mm	-166.65 MPa	2.884e-003 MPa
Maximum	161.76 MPa	0.81556 mm	169.88 MPa	3.9893e-002 mm	6.913 MPa	91.432 MPa

Table 4. 6. Torsional Analysis Results for ASTM A302 Steel Alloy

Type of analysis	Equivalent (von-Mises) Stress	Total Deformation	Maximum Principal Stress	Maximum Shear Stress	Directional Deformation
Minimum	5.1247e-003 MPa	0. mm	-8.4037 MPa	2.8767e-003 MPa	-3.94e-002 mm
Maximum	163.64 MPa	0.80702 mm	180.45 MPa	92.9 MPa	3.9503e-002 mm

Table 4. 7. Torsional Analysis Results for Aluminum 6063 T-6 Alloy

Type of analysis	Equivalent (von-Mises) Stress	Total Deformation	Maximum Principal Stress	Maximum Shear Stress	Directional Deformation
Minimum	5.1556e-003 MPa	0. mm	-6.4884 MPa	2.8784e-003 MPa	-1.1957 mm
Maximum	163.1 MPa	24.48 mm	177.53 MPa	92.493 MPa	1.1981 mm

The maximum equivalent (Von Mises) stress for ASTM A710 steel alloy is 161.76 Mpa and its maximum deformation value is 0.8156mm as shown in the Table 4.5 above. The ultimate tensile strength and the compressive yield strengths of ASTM A710 steel alloy are 515Mpa and 450 Mpa respectively as given on the material property table 3.1.

The factor of safety (FOS) of the chassis frame for ASTM A710 steel alloy is given by:

$$\text{Factor of safety} = \frac{yield\ stress}{1.5\times developed\ stress} \qquad (3.15)$$

$$\text{FOS} = \frac{S_Y}{1.5\times developed\ stress} = \frac{450\ MPa}{1.5\times 161.76 MPa} = 1.86 \qquad \text{(compressive strength)}$$

$$\text{Factor of safety} = \frac{ultimate\ \ stress}{1.5\times developed\ stress}$$

$$\text{FOS} = \frac{S_{UT}}{1.5\times developed\ stress} = \frac{515\ MPa}{1.5\times 161.76 MPa} = 2.12 \qquad \text{(Tensile strength)}$$

The maximum equivalent (Von Mises) stress for ASTM A302 steel alloy is 163.64 MPa and its maximum deformation value is 0.807 mm as shown in the Table 4.6 above. The ultimate tensile strength and the compressive yield strengths of ASTM A302 steel alloy are 590 MPa and 340 MPa respectively as given on the material property table 3.1.

The factor of safety (FOS) of the chassis frame for ASTM A302 steel alloy is given by:

$$\text{Factor of safety} = \frac{yield\ stress}{1.5 \times developed\ stress}$$

$$\text{FOS} = \frac{S_Y}{1.5 \times developed\ stress} = \frac{340\ MPa}{1.5 \times 163.64 MPa} = 1.39 \qquad \text{(compressive strength)}$$

$$\text{Factor of safety} = \frac{ultimate\ \ stress}{1.5 \times developed\ stress}$$

$$\text{FOS} = \frac{S_{UT}}{1.5 \times developed\ stress} = \frac{590\ MPa}{1.5 \times 163.64 MPa} = 2.4 \qquad \text{(Tensile strength)}$$

The maximum equivalent (Von Mises) stress for Aluminum 6063 T-6 alloy is 163.1 MPa and its maximum deformation value is 24.48 mm shown in the Table 4.7 above. The ultimate tensile strength and the compressive yield strengths of AISI 710 steel alloy are 250 MPa and 220 MPa respectively as given on the material property table 3.1.

The factor of safety (FOS) of the chassis frame for aluminum 6063 T-6 alloy is given by:

$$\text{Factor of safety} = \frac{yield\ stress}{1.5 \times developed\ stress}$$

$$\text{FOS} = \frac{S_Y}{1.5 \times developed\ stress} = \frac{220\ MPa}{1.5 \times 163.1\ MPa} = 0.91 \qquad \text{(compressive strength)}$$

$$\text{Factor of safety} = \frac{ultimate\ \ stress}{1.5 \times developed\ stress}$$

$$\text{FOS} = \frac{S_{UT}}{1.5 \times developed\ stress} = \frac{250\ MPa}{1.5 \times 163.1\ Mpa} = 1.02 \qquad \text{(Tensile strength)}$$

Table 4. 8. Summary of Finite Element Analysis Results for Torsion Case

Material	Von Misses Stress (MPa)	Max.deformation (mm)	Factor of safety		Remark
			Tensile	compressive	
ASTM 710 Steel Alloy	161.76	0.8155	2.12	1.86	Pass
ASTM 310 Steel Alloy	163.64	0.80702	2.4	1.39	Pass
Aluminum 6063 T-3 Alloy	163.1	24.48	1.02	*0.92*	Risk

According to the result of torsional analysis, the design is safe for both ASTM A710 steel alloy and ASTM A302 steel alloy. But aluminum alloy needs an increase in thickness of the chassis to get a factor of safety about 1.5. In addition to this the deformation of the chassis frame is higher for aluminum alloy compared to the two steel alloys.

4.5. FEA results for combined bending and torsion load case

This represents the situation arising if one wheel of the lighter loaded axle is raised on a bump of sufficient height to cause the other wheel on that axle to leave the ground without ignoring the effect of vehicle weight. If the left wheel of the front axle is on the bump, the load on the right wheel of the front axle will be the total axle load R_e=3986N, the torque on the body 2790.2 Nm and R'_R is equal to R_e which is 3986 N. Based on this pre-condition, the FEA showed the following results shown in Tables 4.9, 4.10 and 4.11.

Table 4. 9. Combined Load Analysis Results for ASTM A710 Steel Alloy

Type	Equivalent (von-Mises) Stress	Maximum Principal Stress	Maximum Shear Stress	Total Deformation
Minimum	2.3827e-002 MPa	-12.749 MPa	1.363e-002 MPa	0. mm
Maximum	341.49 MPa	243.53 MPa	193.55 MPa	1.4124 mm

Table 4. 10. Combined Load Analysis Results for ASTM A302 Steel Alloy

Type	Equivalent (von-Mises) Stress	Maximum Principal Stress	Maximum Shear Stress	Total Deformation
Minimum	2.4021e-002 MPa	-21.139 MPa	1.3719e-002 MPa	0. mm
Maximum	344.29 MPa	250.95 MPa	195.91 MPa	1.394 mm

Table 4. 11. Combined Load Analysis Results for Aluminum 6063 T-6 Alloy

Type	Equivalent (von-Mises) Stress	Maximum Principal Stress	Maximum Shear Stress	Total Deformation
Minimum	2.397e-002 MPa	-18.92 MPa	1.3696e-002 MPa	0. mm
Maximum	343.46 MPa	248.98 MPa	195.24 MPa	42.313 mm

The maximum equivalent (Von Mises) stress for ASTM A710 steel alloy is 325.38Mpa and its maximum deformation value is 1.4124 mm as shown in the Table 4.9 above. The ultimate tensile strength and the compressive yield strengths of ASTM A710 steel alloy are 515Mpa and 450 Mpa respectively as given on the material property table 3.1.

The factor of safety (FOS) of the chassis frame for ASTM A710 steel alloy is given by:

$$\text{Factor of safety} = \frac{yield\ stress}{developed\ stress}$$

$$\text{FOS} = \frac{S_Y}{developed\ stress} = \frac{450\ MPa}{325.38\ MPa} = 1.38 \qquad \text{(compressive strength)}$$

$$\text{Factor of safety} = \frac{ultimate\ \ stress}{developed\ stress}, \text{ for tensile strength}$$

$$\text{FOS} = \frac{S_{UT}}{developed\ stress} = \frac{515\ MPa}{325.38\ MPa} = 1.58 \qquad \text{(Tensile strength)}$$

The maximum equivalent (Von Mises) stress for ASTM A302 steel alloy is 327.1 MPa and its maximum deformation value is 1.394 mm as shown in the Table 4.10 above. The ultimate tensile strength and the compressive yield strengths of ASTM A302 steel alloy are 590MPa and 340 MPa respectively as given on the material property table 3.1.

The factor of safety (FOS) of the chassis frame for ASTM A302 steel alloy is given by:

$$\text{Factor of safety} = \frac{yield\ stress}{developed\ stress}$$

$$\text{FOS} = \frac{S_Y}{4 \times developed\ stress} = \frac{340MPa}{327.1MPa} = 1.04 \qquad \text{(compressive strength)}$$

$$\text{Factor of safety} = \frac{ultimate\ \ stress}{4 \times developed\ stress}$$

$$\text{FOS} = \frac{S_{UT}}{4 \times developed\ stress} = \frac{590MPa}{327.1\ MPa} = 1.8 \qquad \text{(Tensile strength)}$$

The maximum equivalent (Von Mises) stress for Aluminum 6063 T-6 alloy is 326.65 MPa and its maximum deformation value is 42.313 mm as shown in the Table 4.11 above. The ultimate tensile strength and the compressive yield strengths of aluminum 6063 T-6 alloy are 250 MPa and 220 MPa respectively as given on the material property table 3.1.

The factor of safety (FOS) of the chassis frame for aluminum 6063 T-6 alloy is given by:

$$\text{Factor of safety} = \frac{yield\ stress}{4 \times developed\ stress}$$

$$\text{FOS} = \frac{S_Y}{developed\ stress} = \frac{220\ MPa}{326.65\ MPa} = 0.67 \qquad \text{(compressive strength)}$$

$$\text{Factor of safety} = \frac{ultimate\ \ stress}{developed\ stress}$$

$$\text{FOS} = \frac{S_{UT}}{developed\ stress} = \frac{250\ MPa}{326.65\ MPa} = 0.76 \qquad \text{(Tensile strength)}$$

Table 4. 12. Summary of Finite Element Analysis Results for Combined Loading Case

Material	Von Misses Stress (MPa)	Max.deformation (mm)	Factor of safety		Remark
			Tensile	Compressive	
ASTM 710 Steel Alloy	325.38	1.318	1.58	1.38	Pass
ASTM 310 Steel Alloy	327.14	1.3007	1.8	1.04	Risk for compressive
Aluminum 6063 T-3 Alloy	326.65	39.482	0.76	0.67	Fail

The result of combined loading analysis showed that ASTM A710 steel alloy is in good condition and ASTM A302 steel alloy needs some increase in thickness of the chassis frame. But the factor of safety for aluminum alloy is very minimum for both tensile and compressive strengths and its deflection is also large compared to the two materials. Aluminum 6063 T-6 alloy felt for all of the three types of static load analysis. So doing further analysis may not be much effective for this material. Since its factor of safety is very lower than the required, increasing the thickness of the chassis frame may result higher weight of the chassis frame.

4.4. Dynamic analysis

ANSYS explicit dynamics engineering simulation solutions are ideal for simulating physical events that occur in a short period of time and may result in material damage or failure. These types of events are often difficult or expensive to study experimentally. Simulation provides insight and a detailed understanding of the fundamental physics taking place and gives engineers a chance to make necessary changes before their products are put into service, when mistakes in design can be costly. Explicit dynamics analysis is used to determine the dynamic response of a structure due to stress wave propagation, impact or rapidly changing time-dependent loads.

4.4.1. Impact analysis results

The FEA results of ASTM A710 and ASTM A302 are shown in Tables below.

Table 4. 13. Results of Impact Analysis for ASTM A710 Steel Alloy

Time [s]	Directional deformation		total deformation [mm]	Equivalent stress [MPa]
	Minimum [mm]	Maximum [mm]		
1.18E-38	0	0	0	0
3.50E-05	-0.34345	4.73E-02	0.3525	610.24
7.01E-05	-0.70138	5.24E-02	0.77648	728.57
1.05E-04	-1.0458	8.18E-02	1.0478	607.72
1.40E-04	-1.461	0.29951	1.4615	767.66
1.75E-04	-1.6162	0.43615	1.617	711.34
2.10E-04	-1.6039	0.29759	1.6039	599.35
2.45E-04	-1.488	0.11932	1.489	769.25
2.80E-04	-1.3824	0.5345	1.3915	572.92
3.15E-04	-1.3069	0.84856	1.3137	766.24
3.50E-04	-1.169	0.91895	1.1726	632.5
3.85E-04	-0.8901	1.012	1.0473	663.51
4.20E-04	-0.50258	1.1501	1.186	777.42
4.55E-04	-0.3373	1.0247	1.317	581.38
4.90E-04	-0.43138	0.8371	1.5001	694.51
5.25E-04	-0.48053	0.78574	1.4842	658.04
5.60E-04	-0.60031	1.0073	1.2491	542.36
5.95E-04	-1.1006	1.2013	1.3118	799.47
6.30E-04	-1.3318	1.4652	1.5747	1095.9
6.65E-04	-1.144	1.6043	1.7298	1042.4
7.00E-04	-0.90627	1.5842	1.7777	724.53

Table 4. 14. Results of Impact Analysis for ASTM A302 Steel Alloy

Time [s]	Directional deformation		Total deformation [mm]	Equivalent stress [MPa]
	Minimum [mm]	Maximum [mm]		
1.18E-38	0	0	0	0
3.50E-05	-0.34281	4.57E-02	0.35246	610.96
7.01E-05	-0.70195	5.16E-02	0.7767	727.54
1.05E-04	-1.0475	8.27E-02	1.0476	617.23
1.40E-04	-1.4591	0.29912	1.4596	791.05
1.75E-04	-1.6061	0.43346	1.6067	694.96
2.10E-04	-1.5898	0.29544	1.5898	578.25
2.45E-04	-1.4648	0.10985	1.4661	777.08
2.80E-04	-1.3604	0.54475	1.3694	572.65
3.15E-04	-1.2834	0.86067	1.2905	799.83
3.50E-04	-1.1353	0.92448	1.139	651.79
3.85E-04	-0.84279	1.0226	1.0523	666.19
4.20E-04	-0.45228	1.1535	1.1913	741.13
4.55E-04	-0.34195	0.98566	1.3162	582.23
4.90E-04	-0.43011	0.8093	1.4929	674.89
5.25E-04	-0.47692	0.82555	1.4739	635.19
5.60E-04	-0.63413	1.0304	1.2235	508.11
5.95E-04	-1.117	1.2402	1.3511	903.8
6.30E-04	-1.3334	1.4879	1.593	1163.2
6.65E-04	-1.1194	1.5914	1.7223	1006.3
7.00E-04	-0.88946	1.5446	1.7504	712.18

The maximum equivalent (Von Mises) stress for ASTM A710 steel alloy is 1095.9 MPa and its maximum deformation value is 1.777 mm as shown in the Table 4.13 above. The ultimate tensile strength and the compressive yield strengths of ASTM A710 steel alloy are 515MPa and 450 MPa respectively as given on the material property table 3.1.

The factor of safety (FOS) of the chassis frame for ASTM A710 steel alloy is given by:

$$\text{Factor of safety} = \frac{yield\ stress}{developed\ stress}$$

$$\text{FOS} = \frac{S_Y}{developed\ stress} = \frac{450\ MPa}{1095.9\ MPa} = 0.41 \qquad \text{(compressive strength)}$$

$$\text{Factor of safety} = \frac{ultimate\ \ stress}{developed\ stress}$$

$$\text{FOS} = \frac{S_{UT}}{developed\ stress} = \frac{515\ MPa}{1095.9\ MPa} = 0.47 \qquad \text{(Tensile strength)}$$

The maximum equivalent (Von Mises) stress for ASTM A302 steel alloy is 1163.2 MPa and its maximum deformation value is 1.7504 mm as shown in the Table 4.14 above. The ultimate tensile strength and the compressive yield strengths of ASTM A710 steel alloy are 590 MPa and 340 MPa respectively as given on the material property table 3.1.

The factor of safety (FOS) of the chassis frame for ASTM A710 steel alloy is given by:

$$\text{Factor of safety} = \frac{yield\ stress}{developed\ stress}$$

$$\text{FOS} = \frac{S_Y}{developed\ stress} = \frac{340\ MPa}{1163.2\ MPa} = 0.29 \qquad \text{(compressive strength)}$$

$$\text{Factor of safety} = \frac{ultimate\ \ stress}{developed\ stress}$$

$$\text{FOS} = \frac{S_{UT}}{developed\ stress} = \frac{590\ MPa}{1163.2 MPa} = 0.51 \qquad \text{(Tensile strength)}$$

Table 4. 15. Summary of Impact Analysis Results for ASTM A710 and ASTM A302

Material	Von Misses Stress (Mpa)	Maximum deformation (mm)	Factor of safety		Remark
			tensile	Compressive	
ASTM 710 Steel Alloy	724.53	1.777	0.47	0.41	Failed
ASTM 310 Steel Alloy	712.18	1.7504	0.29	0.51	Failed

The impact analysis result showed that the factor of safety for both ASTM A710 steel alloy and ASTM A302 steel alloy are lower than the required for both tensile and compressive strengths. to bring the required factor of safety an increase of large thickness of the chassis frame is needed.

This also leads to higher increase in weight of the chassis frame. So, it is better to change the design with a material having better tensile and compressive strengths. AISI 4140 steel alloy quenched and tempered at 205 ^{o}C which have the mechanical properties given in Table 3.1 is selected.

4.4.2. Results of combined loading for AISI 4140 steel alloy

Table 4. 16. Results of Combined Loading for AISI 4140 Steel Alloy

Type	Equivalent (von-Mises) Stress	Maximum Principal Stress	Maximum Shear Stress	Total Deformation
Minimum	2.3873e-002 MPa	-14.732 MPa	1.3652e-002 MPa	0. mm
Maximum	342.07 MPa	245.28 MPa	194.07 MPa	1.4518 mm

The allowable tensile and compressive strengths of AISI 4140 Q&T at 205 ^{o}C steel alloy are 1770 MPa and 1640 MPa respectively as given in the material property table 3.1. The factor of safety (FOS) of the chassis frame for this material is given by:

$$\text{Factor of safety} = \frac{yield\ stress}{developed\ stress}$$

$$\text{FOS} = \frac{S_Y}{developed\ stress} = \frac{1640\ MPa}{342.07\ MPa} = 4.79 \qquad \text{(compressive strength)}$$

$$\text{Factor of safety} = \frac{ultimate\ \ stress}{developed\ stress}$$

$$\text{FOS} = \frac{S_{UT}}{developed\ stress} = \frac{1770\ MPa}{342.07\ MPa} = 5.17 \qquad \text{(Tensile strength)}$$

The factor of safety for both tensile and compressive strengths showed that the design is much safe for combined load analysis. To bring the factor of safety about 1.5, the thickness of the chassis frame can be reduced if the same condition happens to the impact analysis.

4.4.3. Results of impact analysis for AISI 4140 steel alloy

The maximum equivalent (Von Mises) stress is 1112.5 MPa and the maximum deflection is 1.88mm as shown in Table 4.17 below. The ultimate tensile strength and the compressive yield strengths of AISI 4140 steel alloy are 1770 MPa and 1640 MPa respectively as given on the material property table 3.1.

Table 4. 17. Impact Analysis Results for AISI 4140 Steel Alloy

Time [s]	Directional deformation		Total deformation [mm]	Equivalent stress	
	Minimum [mm]	Maximum [mm]		Minimum [MPa]	Maximum [MPa]
1.18E-38	0	0	0	0	0
5.00E-04	-0.51568	1.4515	1.5747	0.31072	596.6
1.00E-03	-0.8716	0.98245	1.4992	0.41903	688.76
1.50E-03	-0.87175	0.99583	1.2258	0.45869	592.93
2.00E-03	-1.3322	0.11698	1.8815	0.84377	760.73
2.50E-03	-1.2138	0.99112	1.5844	0.32858	711.83
3.00E-03	-0.78075	1.059	1.5947	0.92714	635.56
3.50E-03	-0.37341	1.093	1.7717	0.93824	728.35
4.00E-03	-0.94203	1.2543	1.7986	0.6032	571.92
4.50E-03	-1.3615	0.73826	1.9182	0.70984	684.54
5.00E-03	-1.1531	1.1565	1.7481	0.8267	571.71
5.50E-03	-1.4485	0.95203	1.7393	1.0934	712.28
6.00E-03	-0.38561	1.5124	1.605	0.78271	733.84
6.50E-03	-1.5797	1.1447	1.5808	1.2416	543.56
7.00E-03	-1.1052	1.487	1.5155	0.55968	675.53
7.50E-03	-1.1382	0.87163	1.1739	0.67257	688.49
8.00E-03	-0.61449	0.82514	1.0779	1.3221	526.93
8.50E-03	-0.93459	1.0264	1.3908	0.8936	677.98
9.00E-03	-0.958	0.57556	1.0266	0.77834	1050.5
9.50E-03	-1.1949	0.74694	1.5676	1.1075	1112.5
1.00E-02	-0.85788	0.83614	1.5007	0.70881	626.5

The factor of safety (FOS) of the chassis frame for AISI 4130 steel alloy is given by:

Factor of safety = $\frac{yield\ stress}{developed\ stress}$

FOS = $\frac{S_Y}{developed\ stress} = \frac{1640\ MPa}{1112.5\ MPa} = 1.47$ (compressive strength)

Factor of safety = $\frac{ultimate\ \ stress}{developed\ stress}$

FOS = $\frac{S_{UT}}{developed\ stress} = \frac{1770\ MPa}{1112.5\ MPa} = 1.59$ (Tensile strength)

The factor of safety for impact analysis result showed that AISI 4140 quenched and tempered at 205 ^{o}C is appropriate for this design.

4.5. Modal analysis

Modal analysis is a powerful tool to identify the dynamic characteristics of structures. Every structure vibrates with high amplitude of vibration at its resonant frequency.

After constructing finite element model of chassis and appropriate meshing with shell elements, model has been analyzed and first 10 frequencies that play important role in dynamic behavior of chassis, have been expanded.

The engine works in the range of 0 to 3000 rpm engine speed which is equivalent to an excitation frequency of 0-50 Hz. At low speed, there is no risk of vibration effect due to engine excitation but excitation of road disturbance is more risky and which ranges from 0- 100Hz (Dr.R.Rajappan and M.Vivekanandhan, 2013).

4.5.1. Deformation and mode shape of AISI 4130 steel alloy

Table 4. 18. Modal Analysis Results of AISI 4130 Steel Alloy

Mode	Frequency	Max. displacement (mm)	DISPLACEMENT
1	141.59	3.75	Bending about x-axis
2	206.9	5.11	Bending about z-axis and twisting about vertical axis
3	212.76	5.49	Bending about z-axis and twisting about x-axis
4	249.08	4.42	Bending about z-axis and x-axis
5	293.12	6.71	Bending about z-axis
6	299.37	7.15	Bending about z-axis and twisting about x-axis
7	321.15	4.25	Bending about z-axis and twisting about x-axis
8	394.56	4.18	
9	441.59	8.31	
10	469.52	4.84	

The result for modal analysis of AISI 4140 Q&T at 205 ^{o}C showed that the minimum natural frequency of the chassis frame is 141.59 Hz which is about 2.83 times the maximum engine excitation frequency and 1.42 times the maximum road excitation frequency and so there is no risk for happening of resonant frequency. Therefore the design is safe for this material.

CHAPTER FIVE

SUMMARY, CONCLUSION AND RECOMENDATION

5.1. Summary

Chassis refers to the Frame or Basic Structure of the vehicle and is called as Carrying Unit of a vehicle. The components of the vehicle like Power plant (Engine), transmission System, Axles, Wheels and Tires, Suspension, Controlling Systems like Braking, Steering and also electrical system parts are mounted on the Chassis frame. Being the main load bearing structure of the vehicle, well-conditioned design of the Chassis frame is paramount to the success of the vehicle as a whole. Conventional frame, integral frame and semi-integral frames are the three main types of chassis frames. The Conventional type of chassis frame has two long side members and 5 to 6 cross members joined together with the help of rivets and bolts. The frame sections used are generally classified as Channel Section, Tabular Section and Box Section.

Various loads acting on the chassis frame are Static Loads - Loads due to chassis parts and weight of vehicle, Inertia Load - While applying brakes, Momentary duration Load - While taking a curve and Impact Loads - Due to the collision of the vehicle. In addition to being at rest, when the Vehicle is moving at a constant velocity on an even road the loads are treated as static loading type and can be solved using static equilibrium balance. On the other hand Dynamic loads include the load types during Vehicle moving on a bumpy road even at constant velocity loads during collision of a vehicle. Such problems can be solved using dynamic equilibrium balance.

The finite element method (FEM), sometimes referred to as finite element analysis (FEA), is a computational technique used to obtain approximate solutions of boundary value problems in engineering. Both static analysis such as bending load analysis, torsional load analysis, combined load analysis and dynamic load such as impact analysis and modal analysis can be done with Finite Element Analysis software, ANSYS.

5.2. Conclusion

In this thesis work, ladder type chassis frame for Agricultural Rotary Dibber Machine was designed and analyzed using ANSYS 18.1 software. From the results, it is observed that;

- Aluminum alloy 6063 T-6 had good strength for only torsional analysis, but it has lower factor of safety and higher deflection for all other static and dynamic analysis compared to other three materials.
- Even if ASTM A710 and ASTM A302 steel alloys have good factor of safety for static analysis, the result of impact analysis showed that these two materials could not be used for this chassis frame with the given chassis frame thickness. The factor of safety (0.41 and 0.47 respectively for ASTM A710 and ASTM A302) showed that a double of its original thickness is required to have appropriate strength of the chassis frame with these materials which resulted a higher mass of the chassis frame.
- The result of AISI 4140 steel alloy tempered and quenched at 205 ^{o}C had appropriate factor of safety for both static and dynamic analysis. It has a compressive and tensile factor of safety of 4.79 and 5.17 respectively for combined bending and torsional analysis in the case of static analysis. Whereas, in the case of impact analysis it had a factor of safety of 1.47 and 1.59 for compressive and tensile strengths respectively.

In addition, the results for modal analysis for AISI 4140 steel alloy tempered and quenched at 205 ^{o}C showed that the Values of natural frequency obtained by finite element method were in good condition. The first ten frequency modes of the chassis frame that determine its dynamic behavior are above 140 Hz and vary from 141.59 to 469.52 Hz. According to this result, the minimum natural frequency of the chassis frame for AISI4130 steel alloy exists at the first modal analysis which is around 1.42 times the maximum road excitation frequency. So the happening of resonance is not the risk for this material.

Therefor based on all the analysis made, the chassis frame with thickness of 8.5 mm for longitudinal members and channel section cross members is taken as the final design with the given chassis length and width. The tubular cross members have outer diameter of 90 mm and thickness of 10mm. AISI 4140 steel alloy tempered and quenched at 205 ^{o}C had been taken for all longitudinal members and cross members which made the design safe.

5.3. Recommendation

- Since agriculture is the backbone for Ethiopian economy, both the government and research centers should give high emphasis for agricultural mechanization that fit to low farm land holder Ethiopian farmers.
- In a chassis design, materials that has appropriate strength in dynamic analysis will not fail for static analysis. So giving more emphasis for dynamic analysis is better.
- In designing of the chassis frame, design and analysis of longitudinal members and cross members individually by identifying the loads shared by each component for each case may be better than doing the analysis of the assembly for material saving and weight reduction.
- It is possible to design ladder type chassis frame that fit to the required power train components and to use for appropriate agricultural operations.

5.3.Future Work

1. Strength analysis of the rotary mechanism
2. Finding the factor of safety and weight minimization of the chassis frame by doing analysis for each component. So any one who is interested to do this task can proceed taking this work as a starting point.

REFERENCES

A.Hari Kumar and V.Deepanjali (2016) 'Design & Analysis of Automobile Chassis', *Volume 5, Issue1*:*International Journal of Engineering Science and Innovative Technology (IJESIT),* 187-195 pp.

Ashutosh Dubey and Vivek Dwivedi (2009) 'Vehicle Chassis Analysis, Load Cases & Boundary Conditions for Stress Analysis', Vol. 11, No. 4/5: *International Jornal of Vehicle Design,* 3-5 pp.

Atsbaha Gebre-Selassie and Tessema Bekele (2010) 'Roles,Policy and Small Scale Farming Systems', A Review of Ethiopian Agriculture : *Global Growing Casebook,* 44-56 pp.

Bahattin A. (2008) '*Elasticity of a Farm Trailer's Chassis at Different Twisting Angles'*, Turkey, Proceedings of the Institution of Mechanical Engineers, Part D: Journal of Automobile Engineering.

Cavazzuti Marco, Andrea Baldini, Enrico Bertocchi, Dario Costi, Enrico Torricelli, Patrizio Moruzzi (2010) 'High Performance Automotive Chassis Design',*Springer-Verlag: DOI 10.1007/S00158-010-0578-7*, 45-56.

D.Srinivasa Rao, (2017) 'Design and Analysis of a Truck Chassis Frame Using Catia and Ansys *Volume-3, Issue-8: International Journal of Scientific Engineering and Applied Science (IJSEAS) ISSN: 2395-3470*, 73-81 pp.

David V.Hutton (2004) '*Fundamentals of Finite Element Analysis'*, New York, Ny 10020: ISBN 0-07-239536-2.

Dr. C.N.Sakhale (2016) 'Multipurpose Farm Machine', *Volume:03: International Research Journal of Engineering and Technology (IRJET), Issue: 09 |E-ISSN: 2395 -0056*, 990-995 pp.

Dr.R.Rajappan And M.Vivekanandhan (2013) 'Static and Modal Analysis of Chassis by Using FEA', *Volume 2:The International Journal of Engineering and Science (Ijes): Issue 2*, 63-73 pp.

E.Madenci (2007) '*The Finite Element Method and Application in Engineering Using ANSYS':* SPRINGER.

Erwin A. (2004) 'Compulsory Specification for Agriculture Tractors': *ICS 43.080.99; 53.060*, 2-11 pp.

Gaurav R. Mohite, Pramod T. Korde, Pramod P. Derkar, Nikhil M. Nimkar, Nitish (2016) 'Design and Static Analysis of a Go-Kart Chassis by ANSYS Simulation': *International Research Journal of Engineering and Technology Volume: 03 Issue: 04,* 1426-1428 pp.

Grzegorz Szczęśniak, Paulina Nogowczyk and Rafał Burdzik (2014) 'Basic Tips in Vehicle Chassis and Frame Design', Volume 2: Journal of Measurements In Engineering, Issue 4, 208-214 pp.

Hans Binswanger (2014) 'A Comparative Historical Perspective of Agricultural Mechanization': *Oxford University Press*, 27-75 pp.

Jatin Rajpal,Sandeep, G. Thorat,Basavaraj, S. Kothavale Swapnil, S. Hatwalane (2014) 'Design Considerations For Automobile Chassis for Prevention of Rolling Over of a Vehicle': *Trans Tech Publications, Switzerland:Vol. 612,* 41-49 pp.

Julian Happian-Smith (2002) '*An Introduction to Modern Vehicle Design',*Linacre House, Jordan Hill, Oxford OX2 8DP,A Member of the Reed Elsevier Plc Group:ISBN 07506 50443.

Kallappa Khannukar, Vinayak Kallannavar, Dr. B. S. Manjunath (2015) 'Dynamic Analysis of Automotive Chassis Using FEA', *Volume: 02: International Research Journal of Engineering and Technology,P-ISSN: 2395-0072, Issue: 09*, 2165-2170 pp.

Kataoka, T. (2009) '*Agricultural Machinery Technology':* Hokkaido University Press.

Kehinde Adedeji Adekola (2014) 'China Agricultural Mechanization Development Experience for Developing Countries',Volume 3,:*International Journal of Agriculture Innovations and Research,* ISSN (Online) 2319-1473 , Issue 2, 654-658 pp.

Kiran Ghodvinde and S. R.Wankhade (2014) 'Structural Stress Analysis of an Automotive Vehicle Chassis': *International Journal on Mechanical Engineering and Robotics (IJMER)ISSN : 2321-5747, Volume-2, Issue*-6,44-48pp.

Kolchin (1984) '*Design of Automotive Engine',First Edition,* MOSCOW: MIR PUBLICATION.

M.Rutheravan (2016) 'Summary of Safety Criteria in Design': *Research Gate*, 1-4 pp.

Madhu Ps and Venugopal T.R (2014) 'Static Analysis, Design Modification and Modal Analysis of Structural Chassis Frame': *International Journal of Engineering Research and Applications,ISSN : 2248-9622, Vol. 4, Issue 5*, 06-10 pp.

Marta Birkas (2014) '*Book of Tillage'*, Budapest: Szent Istvan University Press, ISBN:978-963-269-447-4.

MITCHEL J. (2004) 'Minimum Tillage Vegetable Crop Production':*ANR Publication 8132*, 1-8 pp.

Mukhopadhyay, M. C. (2013) 'Modal Analysis of Structural Vibration':*Proceedings of The International Mechanical Engineering Congress & Exposition, IMECE:2013-62533*.

Patel, V. V. (2012) 'Structural Analysis of a Ladder Chassis Frame': *World Journal of Science and Technology ISSN: 2231 – 2587*, 05-08 pp.

Paulina Nogowczyk, G. S. (2014) 'Some Basic Tips In Vehicle Chassis and Frame Design': *Journal of Measurements in Engineering, Volume 2, Issue 4*, 208-214.

Pingali Prabhu (2009) '*Agricultural Mechanization and the Evolution of Farming'*,London: The Johns Hopkins University Press.

Prashanth A. (2017) 'Design and Analysis of a Automobile Chassis by Using Composite Material, E-Glass Epoxy': *International Journal of Innovative Research In Science,Engineering and Technology,ISSN(Online): 2319-8753*, 19597-19605 pp.

Prof. Gaurav R. Mohite (2016) 'Design and Static Analysis of a Go-Kart Chassis by ANSYS Simulation', *International Research Journal of Engineering and Technology (IRJET),Volume: 03 Issue: 04 , P-ISSN: 2395-0072*, 1426-1428.

Rajappan And Vivekanandhan (2013) 'Static and Modal Analysis of Chassis by FEA': *Proceedings of the National Conference on Emerging Trends In Mechanical Enginnering.*

Shree Harsha B T, Saketh Chellur, Aparna Latha A, Sandeep Kumar Y, (2006). Conservation Tillage and Weed Manegement': *ISBN-10:1-60107-392-5*, 1-12 pp.

Vanessa Duarte (2016) 'The Early Evolution of the American Tractor Industry', *Évora - Portugal, Largo Dos Colegiais 2, 7000-803*.

Vijayan, Sendhilkumar S. and Kiran Babu, (2015) 'Design and Analysis of Automotive Chassis Considering Cross-Section and Material': *International Journal Of Current Research:Volume 7,Issue, 05,ISSN: 0975-833X*,15697-1570 pp.

Vinodbabu Chintada, Chiranjeeva Rao Seela, Vykunta Rao Matta (2015) 'Modal and Static Analysis of Automotive Chassis Frame by Using FEA': *International Journal of Applied Engineering Research, ISSN 0973-4562 Vol. 10, No.20*, 19775-19778 pp.

Xinshen Diao (2016) 'Agricultural Mechanization and Mechanization Transformation': *Japan International Cooperation Agency Research Institute (JICA-RI)*, 7-8 pp.

A. APPENDIX

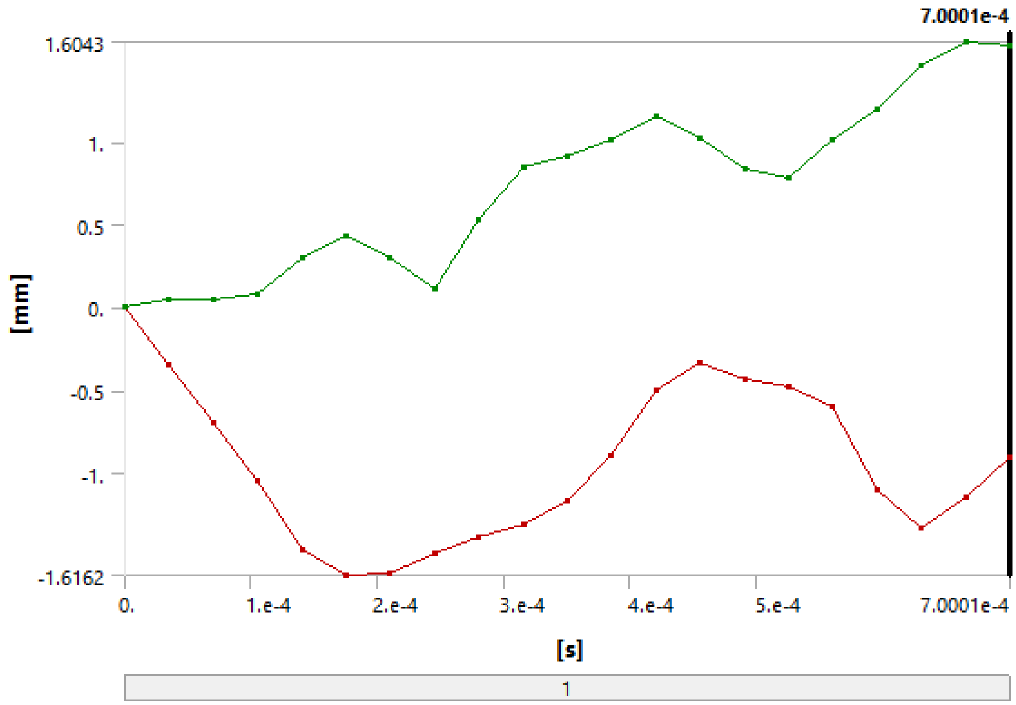

Figure A. 1.Directional deformation graph of ASTM A710 for impact analysis

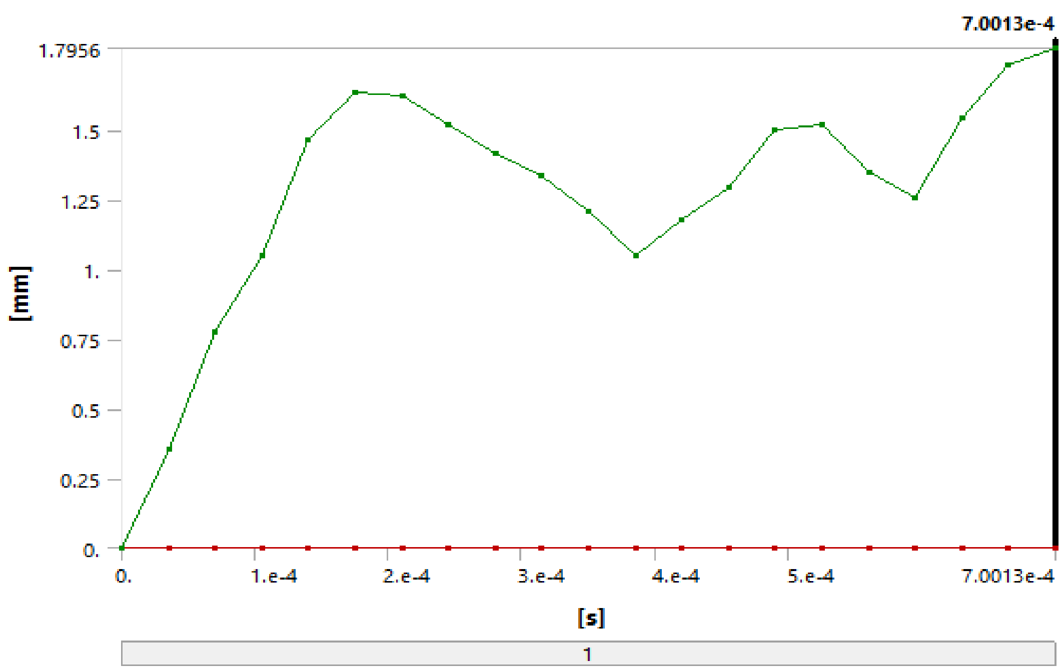

Figure A. 2. Total deformation graph of ASTM A710 for impact analysis

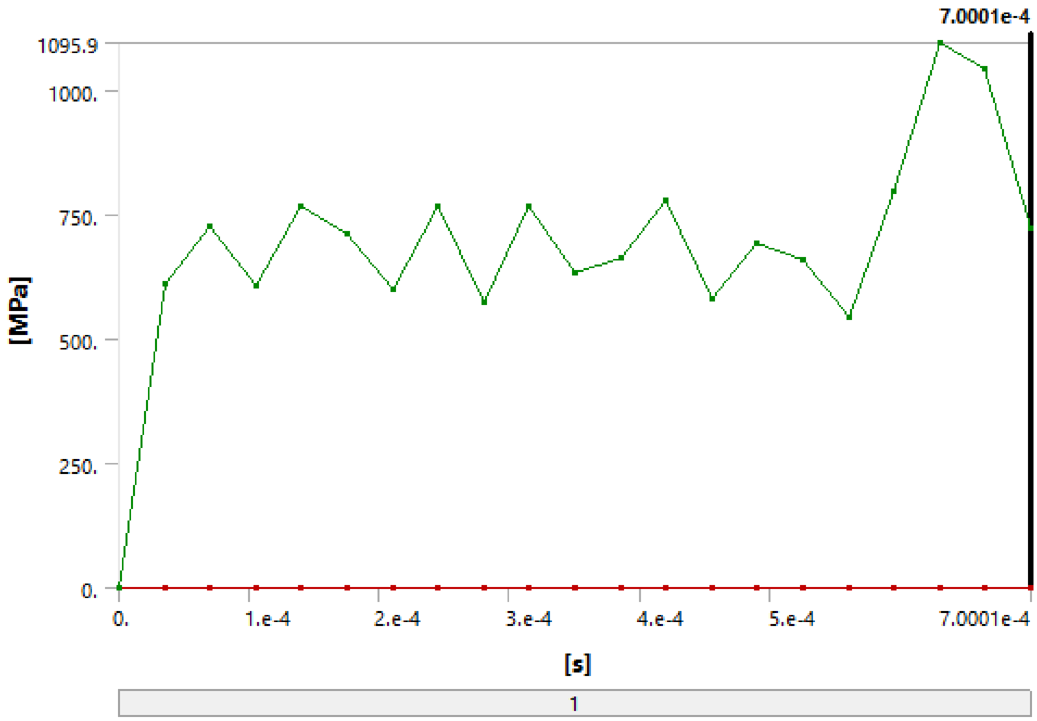

Figure A. 3.Von misses stress graph of ASTM A710 for impact analysis

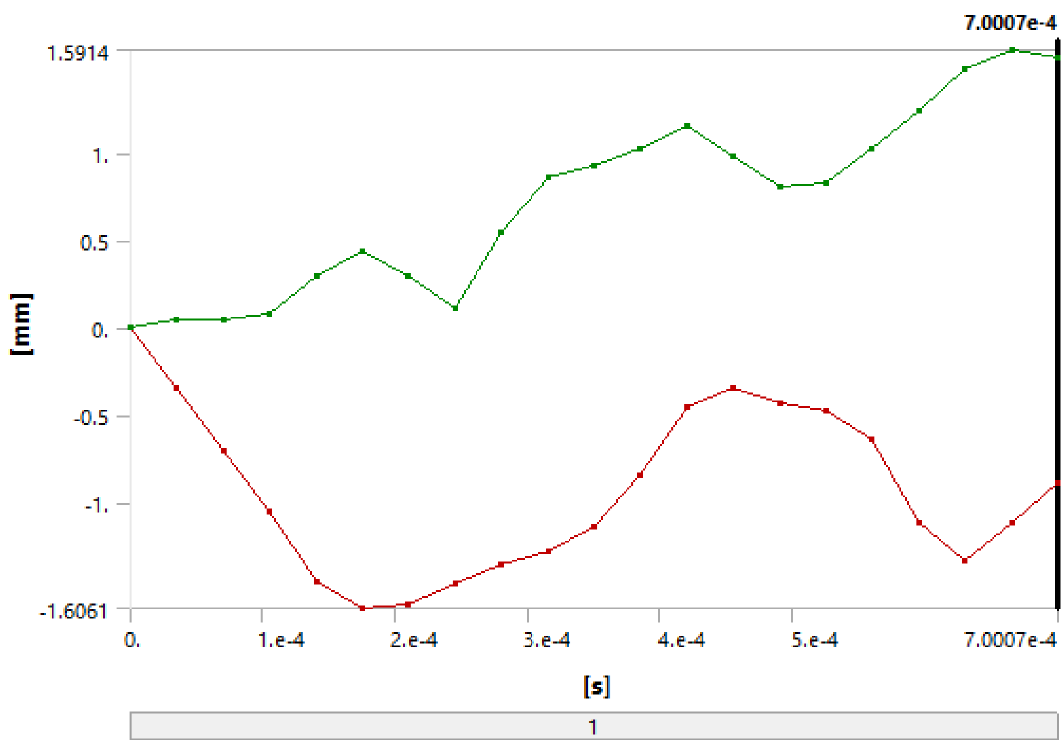

Figure A. 4. Directional deformation graph of ASTM A302 for impact analysis

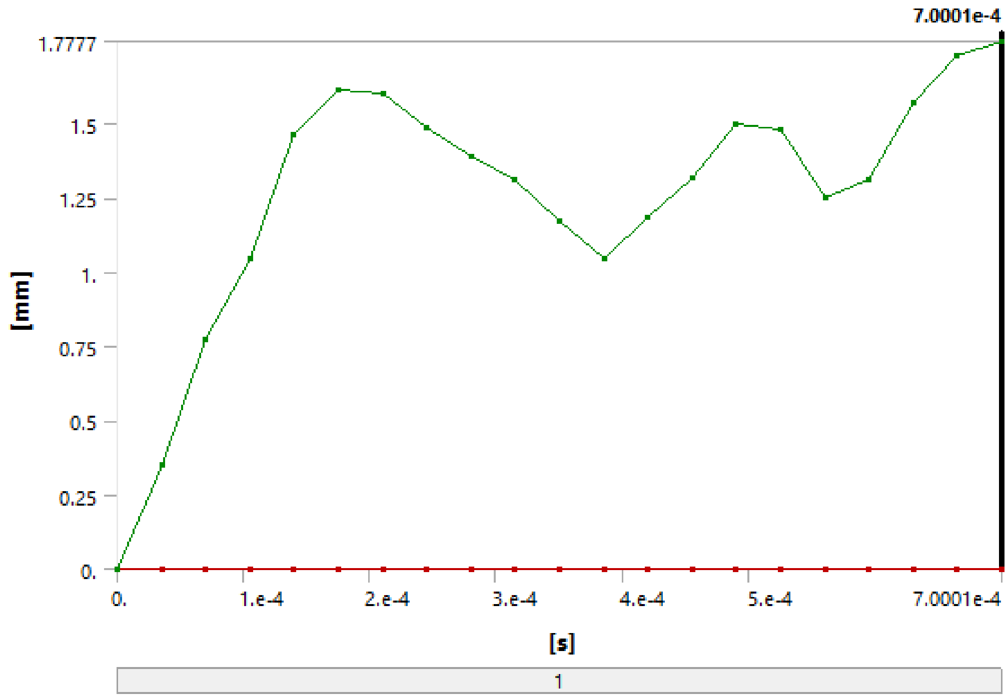

Figure A. 5.Total deformation graph of ASTM A302 for impact analysis

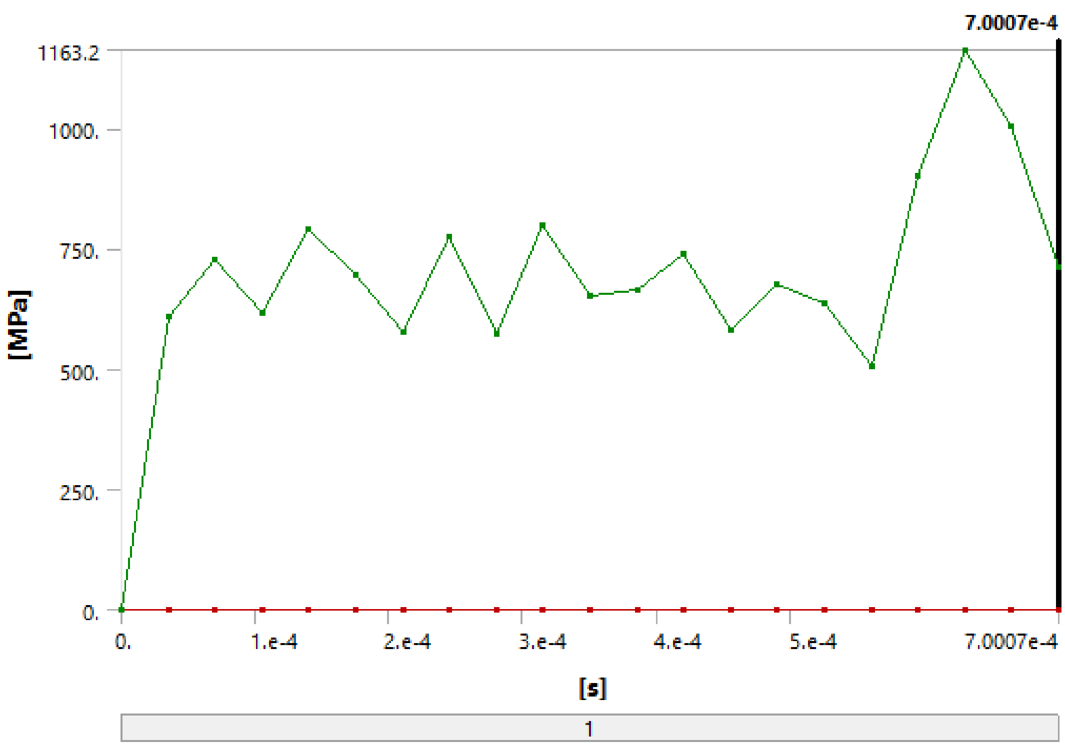

Figure A. 6. Von misses stress graph of ASTM A302 for impact analysis

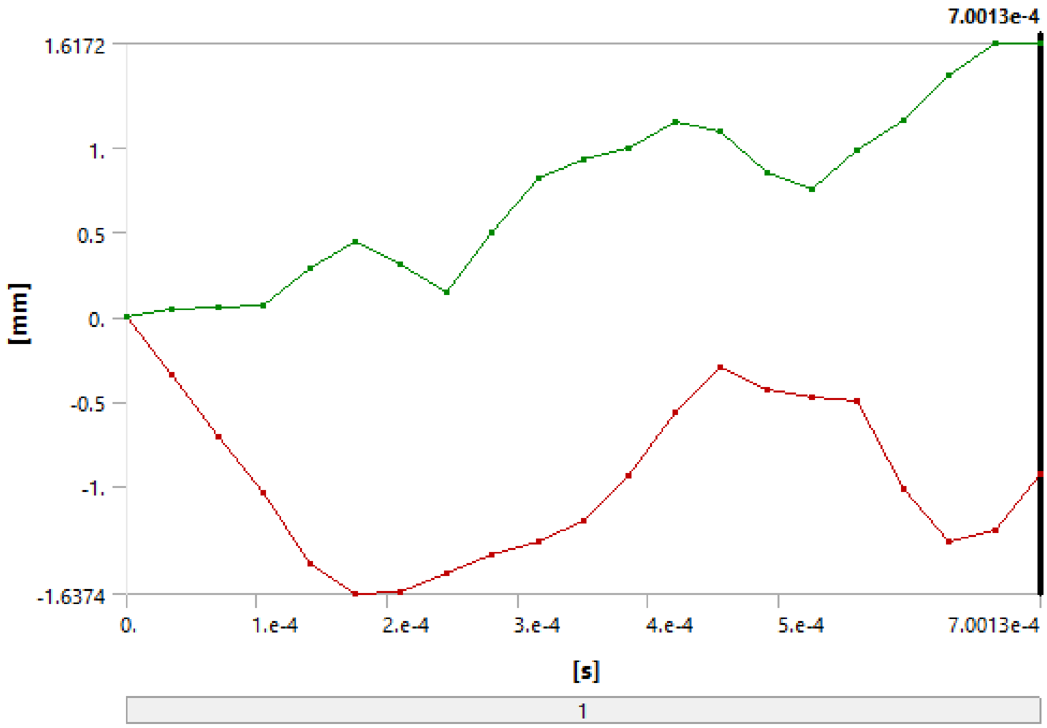

Figure A. 7. Directional deformation graph of ASTM AISI 4140 for impact analysis

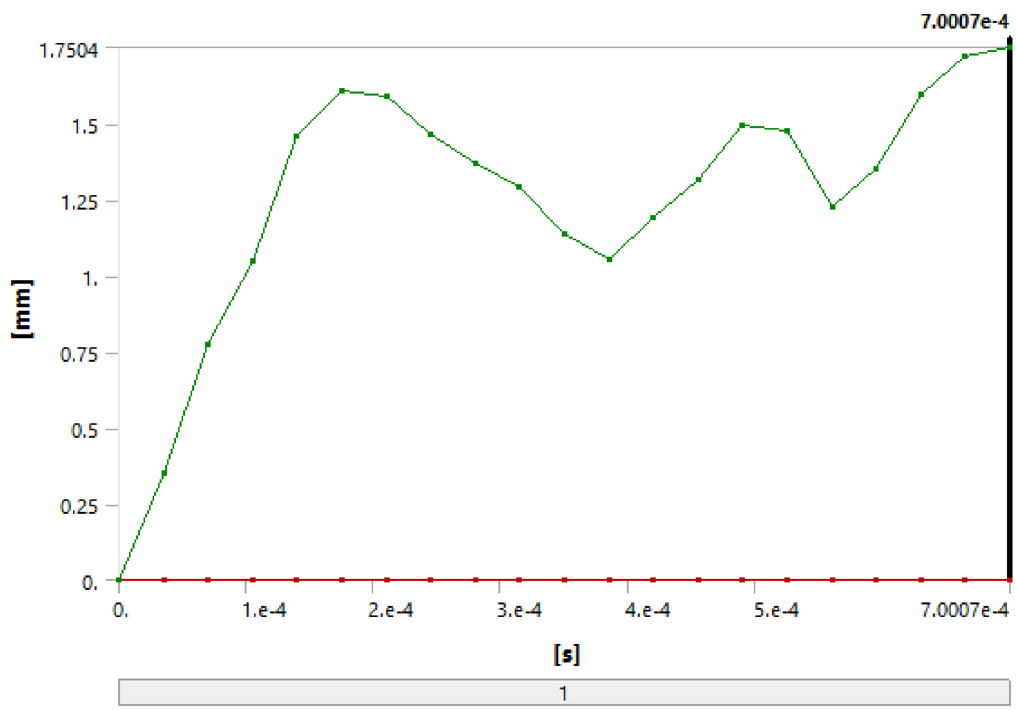

Figure A. 8.Total deformation graph of ASTM AISI 4140 for impact analysis

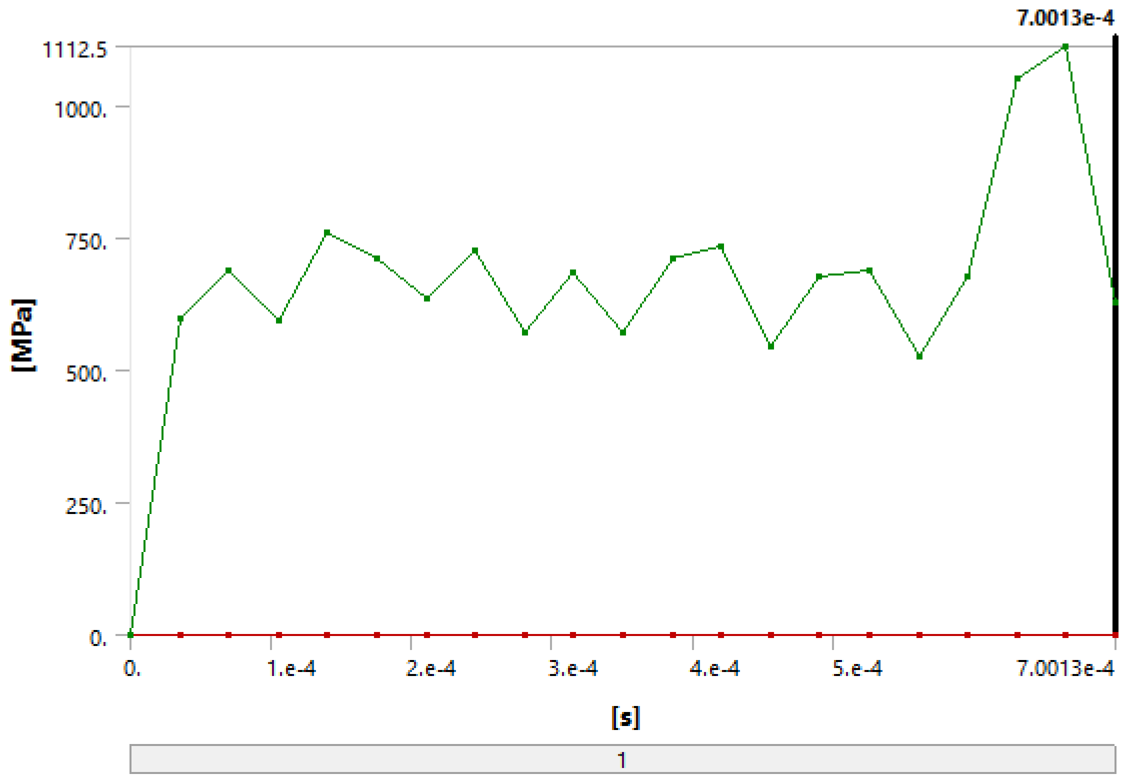

Figure A. 9. Von misses stress graph of AISI 4140 for impact analysis

Table A. 1. FEA Result of ASTM A710 for Impact Analysis

Object Name	*Directional Deformation*	*Total Deformation*	*Equivalent Plastic Strain*	*Equivalent Stress*
State	Not Solved			
Scope				
Scoping Method	Geometry Selection			
Geometry	All Bodies			
Definition				
Type	Directional Deformation	Total Deformation	Equivalent Plastic Strain	Equivalent (von-Mises) Stress
Orientation	X Axis			
By	Time			
Display Time	Last			
Coordinate System	Global Coordinate System			
Calculate Time History	Yes			
Identifier				
Suppressed	No			
Results				
Minimum	-0.90627 mm	0. mm	0. mm/mm	0. MPa
Maximum	1.5842 mm	1.7777 mm	0. mm/mm	724.53 MPa
Minimum Occurs On	ladder c assembly gut.2\Solid	for impact test\Solid	ladder c assembly gut.2\Solid	for impact test\Solid
Maximum Occurs On	ladder c assembly gut.2\Solid			
Minimum Value Over Time				
Minimum	-1.6162 mm	0. mm	0. mm/mm	0. MPa
Maximum	0. mm		0. mm/mm	0. MPa
Maximum Value Over Time				
Minimum	0. mm		0. mm/mm	0. MPa
Maximum	1.6043 mm	1.7777 mm	0. mm/mm	1095.9 MPa
Information				
Time	7.0001e-004 s			
Set	21			
Cycle Number	4947			
Integration Point Results				
Display Option			Averaged	
Average Across Bodies			No	

Table A. 2. FEA Result of ASTM A302 for Impact Analysis

Object Name	*Directional Deformation*	*Total Deformation*	*Equivalent Plastic Strain*	*Equivalent Stress*
State	Not Solved			
Scope				
Scoping Method	Geometry Selection			
Geometry	All Bodies			
Definition				
Type	Directional Deformation	Total Deformation	Equivalent Plastic Strain	Equivalent (von-Mises) Stress
Orientation	X Axis			
By	Time			
Display Time	Last			
Coordinate System	Global Coordinate System			
Calculate Time History	Yes			
Identifier				
Suppressed	No			
Results				
Minimum	-0.88946 mm	0. mm	0. mm/mm	0. MPa
Maximum	1.5446 mm	1.7504 mm	0. mm/mm	712.18 MPa
Minimum Occurs On	ladder c assembly gut.2\Solid	for impact test\Solid	ladder c assembly gut.2\Solid	for impact test\Solid
Maximum Occurs On	ladder c assembly gut.2\Solid			
Minimum Value Over Time				
Minimum	-1.6061 mm	0. mm	0. mm/mm	0. MPa
Maximum	0. mm		0. mm/mm	0. MPa
Maximum Value Over Time				
Minimum	0. mm		0. mm/mm	0. MPa
Maximum	1.5914 mm	1.7504 mm	0. mm/mm	1163.2 MPa
Information				
Time	7.0007e-004 s			
Set	21			
Cycle Number	5345			
Integration Point Results				
Display Option			Averaged	
Average Across Bodies			No	

Table A. 3.FEA Result of AISI 4140 for Impact Analysis

Object Name	*Directional Deformation*	*Total Deformation*	*Equivalent Plastic Strain*	*Equivalent Stress*
State	Solved			
Scope				
Scoping Method	Geometry Selection			
Geometry	All Bodies			
Definition				
Type	Directional Deformation	Total Deformation	Equivalent Plastic Strain	Equivalent (von-Mises) Stress
Orientation	X Axis			
By	Time			
Display Time	Last			
Coordinate System	Global Coordinate System			
Calculate Time History	Yes			
Identifier				
Suppressed	No			
Results				
Minimum	-0.92393 mm	0. mm	0. mm/mm	0. MPa
Maximum	1.6163 mm	1.7956 mm	0. mm/mm	626.5 MPa
Minimum Occurs On	ladder c assembly gut.2\Solid	for impact test\Solid	ladder c assembly gut.2\Solid	for impact test\Solid
Maximum Occurs On	ladder c assembly gut.2\Solid			
Minimum Value Over Time				
Minimum	-1.6374 mm	0. mm	0. mm/mm	0. MPa
Maximum	0. mm		0. mm/mm	0. MPa
Maximum Value Over Time				
Minimum	0. mm		0. mm/mm	0. MPa
Maximum	1.6172 mm	1.7956 mm	0. mm/mm	1112.5 MPa
Information				
Time	7.0013e-004 s			
Set	21			
Cycle Number	4958			
Integration Point Results				
Display Option			Averaged	
Average Across Bodies			No	

COST ESTIMATION

Even if the price of materials vary from time to time, the total cost of the chassis frame is estimated as per todays average cost as follows.

In today's online marketing price, the cost of high quality channel cross-section AISI steels are on the range of $1885-2000 per ton which is equivalent to Ethiopian 60 Birr per kilogram. Based on this price the cost of the chassis frame is given by:

Cost of longitudinal member = 2 × 0.0058 m^3 × 7835 kg/m^3 × 60 Birr/kg = 5453.16 Birr

Cost of I section cross member = 2 × 0.00318 m^3 × 7835 kg/m^3 × 60 Birr/kg = 2989.36 Birr

Cost of 'C' section cross member = 0.00159 m^3 × 7835 kg/m^3 × 60 Birr/kg = 747.46 Birr

Cost of tubular cross member = 2 × 0.00176 m^3 × 7835 kg/m^3 × 60 Birr/kg = 1654.73 Birr

Cost of bolts =56 × 15 = 840 Birr

Total material cost =11684.71 Birr

Assuming transportation and related costs including tax payments equal to the material cost (11684.71Birr) and machine and labor cost of 5000 Birr, the total cost of the chassis frame is:

11684.71 Birr + 11684.71 Birr 5000 Birr = 28369.42 Birr